

**AN EXPERIMENTAL INVESTIGATION INTO THE
EFFICIENCY OF FILTER MATERIALS FOR
PHOSPHATE REMOVAL FROM WASTEWATER**

ALI ALZEYADI

A thesis submitted in partial fulfilment of the requirements of Liverpool John

Moore's University for the degree of Doctor of Philosophy

June 2017

Name of department: Department of Civil Engineering

Faculty of Engineering and Technology

Liverpool John Moores University

Author: Ali Alzeyadi

Title: An Experimental Investigation into the Efficiency of Filter Materials for
Phosphate Removal from Wastewater

Director of study: Dr Edward Loffill

Co-supervisor: Professor Rafid Alkhaddar

Acknowledgment

I would like to express my acknowledgement to my supervisors Dr. Edward Loffill and Professor Rafid Alkhaddar, for giving me the guidance and support me throughout my PhD study. I would like to thank the technical team of the Henry Cotton Labs at Liverpool John Moores University for their valuable assistance, in particular Mal Feegan, Gary Lamb, and Alan Jones.

Special thanks to Mrs. Nicola Dempster and Mr. Campbell Woods from the Faculty of Science at Liverpool John Moores University for helping with conducting the experiments in identifying the chemical characteristics of the materials, which are selected in this study.

I would like to express my gratitude to Mr. Dave Unsworth, the team leader of Fuel & By-Product Logistics at Fiddlers Ferry Power Station for providing the furnace bottom ash used in this work. In addition, I would like to thank Omya UK Ltd for supplying the limestone, particular Les Wright the technical sales representative for organizing the material delivery.

To all my colleagues among the researchers in the Henry Cotton Building at Liverpool John Moores University, I am truly grateful for making my PhD an enjoyable journey, and for your brilliant suggestions and comments.

I appreciate the funding source that made my PhD work possible, the Ministry of Higher Education in Iraq and its representative in the United Kingdom the Iraqi cultural attaché in London.

Finally, I would like to thank my family. For the soul of my father who encouraged me to love science and supported me in chasing my dreams. For my beloved mother

for all her love and encouragement. For all my brothers and sister. For my loving, supportive and encouraging wife. Moreover, for my three lovely daughters for making my life better.

Abstract

Phosphorus is one of the most important nutrients, which significantly influences the extraordinary growth of algae. Consequently, this leads to eutrophication of aquatic life. Eutrophication of water bodies due to phosphorus coming from wastewater is a serious problem. Therefore, additional work on many wastewater treatment plants is required in order to meet the required standards, particularly in relation to nutrient removal. Recently, continuous upflow filters CoUFs have been found to be a suitable technology for upgrading or expanding the wastewater treatment plants. On the other hand, investigation of different sorts of low-cost materials has been shown to be an attractive solution as phosphate sorbent materials PSMs, which represents a sustainable solution based on economical and environmental factors. This PhD study seeks to determine materials that are capable of removing phosphate from wastewater at tertiary treatment within a short time when they are packed in CoUFs.

In order to select the suitable PSMs a comprehensive study has been conducted to describe their physical and chemical characteristics, affinity to retain orthophosphate (phosphate) and bonding time. This work was carried out through subjecting these materials to examinations such as scanning electron microscopy SEM and X-ray fluorescence analysis XRF to identify their characteristics, and conducting a batch test and constructing a lab-scale upflow filter to investigate the filter materials' affinity to phosphate.

Based on the phosphate removal efficiency and characteristics of selected materials an innovative and sustainable coating technology has been proposed to introduce a new type of filter material capable of removing phosphate effectively. Filtration materials coated with metallic oxides are presented as a good method for phosphate

sorption. However, most of the researchers utilize chemicals as a source of metallic oxides and heating process to set the chemicals over the filtration materials. In this study, the method of creating new filter media involves coating a solid material via waste materials containing metallic oxides; the ordinary Portland cement (OPC) was utilized as a binder for the mixture materials. Water is the factor which is responsible for activating the OPC. All factors have been subjected to an optimization process. The results revealed that the limestone particles coated by furnace bottom ash (FBA) indicated a high capacity for phosphate sorption and possibility of regenerating their efficiency.

In conclusion, this study introduces a new approach regarding creating and developing the characteristics of the filter media which fit the sustainability requirements.

List of Publications and rewards

Peer-reviewed papers

Alzeyadi, A., Loffill, E. & Alkhaddar, R. (2015) Investigation into the Optimum Hydraulic Loading Rate for Selected Filter Media Packed in a Continuous Up-flow Filter. *International Journal of Civil, Environmental, Structural, Construction and Architectural Engineering* 9, 710-713. (Published)

Alzeyadi, A.; Loffill, E.; Alkhaddar, R. M., Ali W. Alattabi (2016) Performance investigation of furnace bottom ash as a filter media for phosphate removal. *Environmental Protection Engineering journal*. (Accepted)

Alzeyadi, A., Loffill, E., Alkhaddar, R. & Alattabi, A. (2017) A novel coating method for creating a filter media for the effective removal of phosphate from wastewater. *Journal of Water Process Engineering*. (Under Review)

Conference papers

Alzeyadi, A.; Loffill, E.; Alkhaddar, R. M. (2014) An experimental investigation into the efficiency of aerated up flow filters for wastewater treatment. *The 9th Built Environment and Natural Environment Conference*. Liverpool United Kingdom: Liverpool John Moores University. (Published)

Alzeyadi, A., Loffill, E. & Alkhaddar, R. (2015) A Study of the Physical and Chemical Characteristics of Ca-Rich Materials for Use as Phosphate Removal Filter Media: A Process Based on Laboratory-Scale Tests. *World Environmental and Water Resources Congress* Texas, USA: ASCE library. (Published)

Alzeyadi, A., Loffill, E. & Alkhaddar, R. (2016) Study of influent transfer inside filter media packed in a laboratory up-flow filtration regime. *The 2ed British University in Dubai Conference*. Dubai, UAE. (Published)

Alzeyadi, A., Loffill, E. & Alkhaddar, R. (2016) Evaluating the performance of phosphate adsorption by materials packed in an up-flow filter. *The 2ed Faculty Research Week Conference*. Liverpool, UK: Liverpool John Moores University. (Published)

Alzeyadi, A., Loffill, E., Alkhaddar, R., Alattabi, A. & Abdulredha, M. (2017) Phosphate removal by utilizing different sorption materials as filter media: A comparative study. *The 3ed British University in Dubai Conference*. Dubai, UAE. (Published)

Rewards

Medal of excellence awarded by The Iraqi Minister of Higher Education for the best Iraqi researchers in the United Kingdom according to their scientific contribution and publications.

Certification of appreciation and recognition awarded by The Dean of The Faculty of Engineering and Technology for achievements while studying at LJMU with regards to research, publication and promoting LJMU.

Table of Contents

CHAPTER 1 INTRODUCTION	1
1.1 General introduction	1
1.2 The environmental effects of nutrients	2
1.3 Continuous, Up-flow filters	3
1.4 Scope of thesis	4
1.5 Aim of the thesis	5
1.6 Thesis structure and outline:	8
CHAPTER 2 LITERATURE REVIEW	11
2.1 Chapter Introduction	11
2.2 Background	11
2.2.1 EU Water Directive Framework WFD	11
2.2.2 Phosphorus sources	13
2.2.3 Phosphorus structure in municipal wastewater	14
2.2.4 Continuous up flow Filter Principles of Operation	15
2.2.5 History of continuous up flow filter development	18
2.2.6 Tertiary treatment	20
2.3 Phosphorus removal processes:	21
2.3.1 Physical Treatment	21
2.3.2 Chemical precipitation or Precipitation of phosphorus by metal salts	23
2.3.3 Biological phosphorus removal	26
2.3.4 Constructed wetlands	27
2.3.5 Phosphorus sorbing materials PSMs	28
2.4 Factors' influence on the phosphate removal	31
2.4.1 Filter media	31
2.4.2 pH	33
2.4.3 Operational conditions	34
2.4.4 Residence time distribution	35
2.4.5 Isothermal adsorption models	38
2.5 Filter media coating technologies	40
2.5.1 Overview of literature relevant to coating technologies	40
2.5.2 Coating material	45
2.6 Chapter summary	48

CHAPTER 3 RESEARCH METHODOLOGY	49
3.1 Chapter introduction	49
3.2 Material selection	52
3.3 Investigate the characteristics of research candidate materials	53
3.3.1 Particle size distribution PSD.....	54
3.3.2 Coefficient of permeability K	55
3.3.3 Specific gravity S.G	57
3.3.4 Porosity and Bulk density	58
3.3.5 Scanning electron microscopy (SEM)	58
3.3.6 X-ray fluorescence analyser (XRF)	59
3.3.7 Atomic absorption spectrometry (AAS)	60
3.3.8 Residence time distribution (RTD)	61
3.4 Research procedure	62
3.4.1 Risk assessment.....	62
3.4.2 Synthetic influent	63
3.4.3 Effluent sampling	63
3.4.4 Phosphate measurement:	64
3.4.5 Batch tests	65
3.4.6 Lab-scale filter	66
3.5 Data analysis tools	67
3.6 Chapter Summary	69
CHAPTER 4 INVESTIGATING THE SUITABILITY OF SELECTED MATERIALS AS PHOSPHATE FILTERS	71
4.1 Chapter introduction	71
4.2 Material collection.....	72
4.3 Investigation of the materials characteristics	73
4.3.1 Physical characteristics	74
4.3.2 Chemical characteristics.....	82
4.3.3 Surface characteristics.....	85
4.4 Investigating the efficiency of materials for phosphate sorption	87
4.4.1 Preparation of the phosphate calibration curve for spectrophotometer	87
4.4.2 Batch experiments	90
4.5 Chapter discussion.....	93
4.6 Chapter summary	94

CHAPTER 5 FILTER MEDIA COATING TECHNOLOGY.....	97
5.1 Chapter introduction.....	97
5.2 Materials bonding mechanism.....	98
5.3 Filter media preparation	99
5.4 Composite materials characteristics	101
5.4.1 Physical properties	101
5.4.2 Chemical properties	103
5.4.3 Surface characteristics.....	104
5.5 SEM image processing.....	106
5.6 Investigating the efficiency of new materials for phosphate sorption.....	110
5.7 Lab-scale filter.....	113
5.7.1 Study of influent transfer inside lab-scale filter.....	113
5.7.2 Investigating the filter materials efficiency.....	121
5.8 Safety examination	124
5.9 Adsorption isotherm study	124
5.9.1 Batch technique and adsorption Isotherms	125
5.9.2 Adsorption isotherm models	125
5.10 Chapter discussion.....	129
5.11 Chapter summary	131
CHAPTER 6 OPTIMIZATION OF COATING PROCESS.....	133
6.1 Chapter introduction.....	133
6.2 Obtain optimal filter media	134
6.2.1 Optimization process.....	134
6.2.2 Water ratio.....	135
6.2.3 OPC ratio.....	137
6.2.4 Coating dosage	139
6.2.5 Curing time	140
6.3 Multiple regression technique	142
6.3.1 Assumptions of multiple regression model.....	143
6.3.2 Model parameters.....	150
6.4 Chapter discussion.....	153
6.5 Chapter summary	155
CHAPTER 7 EVALUATING THE LFBA SUITABILITY FOR FIELDWORK ..	157
7.1 Chapter introduction.....	157

7.2	Filter media longevity	158
7.3	LFBA regeneration.....	162
7.3.1	Point zero charge PZC	163
7.3.2	Measuring the PZC of LFBA.....	165
7.3.3	Process of washing LFBA.....	167
7.3.4	Measuring the efficiency of LFBA after regeneration process.....	168
7.4	Cost analysis of LFBA	171
7.4.1	Method of pricing.....	172
7.4.2	Calculate the filter material cost	173
7.5	Phosphate removal from wastewater sample	176
7.6	Effect of LFBA bed height.....	179
7.7	Comparison with related work	183
7.8	Chapter discussion.....	187
7.9	Chapter summary	188
CHAPTER 8 CONCLUSION AND RECOMMENDATIONS.....		191
8.1	Chapter introduction.....	191
8.2	Thesis primary aim.....	191
8.3	Major conclusions	191
8.4	Thesis contribution to knowledge	192
8.5	Minor contributions.....	192
8.6	Thesis recommendations	193
References.....		195
Appendices.....		205

List of Figures

Figure 1.1. Percentage of total river length with average concentrations >30mg/l (nitrates) and > 0.1mg/l (phosphates) (Defra, 2014a)	3
Figure 1.2. Aerated COUFs at Biddulph WWTW, Cheshire, England (Loffill, 2011)4	4
Figure 2.1. Algae growth in the Tualatin River (Shock and Pratt, 2003)	12
Figure 2.2. Sources of phosphors entering surface waters, statistical results for 12 European countries, including the UK (Morse et al., 1993)	13
Figure 2.3. Phosphorus compound structure in domestic wastewater	15
Figure 2.4. Schematic of CoUF (Schauer et al., 2006)	16
Figure 2.5. Schematic of membrane filter (MECO, 2016)	23
Figure 2.6. The main strategies for phosphate removal chemically in wastewater treatment plants (Lenntech, 2016).....	25
Figure 2.7. A basic biological phosphorus removal process (Lenntech, 2016)	27
Figure 2.8. Schematic of constructed wetland, effluent flows horizontally through the bed (UNEP, 2016).....	28
Figure 2.9. Ligand exchange reactions on metals oxide surface (Klimeski et al., 2012)	30
Figure 2.10. Methods of tracer injection through the reactors	38
Figure 2.11. The experimental conditions for the preparation of BCSCP	45
Figure 2.12. Schematic layout of a coal-fired electrical generating station illustrate the production of bottom and fly ash	47
Figure 3.1. Research methodology flow chart	51
Figure 3.2. Material selection priorities	52
Figure 3.3. Sieve analysis	55
Figure 3.4. Hydraulic conductivity measurement (a) Dolomite (b) Limestone	56
Figure 3.5. Filter media specifications for multimedia filter	57
Figure 3.6. Scanning electron microscopy	59
Figure 3.7. Energy dispersive X-ray fluorescence	60
Figure 3.8. Spectrophotometer device	64
Figure 3.9. Steps of the phosphate concentration measurement; according to the Amino Acid method	65
Figure 3.10. Schematic diagram of upflow filter set-up (dimensions unit is cm).....	66
Figure 4.1. Particle size distribution curve PSD	78
Figure 4.2. SEM comparison of limestone surface (a), white dolomite surface (b), sand surface (c), BBA surface (d) and FBA surface (e)	86
Figure 4.3. Wavelength determination for phosphate samples by utilizing spectrophotometer	88
Figure 4.4. Spectrophotometric absorption for phosphate samples at wavelength 830 nm.....	90
Figure 4.5. Batch experiments results	91
Figure 5.1. Grinder with pestle and mortar, 2L capacity	99
Figure 5.2. Bench mixer, 5 L capacity	100
Figure 5.3. Samples of new-coated materials	100

Figure 5.4. SEM comparison of material surface before and after coating, (a1) limestone, (a2) LFBA, (a3) LBBA, (b1) white dolomite, (b2) DFBA, (b3) DBBA, (c1) sand, (c2) SFBA and (c3) SBBA.....	105
Figure 5.5. SEM image processing analysis for LFBA and LBBA.....	108
Figure 5.6. SEM image processing analysis for DFBA and DBBA.....	109
Figure 5.7. SEM image processing analysis for SFBA and SBBA.....	109
Figure 5.8. Batch experiments results for coated materials.....	111
Figure 5.9. Phosphate sorption comparison between coated and uncoated material.....	112
Figure 5.10. Determination of the best wavelength for absorbance of RDD samples, first attempt.....	115
Figure 5.11. Determination of the best wavelength for absorbance of RDD samples, second attempt.....	116
Figure 5.12. Spectrophotometric absorbance values at 525 nm that correspond to known concentrations of RDD.....	117
Figure 5.13. The residence time distribution curves for LFBA, SFBA and SBBA at different flow rates: (a) 0.5 l/min; (b) 1 l/min; (c) 1.5 l/min.....	118
Figure 5.14. Investigate the efficiency of the filter materials for phosphate removal.....	123
Figure 5.15. Adsorption isotherms of phosphate on LFBA.....	126
Figure 5.16. Langmuir isotherm model (1/Ce vs. 1/qe).....	127
Figure 5.17. Freundlich isotherm model (log Ce vs. log qe).....	128
Figure 6.1. Effect of water ratio on the removal of phosphate.....	136
Figure 6.2. Effect of OPC ratio on the removal of phosphate.....	138
Figure 6.3. Effect of FBA dosage on the removal of phosphate.....	140
Figure 6.4. Effect of curing time on the removal of phosphate.....	141
Figure 6.5. Plot of regression standardised residual.....	148
Figure 6.6. Data distribution for all variables, (a) data histogram (b) normal P-P plot.....	149
Figure 7.1. Phosphate removal via LFBA over the operating sessions.....	160
Figure 7.2. Δ pH versus initial pH of LFBA at different temperatures.....	166
Figure 7.3. Phosphate removal efficiency via LFBA samples versus washing time.....	168
Figure 7.4. LFBA efficiency after washing with solution at pH 9.5.....	169
Figure 7.5. LFBA efficiency after washing with solution at pH 10.....	170
Figure 7.6. Treating wastewater influent via lab-scale upflow system (a) submersible pump (b) lab-scale upflow filter.....	177
Figure 7.7. Adsorption of phosphate onto LFBA for wastewater and synthetic phosphate solutions (flow rate 1 L/min, temperature (20 \pm 2 oC)).....	178
Figure 7.8. The second constructed lab-scale flow filter for measure phosphate removal at various LFBA depths.....	180
Figure 7.9. Phosphate adsorption at different depths, when LFBA fresh.....	181
Figure 7.10. Phosphate adsorption at different depths, when LFBA semi saturated.....	182

List of Tables

Table 2.1. pH Influence on Phosphate Removal.....	34
Table 4.1. The results of sieve analysis for Sand sample.....	75
Table 4.2. The results of sieve analysis for Limestone sample.....	75
Table 4.3. The results of sieve analysis for White dolomite sample	76
Table 4.4. The results of sieve analysis for BBA sample	77
Table 4.5. The results of sieve analysis for FBA sample.....	77
Table 4.6. The basic parameters that can be determined from particle size distribution curves.....	79
Table 4.7. The physical properties of the material.....	80
Table 4.8. Materials characterization according to their Bulk Density.....	82
Table 4.9. The X-ray fluorescence analysis for the selected material	84
Table 4.10. Absorbance of the prepared standard samples	89
Table 5.1. The physical properties of new composite material.....	102
Table 5.2. The x-ray fluorescence analysis for the new created media	104
Table 5.3. Process parameters and the MRT values for all filter materials	120
Table 5.4. Langmuir and Freundlich isotherm models' parameters for PO ₄ -3 adsorption on LFBA.....	127
Table 6.1. Optimization process the factors which influence on the efficiency of created mixture for phosphate sorption.....	135
Table 6.2. Tolerance and VIF values for each independent variable.....	145
Table 6.3. Critical values for the MDs (Pallant, 2005)	147
Table 6.4. Model summary	150
Table 6.5. Coefficients of multi regression model.....	151
Table 7.1. Regeneration efficiency of LFBA according to pH and method of washing	171
Table 7.2. Materials and energy costs for LFBA production.....	174
Table 7.3. Materials and energy costs for IOCS production.....	175
Table 7.4. Experimental conditions at each selected depth	181
Table 7.5. LFBA and other filter materials used in flow column experiments.....	184

List of Equations

Equation 2.1	35
Equation 2.2	35
Equation 2.3	36
Equation 2.4	36
Equation 2.5	36
Equation 2.6	38
Equation 2.7	39
Equation 2.8	39
Equation 2.9	39
Equation 2.10	40
Equation 3.1	56
Equation 3.2	58
Equation 3.3	58
Equation 4.1	79
Equation 4.2	79
Equation 5.1	128
Equation 6.1	144
Equation 6.2	145
Equation 6.3	145
Equation 6.4	151
Equation 6.5	152
Equation 7.1	159
Equation 7.2	170
Equation 7.3	173

Abbreviations

AAS	Atomic absorption spectrometry
Al	Aluminium
Al (OH) ₃	Aluminium hydroxide
Al ₂ O ₃	Aluminium oxide
AlPO ₄	Aluminium phosphate
AsO ₃	Arsenite
BBA	Biomass bottom ash
BCSCP	Blast furnace dust clay sodium silicate ceramic particles
BET	Brunauer–Emmett–Teller
BFD	Blast furnace dust
Ca	Calcium
CaCO ₃	Calcium carbonate
CaO	Calcium oxide
C _c	Coefficient of gradation
Cd	Cadmium
COD	Chemical oxygen demand
CoUF	Continuous up-flow filter
C-S-H	Calcium-silicate-hydrates
Cu	Copper
CW	Constructed wetland
DBBA	Dolomite- biomass bottom ash
Defra	Department for Environment Food & Rural Affairs
DFBA	Dolomite- furnace bottom ash

EU	European Union
FBA	Furnace bottom ash
Fe	Iron
FeCL ₃	Iron(III) chloride
Fe ₂ O ₃	Iron oxide
IOCS	Iron-oxide-coated sand
IVs	Independent parameters
K	Coefficient of permeability
KH ₂ PO	Potassium dihydrogen orthophosphate
LBBA	Limestone- biomass bottom ash
LECA	Light expanded clay aggregates
LFBA	Limestone- furnace bottom ash
LWA	Light-weight aggregates
LWTW	Liverpool wastewater treatment works
MC	Multicollinearity
MDs	Mahalanobis distances
Mg	Magnesium
MgO	Magnesium oxide
MRT	Mean residence time
NaOH	Sodium hydroxide
NH ₃ -N	Ammonia nitrogen
Ni	Nickel
OPC	Ordinary Portland cement
P	Phosphorus

Pb	Lead
pH	Measure of the acidity or basicity of an aqueous solution
PO ₄ ⁻³	phosphate
PSD	Particle size distribution
PSMs	Phosphate sorption materials
PZC	Point zero charge
q _e	Mass of adsorbed per mass unit of adsorbent
R _L	Equilibrium parameter
RO	Reverse osmosis
RT	Retention time
RTD	Residence time distribution
RDD	Red drain dye
SBBA	Sand- biomass bottom ash
SEM	Scanning electron microscopy
SeO ₃	Selenium trioxide
SFBA	Sand-furnace bottom ash
S.G	Specific gravity
SR	Standardised residual
TP	total phosphorus
TSS	Total suspended solid
UC	Uniformity coefficient
UK	United Kingdom
VIF	Variance Inflation Factor
WFD	Water Framework Directive

WWTPs	Wastewater treatment plants
XRF	X-ray fluorescence analyser
Zn	Zinc

CHAPTER 1 INTRODUCTION

1.1 General introduction

Urban and industrial wastewater is generated as a consequence of modern society. Disposal of wastewater produces a continuous threat to freshwater quality on a worldwide scale (Montaigne and Essick, 2002). Consequently, wastewater should not be dumped straight into water bodies, and removing pollutants from wastewater is usually obligatory to reduce their adverse effects on human health and the environment. Phosphorus, ammonium, and nitrates are forms of nutrients; they are released from different sources. High nutrient levels contribute to the eutrophication of water bodies by accelerating the extraordinary growth of algae. The implementation of the EU water framework directive concerning meeting effluent standards, particularly about nutrient removal, required additional work on many wastewater treatment plants to meet the required standards. Conventional wastewater treatment technologies consist of a combination of treatment methods but at a very high cost (Chang et al., 2009). Continuous, up-flow filters are a promising technology for upgrading or expanding the wastewater treatment plants, but the process still requires some optimisation, particularly regarding media type, loading rates and control of environmental factors to improve its performance. Phosphate is recognized as one of the major nutrients (Krishnaswamy et al., 2011); phosphate removal by continuous, up-flow filter is the target of this study.

1.2 The environmental effects of nutrients

Nutrients are responsible for eutrophication of lakes, rivers, and seas (Lau et al., 1997, vanLoon and Duffy, 2000). Eutrophication is characterised by the plentiful growth of phytoplankton called algal blooms that may prevent sunlight from reaching aquatic vegetation; these algal blooms lower the levels of dissolved oxygen as decomposition of their organic matter consumes the dissolved oxygen. The outcomes are anoxic, acidic, detrimental conditions which are preventing the development of higher forms of aquatic life and lead to diversity reduction in the water system (Gray, 2012). The anaerobic conditions of the aquatic body lead to an increase in the growth of toxic bacteria; the result is declining water quality. The intensive growth of algal blooms and photosynthetic bacteria in waters can also block the intake point of water systems; this causes difficulty in pumping the water to water pipes. Additionally, algal blooms reduce water clarity and aesthetic qualities.

The presence of the nutrients in municipal effluents is a threat to water quality. Therefore, the wastewater that is discharged from wastewater treatment plants without adequate treatment is considered as a point source of a nutrient. Lau et al. (1997) alluded to an excessive nutrient content in the effluent discharged from the wastewater treatment plants (WWTPs); phosphate P in the form of orthophosphates and inorganic nitrogen in the form of nitrate are the most notable nutrients.

Ammonia is produced by the breakdown of organic sources of nitrogen. Municipal wastewaters contain large amounts of organic waste, so the wastewater will have a high ammonia concentration. With this high concentration of ammonia, the wastewater would harm downstream ecosystems by enrich the eutrophication phenomenon.

The percentage of total river length in England with nitrate levels over 30 mg NO₃ per litre, and phosphorus (as phosphate) levels over 0.1 mg P per litre is shown in Figure 1.1. Recently, there has been an increase in interest in the protection of water resources. The availability of data for the period after 2000 in comparison with the period from 1990 to 2000 in Figure 1.1 reflects the increase in awareness of the risks, which results from nutrients released into the water bodies. Also, the EU has enacted legislation in the form of the Water Framework Directive (WFD) regarding the tightening of nutrient discharge (Loffill, 2011). The nutrient removal from wastewater is especially troublesome and adopting adequate processes to protect water bodies from contamination has become an urgent requirement.

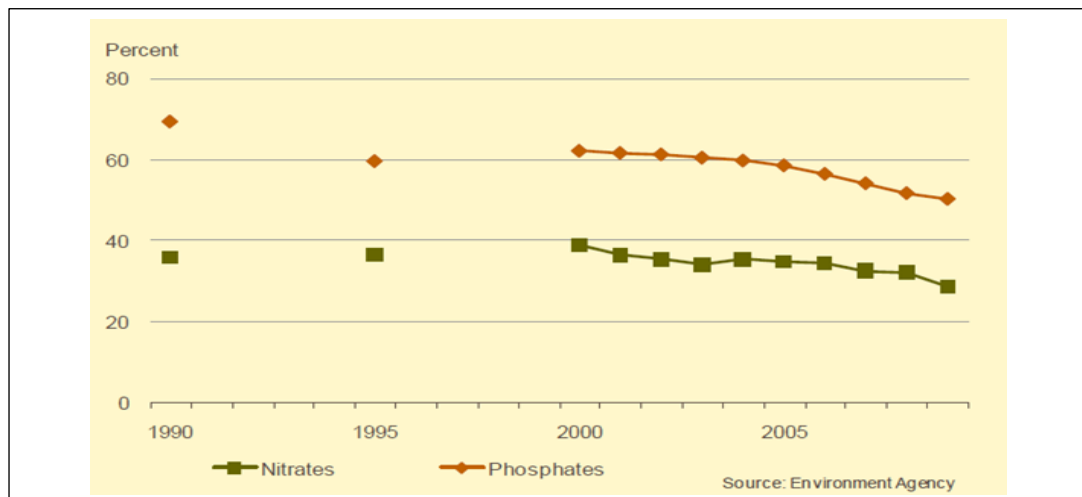


Figure 1.1. Percentage of total river length with average concentrations >30mg/l (nitrates) and > 0.1mg/l (phosphates) (Defra, 2014a)

Permission to use this figure has been granted by Department for Environment,
Food and Rural Affairs

Continuous, Up-flow filter CoUF is the technology that will be applied in this project; it is an up flow, deep bed, and granular media filter with continuous cleaning. The filter deep media bed allows it to bear high levels of suspended solids; meanwhile, the

media is cleaned by a simple internal washing system that does not require backwash pumps or storage tanks. The absence of backwash pumps means low energy consumption. Recently, researchers have paid particular attention to using this technology in removing the nutrients in line with environmental legislation.



Figure 1.2. Aerated COUFs at Biddulph WWTW, Cheshire, England (Loffill, 2011)

Permission to use this figure has been granted by author

1.4 Scope of thesis

Excess algae growth because of excessive release of P into aquatic systems, is leading to oxygen depletion and is damaging the aquatic life. P concentrations in lakes higher than $\sim 50 \mu\text{g/l}$ may cause eutrophication (Smil, 2000). Hence, mitigation of P is one of the essential requirement to achieve a good water quality. Thus, this work focuses on decreasing the P concentration, specifically orthophosphate.

According to (Cucarella, 2009) the agricultural runoff, soil erosion and industrial and municipal wastewaters are the primary sources that increase the P concentrations in surface waters. Wastewater is considered as one of the major point sources of the P;

Farmer (2001) illustrated that more than half of the phosphates discharged in Europe comes from the point sources of P. Many substantial efforts are exerted to minimize the flow of P from municipal wastewater to the water bodies. However, P remains a serious and costly issue in all over the world. Therefore, phosphate removal from wastewater by utilizing the continuous upflow filter is a priority in this research.

Filter media is considered a vital factor in contaminants' mass transfer; it significantly influences the hydraulic characteristics of the filtration system. Media selection is crucial in filtration processes in order to get the required effluent quality (Yu et al., 2008). The application of phosphate sorbing materials PSMs as a filter media provides a potential solution for treating wastewater (Klimeski et al., 2012). One of the important aspects of this thesis is to determine the PSMs that are eligible for removing phosphate at tertiary treatment.

The goal of this research has been achieved according to two main stages. Firstly, investigation of the eligibility of some materials to act as phosphate filter media by subjecting them for physical and chemical tests. Secondly, determine the most efficient material for phosphate removal according to batch and column tests.

1.5 Aim of the thesis

Recently, the continuous upflow filter has been considered one of the promising technologies in wastewater treatment; the development of this technology will lead to opening new horizons in the filtration process. The core goal of this thesis is to identify the media that are capable of removing the phosphate from wastewater by utilizing the continuous upflow filter.

Objectives:

- Achieving a sustainable solution through balancing the environmental and economic factors is one of the essential research targets. Therefore, an extensive literature review has been undertaken so as to select a better filter media material from the waste by-products, in addition to the cheapest and most easily available natural material. In this work two types of bottom ash were selected as filter media; limestone, white dolomite, and sand were selected as naturally available material.
- The most efficient phosphate sorption materials PSMs tend to be those that contain Fe/Al hydroxides or easily soluble Ca/Mg compounds. The chemical composition of filter media has been analysed by the energy dispersive X-ray fluorescence XRF to determine their chemical characteristics.
- The contact between effluent and the material surface is a vital factor in the sorption process. Hence, identifying the physical properties of the material surface is significant to understand the material reactivity to the phosphate. The selected material has been subjected to a series of tests (Particle size distribution PSD and scanning electron microscopy SEM) to illustrate the size, shape, and porosity of the media particles.
- Conduct bench-scale experiments to evaluate the eligibility of the selected media for phosphate sorption. It is applied by bringing the media to be in contact with phosphate solution in a batch experiment.
- Lab-scale filters have been constructed. They have an upflow configuration to simulate the performance of the upflow filter.

- Residence time distribution RTD study was carried out to understand and compare the transfer behaviour of contaminants through the selected filter media that were packed in the lab-scale filters.
- Based on the phosphate removal efficiency and characteristics of selected materials an innovative and sustainable coating technology will be applied to introduce a new type of filter materials capable of removing phosphate effectively.

The research novelty:

- Screen the eligibility of a selected waste material to act as PSMs in upflow continuous filtration system.
- Set up a framework for the PSMs selection; include the experiments that identify the material's physical and chemical characteristics.
- Create a novel filter media as PSM by mixing available waste material. Thus, promote the media's physical and chemical properties that will reflect positively on the phosphate removal.
- The process of optimising the mixing percentages of the new filter media will provide a promising way for researchers regarding creation or enhancing the properties of filter media.
- Develop the process of the continuous upflow filtration system by adding a washing process to regenerate the media surface for phosphate sorption. NaOH solution was pumped to achieve desorption of the phosphate that remains on the media surface.

1.6 Thesis structure and outline:

Chapter one: Introduction of the thesis, this chapter includes background to the thesis topic, indicates the central problem and aim of the thesis and its novelty.

Chapter two: literature review, comprehensive overview of the thesis topic. It includes an overview of the phosphate structure in the wastewater. Regulations and legislations enacted to protect the water bodies from nutrients. The main methods of phosphate removal in wastewater facilities, what has been done in coating technology by previous researchers, and how this current research will contribute to introducing an innovative coating technology more consistent with the sustainable approach.

Chapter three: Thesis methodology, this chapter will explain the steps that were followed to carry out this research. It will also explain the methods of utilizing laboratory tools and devices which contributed in obtaining the research data, and the methods that were implemented to analyse the data.

Chapter four: Investigate the suitability of selected materials to act as phosphate sorption materials for upflow filtration systems. It is applied by studying their physical and chemical characteristics and uses batch experiments to examine their eligibility for phosphate removal.

Chapter five: Implementing coating technology, create novel filter media capable of remove phosphate effectively.

Chapter six: Optimization of the coating process; an optimization process has been conducted to determine the optimal mixture percentages which achieve best phosphate removal.

Chapter seven: Filter media regeneration, provide a method for regeneration of the filter media that leads to increasing the filter media lifespan.

Chapter eight: Thesis conclusion, includes the achieved research aim and how it is contributing to filling the gap in knowledge in previous researches regards the filter media coating technologies. In addition, the limitations that were found in this study and the necessary recommendations that should be undertaken to solve these limitations.

CHAPTER 2 LITERATURE REVIEW

2.1 Chapter Introduction

The literature review consists of four parts. The first part provides a background about the legislations and policies for protection of water bodies, phosphorus sources and their forms in wastewater, and the technology of the continuous upflow filter CoUF including its development over history. The second part presents the recent theories of capture methods for phosphorus. The third part includes the factors influencing the filter performance and the potential manner to deal with them positively. Finally, the fourth part reviews the technologies of filter media coating and the material applied in this present work.

2.2 Background

This part of the literature review provides information about the creation of the European Water Directive Framework (WDF). Especially, in regards to nutrients' release. In addition, characterisation of the phosphorus sources and the operational process of CoUF.

2.2.1 EU Water Directive Framework WFD

Approximately half the EU population lives in countries suffering 'water-stress', where the freshwater abstraction from its sources is too high. As a result, on 23 October 2000, the European Union established a Water Framework Directive WFD in the field of water policy to present a new legislative approach to managing and protecting water bodies. The Water Framework Directive calls for the member states

in the European Union to commit to standards that achieve good qualitative and quantitative status of all water bodies by 2015.

The protection of water bodies from nutrient release is one of the criteria that should be applied to achieve the aims of the WFD. Elevated concentrations of nutrients can cause adverse impacts on plenty of species in the aquatic life as shown in figure 2.1. (Shock and Pratt, 2003) determined the algal growth rate in order to calculate the density of algae which are available in water (g/l), as a function of the orthophosphate concentration as an average over the year. Therefore, a degradation in water quality will take place such as decreasing oxygen levels. The negative variations can then lead to undesirable implications to the animals and plants that live in the water system. Phosphorus concentrations increased because of release from various sources.

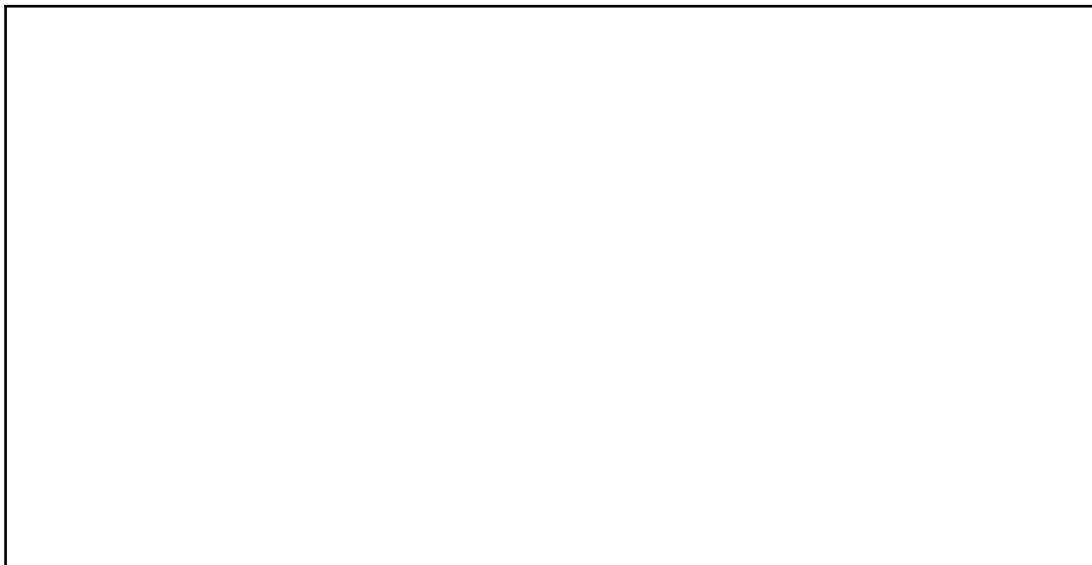


Figure 2.1. Algae growth in the Tualatin River (Shock and Pratt, 2003)

Permission to use this figure has been granted by author

The diagram originally presented here cannot be made freely available via LJMU Digital Collections because of 'copyright'. The diagram was sourced from (Shock and Pratt, 2003)

‘The Water Framework Directive (WFD) (2000/60/EC) introduced a comprehensive river basin management planning system to help protect and improve the ecological health of our rivers, lakes, estuaries and coastal and ground water. This is underpinned by the use of environmental standards to help assess risks to the ecological quality of the water environment and to identify the scale of improvements that would be needed to bring waters under pressure back into good condition’ (Defra, 2014).

2.2.2 Phosphorus sources

Phosphorus is released into the aquatic environment as a result of many human activities; generally, phosphorus sources can be categorised into point sources (such as wastewater treatment works) and diffuse sources such as the runoff from agricultural land (Dils et al., 2001). Figure 2.2 (Morse et al., 1993) shows the main sources of phosphorus (as P total) entering surface waters in the EU (this includes 12 countries, including the UK).



Figure 2.2. Sources of phosphorus entering surface waters, statistical results for 12 European countries, including the UK (Morse et al., 1993)

The diagram originally presented here cannot be made freely available via LJMU Digital Collections because of 'copyright'. The diagram was sourced from (Morse et al., 1993)

In spite of the legislations that restrict the flow of phosphate into water bodies without treatment, still the contribution of human and household waste is very high. Excessive quantities of phosphorus are released into ponds, lakes and rivers from wastewater treatment plants WWTPs. Therefore, controlling the release of phosphorus from these sources must be taken seriously to protect the environment from damage.

2.2.3 Phosphorus structure in municipal wastewater

Phosphorus P in wastewater is categorized as either inorganic or organic phosphorus. Inorganic phosphorus includes relatively simple forms of phosphates such as orthophosphates. It consists of one phosphate ion and zero to three hydrogen ions, depending on the pH level. Condensed phosphates or polyphosphates, also categorized as inorganic phosphorus, are somewhat more complex chemical structures with more than one phosphorus atom linked together in each molecule. Most polyphosphates originate from detergents and other cleaning products and eventually decompose into orthophosphates. While organic phosphorus includes phosphorus incorporated into undigested food residue and dead and living bacteria that are present in faeces (NESC, 2013). Organic phosphorus represents the most common form of phosphorus in the environmental systems. However, by a bacterial action the organic phosphorus decomposes to orthophosphate. Total phosphorus represents both forms - the organic and inorganic. According to UNEP (2004) it is existing in wastewater at a concentration range 5 - 15 mg P/l. Inorganic phosphorus exists in wastewater 4 - 10 mg/l as an orthophosphate and Polyphosphate. On the other hand, the organic form of phosphorus exists 1 - 5 mg/l.

According to (Rybicki, 1997), numerous authors used to present a table set by Jenkins et al. (1971) to show a structure of phosphorus compounds in municipal wastewater.

Jenkins and Hermanowicz (1991) completed a revision of this table, which showed the influence of changes in phosphorus unit load on the structure of phosphorus compounds. An extraction of these tables is presented in figure 2.3. A comparison of data from 1971 and 1991 shows a decrease of total phosphorus content in raw wastewater. Most authors agree that orthophosphates are dominating other phosphorus compounds in municipal wastewater.

Phosphorus compound group	<i>Jenkins 1971</i>	<i>Jenkins & Hermanowicz 1991</i>
	ppm (mg P/L)	ppm (mg P/L)
Orthophosphates	5	3 - 4
Tripolyphosphates	3	2 - 3 (tripoly- and pyro- together)
Pyrophosphates	1	
Organic phosphates	<1	1
Total phosphorus	<10	<7

Figure 2.3. Phosphorus compound structure in domestic wastewater

Permission to use this figure has been granted by Elsevier

Phosphorus P is an extremely reactive element; it combines with oxygen easily to create the phosphate PO_4 . Therefore, in the natural environment the P does not exist as a free element. In accordance with the previously mentioned, the P in wastewater exists in various forms as a compound such as organic, phosphate, polyphosphates, and the dominant form orthophosphate (Crites and Tchobanoglous, 1998).

2.2.4 Continuous up flow Filter Principles of Operation

The general characteristics of the CoUF have been previously provided in the introduction along with reasons that make it a promising technology in wastewater

treatment. According to Schauer et al. (2006) Figure 2.4 shows the operating process in more detail.

The hydraulic head loss is relatively stable as a result of the continuous cleaning process for the filter bed. In addition, the continuous cleaning operation excludes system interruptions and keeps the quantity and quality of treatment at a constant rate. The required maintenance will be reduced and provides a good opportunity to minimise the plugging and short-circuit. On the other hand, a variety of wastewater treatments like biological, physical-chemical or a combination could be applied within the CoUF, which makes it suitable to treat various contaminants such as suspended solids, nutrients and metals.

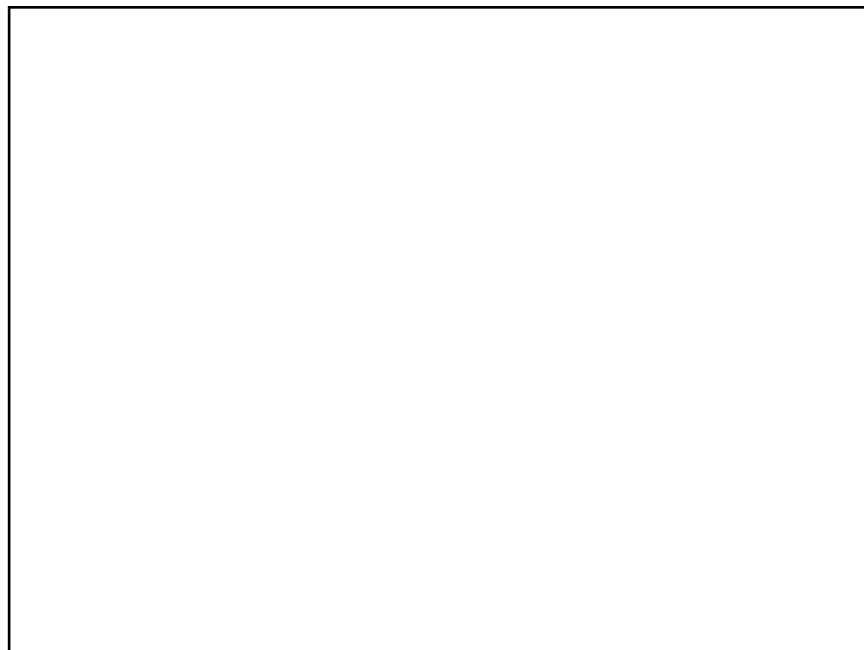


Figure 2.4. Schematic of CoUF (Schauer et al., 2006)

The diagram originally presented here cannot be made freely available via LJMU Digital Collections because of 'copyright'. The diagram was sourced from (Schauer et al., 2006)

Nomenclature:

- (A) Wastewater feeds into the system at the top of the filter and,
- (B) The wastewater continues to flows downward through an annular pipe between the wastewater feed pipe and (N) airlift housing.
- (C) The wastewater is introduced into the bottom of the filter bed through a number of distribution arms that are open at the bottom.
- (D) At the same time as the filter bed is moving downward, the influent flows upward (M) through it and
- (E) Clean effluent exits over the (J) filtrate weir and finally flows out through the effluent pipe.
- (F) The sand bed containing captured solid particles is drawn downward into the bottom of the filter where the airlift pipe is located. At the bottom of the airlift, a small portion of compressed air is supplied, leading the filter media to be dragged into the airlift pipe. At a specific intensity, the airlift pipe scours the sand; the scouring process removes any solid particles that have attached to the sand.
- (G) Airlift continues to push the solid media to the top of the pipe and
- (H) They fall into the reject compartment.
- (I) The sand falls from the reject compartment into the sand washer, driven by the water level difference between the reject weir and the filtrate pool. The denser, coarse solid particles fall into the wash chamber through counter current flow. The cleaned, recycled sand is redistributed on top of the sand bed where it

starts the cleaning process of the wastewater and its ultimate movement to the bottom of the filter over again; whereas the remaining impurities are sent to the reject compartment.

(J) The cleaned, polished effluent continues to move upward and departs from the filter at the top, over the filtrate weir.

(K) Lighter reject solids are carried over the reject weir and

(L) Carried out by the reject pipe.

It is a suitable technology to utilize in tertiary treatment because it is ideal to achieve the stringent discharge standards that are enacted by environmental bodies (World, 2016).

Despite all the positive features of CoUF that were mentioned previously the development of this technology still represent a challenge for the researchers in line with the requirements of protecting the receiving environment from the effluent.

2.2.5 History of continuous up flow filter development

According to (Mendoza and Stephenson, 1999), the combination process between solid removal and bioreactor was first described in 1964. Work continued in the late 1960s and early 1970s to enhance the filter capability by examining different materials to use as filter media. Specifically, in 1975 various filter media were investigated as a packed-bed such as anthracite coal, silica sand, and plastic media (Young et al., 1975). Mendoza and Stephenson (1999) pointed out that all these processes were focused on the removal of organic matter, ammonia and suspended solids S.S, without indication of the process of filter cleaning.

In Europe, in the late 1970s and early 1980s a sand filter was developed to merge the removal of solids with the bioreactor (Pujol et al., 1994). This process was introduced in the USA and followed by France and Canada in years 1978, 1979 and 1981 respectively; they are known as submerged aerated filters or packed bed reactors. This new system can remove contaminants like organic matter and nutrient; at the same time, the need for a further solid separation unit is avoided.

The reactors' hydrodynamic effect on the treatment process within the filtration system such as its impact on the physiological structure of biofilms (Wilderer et al., 1995) must be considered.

In recent years, there has been a tendency to use the up flow filters because they have been able to achieve a high level of pollutant removal at a high flow velocity in comparison with down flow filters, especially when treating wastewater with a high loading rate. It is supposed that the up flow system can handle a higher wastewater flow rate than the down flow system.

When the system is provided with concurrent air/wastewater flow, this will maximise the filter operation time by avoiding the formation of air pockets, and achieve more effective oxygenation (Iida and Teranishi, 1984).

Only in the late 1970s and early 1980s was the continuous up flow filter developed as a new filtration system in tertiary wastewater treatment (Loffill, 2011). During the 1980s, work continued on the development of the filtration system, especially for secondary and tertiary treatment in Europe, Japan and North America (P. and M., 1994). From the late 1980s and until the present time, filtration system development has continued with several systems being available. In Europe, at the present, many

full-scale systems are operating, and they are used for different removal processes (Rogalla et al., 1990).

2.2.6 Tertiary treatment

All over the world the standards of environmental protection became more rigorous; and one of the most important examples is the regulations that were introduced by the EU Water Framework Directive in 2000 (Ntifo, 2004). Hence, the secondary wastewater treatment became no longer enough to guarantee the effluent quality (Henry and Heinke, 1989). Advanced wastewater treatment is required for further control on the residual contaminant from SST; nowadays, tertiary treatment has become an essential stage in any wastewater treatment plants WWTPs. Various technologies have been introduced as tertiary treatment options such as chemical oxidation and precipitation, activated carbon adsorption, constructed wetland and membrane filtration with the aid of coagulants (Tchobanoglous et al., 2003). Decision makers and directors of wastewater considered the enforcement of tertiary treatments in WWTPs extremely important.

In general, approximately 1-2 mg/l of phosphorus can be removed by secondary treatment (Lenntech, 2016); this will lead to an excessive discharge of phosphorus in the final effluent. Therefore, to minimize the negative influence of the phosphorus load, several WWTPs implemented or upgraded the tertiary treatment for phosphorus removal in their schemes. Neethling et al. (2005) stated that advanced physical, chemical and biological processes have been utilized to decrease the total phosphorus to 0.2-0.3 mg/l; some processes capable of performing even better.

Tertiary treatment has a spectacular impact on the final quality of wastewater in terms of phosphorus removal but the cost represents a substantial obstacle in implementing these technologies. Hence, the application of design or upgrade of tertiary treatment systems is based on economic feasibility that achieves the harmony between the environmental and economic requirements.

2.3 Phosphorus removal processes:

Currently, several methods are utilized to remove phosphorus in the industry of wastewater treatment. In most methods, the removal process is performed by converting the ions of phosphorus into a solid fraction. Phosphorus as a solid fraction can be formed in various forms such as precipitate, as an insoluble salt or biomass in a constructed wetlands and activated sludge. The concept of these strategies does not include phosphorus recycling because it is removed with the waste directly. The non-solubilized Phosphorus is buried at landfills after burning of the organic matter; if the treatment units are capable of removing toxic components and human pathogens, the non-solubilized Phosphorus can be used as sludge fertilizer (de-Bashan and Bashan, 2004). As a response to the growing interest in the eutrophication issue in the 1950s the development of phosphorus removal technologies started to reduce the phosphorus concentration that was discharged into water bodies (Morse et al., 1998).

2.3.1 Physical Treatment

2.3.1.1 Filtration for particulate P

The filtration systems are typically applied to handling streams containing suspended solids; it is a solid-liquid separation process in which the liquid passes through a porous medium to remove as much fine suspended solids as possible. Suspended solid

in the fluid is removed by a variety of mechanisms. These mechanisms are: Straining, Sedimentation, Impaction, Interception, Adhesion, Adsorption, and Flocculation (Kocamemi, 2014).

Strom (2006) assuming that 2-3% of organic solids is phosphorus, so the removal of total suspended solid TSS by filtration process will help to reduce the phosphorus in the effluent.

Sand filtration or other TSS removal technics are probably indispensable for treatment facilities with low total phosphorus TP effluent (Reardon, 2006).

2.3.1.2 Membrane technologies

In general, the membrane technologies became a familiar method for wastewater treatment, moreover, for phosphorus removal in specific. Membranes are able to remove the phosphorus in the TSS and the dissolved phosphorus. Tertiary membrane filtration (after secondary treatment), and reverse osmosis RO systems have all been used in full-scale plants with good results. According to (Reardon, 2006) many wastewater treatment facilities have achieved <0.1 mg/l TP in their final effluent, and proposed that the tertiary membrane filtration technology and reverse osmosis RO could be efficient to reduce the phosphorus to 0.04 mg/l and 0.008 mg/l respectively.

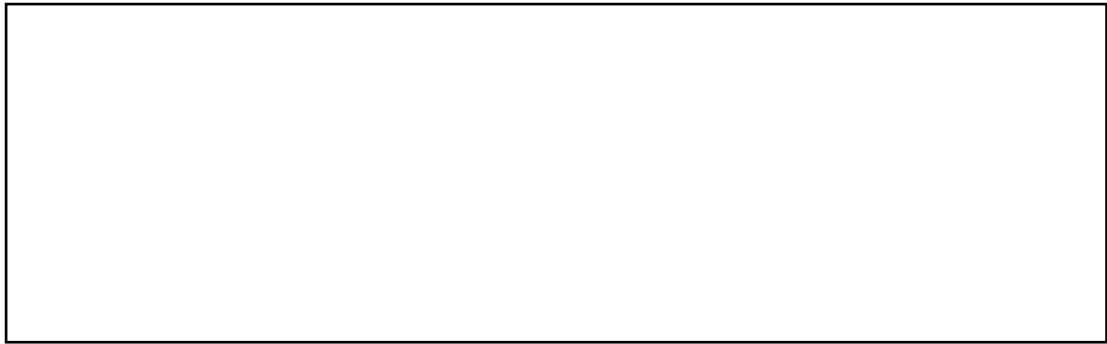


Figure 2.5. Schematic of membrane filter (MECO, 2016)

The diagram originally presented here cannot be made freely available via LJMU Digital Collections because of 'copyright'. The diagram was sourced from (MECO, 2016)

2.3.2 Chemical precipitation or Precipitation of phosphorus by metal salts

This method is characterized as a simple and firmly established technology in numerous countries. Chemical precipitation is in substance a physicochemical process, involving the addition of a divalent or trivalent metal salt to wastewater, producing a precipitate from an insoluble metal phosphate that is settled out by sedimentation. Commonly, the most appropriate metals are iron and aluminium; they are added as sulphates or chlorides. Lime also can be applied to precipitate calcium phosphate. Anionic polymers may be utilized to aid solids separation (Morse et al., 1998). Currently, most commercial processes for phosphorus removal from wastewater effluents are chemical precipitation (Donnert and Salecker, 1999b, Penetra et al., 1999).

The common phosphorus removal by chemical precipitation:

- 1- Calcium phosphorus precipitation: is the most distinguished technology for phosphorus removal; may be because of low cost and ease of handling. Removal process is accomplished by direct precipitation of calcium phosphate

(hydroxyapatite, $\text{Ca}_5(\text{PO}_4)_3\text{OH}$) (Yi and Lo, 2003), using calcite as seeding material (Donnert and Salecker, 1999b, 1999a).

2- Alum phosphorus precipitation: Aluminium hydroxide, $\text{Al}(\text{OH})_3$, is a robust adsorption agent for orthophosphate and condensed phosphate. It precipitates them almost instantly. It precipitates organic phosphate only at the low pH of 3.6. A theoretical analysis of $\text{Al}(\text{OH})_3$ and precipitation of AlPO_4 demonstrates that orthophosphate removal is not achieved via the precipitated AlPO_4 when applying conventional alum to the wastewater, but via precipitation of aluminium hydroxide phosphate. Laboratory tests of mixtures of alum sludge and wastewater indicated that phosphate is removed almost exclusively in the particulate fraction of the sludge. The removal of orthophosphate decreased with aging of the alum sludge (Galarnau and Gehr, 1997).

3- Iron–phosphorus precipitation is widely used for phosphorous removal. For example, an industrial by-product, blast furnace slag, has a very high phosphorus adsorption capacity (Sakadevan and Bavor, 1998). Iron-based, layered double hydroxides were synthesized. The compounds released metal cations (Mg, Ca, and Fe). The released cations and their hydroxides effectively serve as coagulants for phosphorus removal (Seida and Nakano, 2002).

Chemical precipitation is a very flexible approach to phosphorus removal and can be applied at several stages during wastewater treatment as shown in Figure 2.6

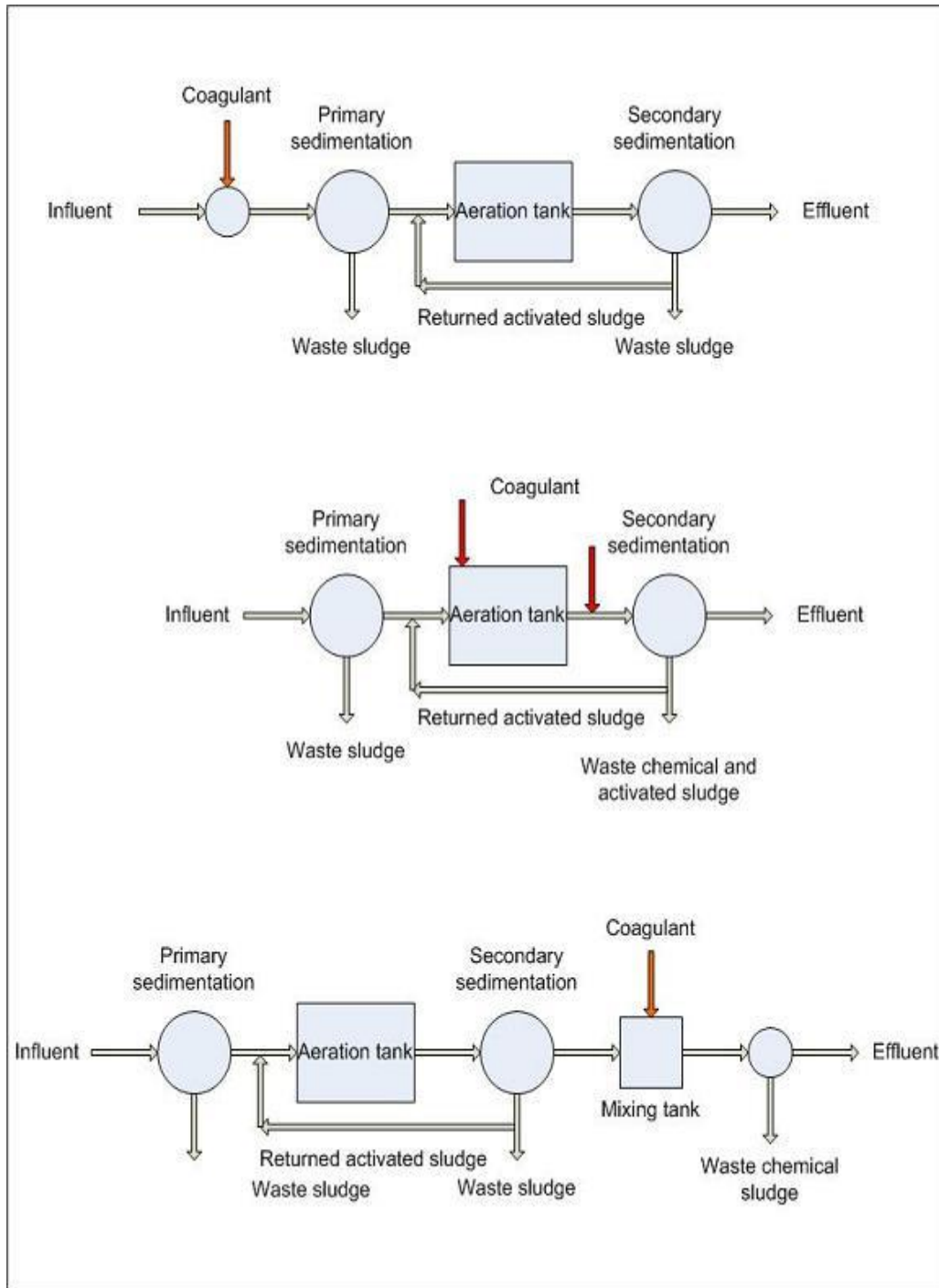


Figure 2.6. The main strategies for phosphate removal chemically in wastewater treatment plants (Lenntech, 2016)

Permission to use this figure has been granted by Lenntech

2.3.3 Biological phosphorus removal

Phosphorus removal biologically is a microbial treatment process; it is applied in wastewater treatment facilities to protect the water bodies from nutrients (Despland et al., 2014). The process is performed in wastewater treatment plants through absorption for the organic phosphate, polyphosphate and dissolved orthophosphate by the living microorganisms such as bacteria, protozoa, fungi, yeast, microalgae.

Marais (1983) determined the essential conditions to be achieved for phosphorus removal biologically based on a review of the biological phosphorus removal observations.

- anaerobic (i.e. oxygen and nitrate free) zone must be included;
- phosphorus uptake happens if phosphorus release had been obtained and oxygen and nitrate is present; a series of anaerobic-aerobic conditions is essential;
- to acquire phosphorus removal, it is required to provide a high amount of readily biodegradable carbon sources for the anaerobic zone,
- Bacteria cells are growing while passing through aerobic phase after the anaerobic zone.

The researchers assert that the effectiveness of phosphorus removal not only depend on the suitable microorganisms to be present but also specific conditions have to be considered. In comparison with chemical precipitation, the main good features for biological phosphorus removal are the low cost and less sludge production.

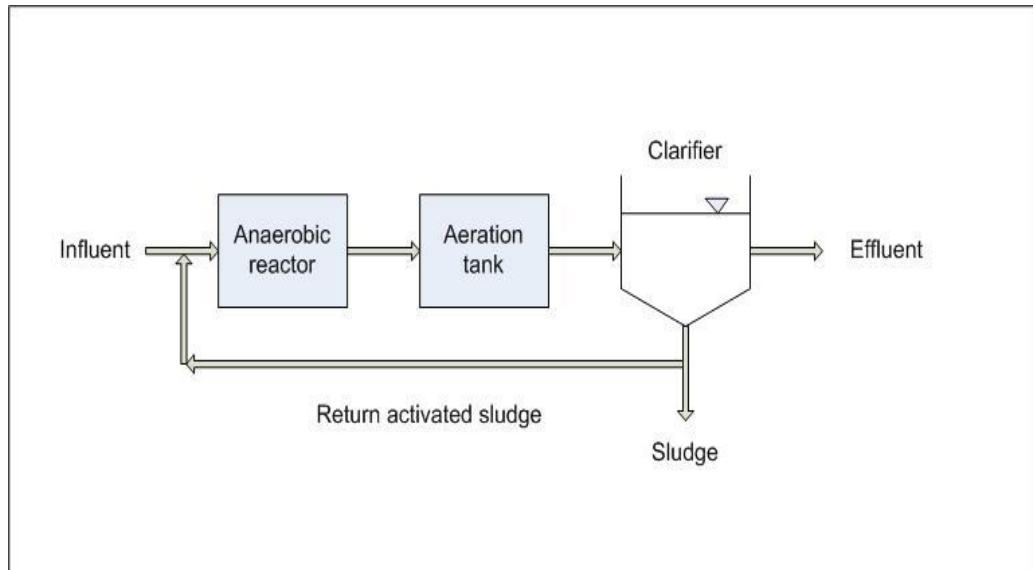


Figure 2.7. A basic biological phosphorus removal process (Lenntech, 2016)

Permission to use this figure has been granted by Lenntech

2.3.4 Constructed wetlands

In general, constructed wetland CW systems are utilized as a tertiary or polishing treatment to enhance the pollutants' removal physically, chemically and biologically (Kadlec and Wallace, 2009). 'It is a container (as small as a bucket or as big as a very large pond) planted with mainly aquatic, but sometimes with terrestrial plants. Inflow wastewater current slowly flows either horizontally or vertically from one end to the other end and, in the process, the outflow is cleaner' (de-Bashan and Bashan, 2004). Plant root zones and the substrate offer the reactive surface area for adsorption of complexing ions such as phosphates. The capacity of sorption depends on the contact time, initial concentration of ions, substrate binding capacity, biomass uptake capacity and effluent pH (Rhue and Harris, 1999, Akhurst et al., 2006, Kadlec and Wallace, 2009). Furthermore, the plant roots and substrate play a vital role in developing the microorganisms growing by acting as a biomass (Kadlec and Wallace, 2009, Madigan et al., 2012).



Figure 2.8. Schematic of constructed wetland, effluent flows horizontally through the bed (UNEP, 2016)

The diagram originally presented here cannot be made freely available via LJMU Digital Collections because of 'copyright'. The diagram was sourced from (UNEP, 2016)

2.3.5 Phosphorus sorbing materials PSMs

An attractive solution for treating municipal wastewater can be offered by applying the phosphorus sorbing materials PSMs in the WWTPs. (Klimeski et al., 2012). According to their origin, PSMs are often classified into three groups: natural material, industrial by-products and manufactured materials (Cucarella and Renman, 2009). A wide range of natural materials have been tested as PSMs, including apatite, bauxite, gravels, sand, clays, sub-soil, opoka, peat, shellsand, wollastonite, zeolites and tree bark. Furthermore, there are several Industrial by-products that have been tested for wastewater treatment such as fly ash, water treatment residuals, ochre, slag, blast furnace and mine residuals. Manufacture materials such as light-weight aggregates (LWA) or light expanded clay aggregates (LECA), Filtrate-P (LECA modified material), iron oxides and concrete have also been tested in both laboratory and field

studies (Johansson Westholm, 2006b, Cucarella and Renman, 2009, Klimeski et al., 2012).

PSMs can also be classified according to their chemical composition: metals, mainly Fe/Al-containing materials, materials containing soluble Ca and Mg or a mixture of the two (Klimeski et al., 2012).

The overall phosphorus removal capacity is strongly dependent on the sorption characteristic for the phosphorus-filter such as size and PSM type. Therefore, considerable attention must be given to the selection of a suitable PSM in order to ensure optimal phosphorus retention over the long term. It is also important to understand the underlying mechanism behind phosphorus sorption by PSM in order to choose the right one for treatment systems, as pointed out in a review by Klimeski et al. (2012).

2.3.5.1 Phosphate sorption to metal oxides

Adsorption describes sorption reactions taking place at the surface of particles. This can occur by electron donor and electron acceptor interaction, electrostatic attraction or covalent bonding. Phosphate adsorbs to Fe and Al oxides by surface complexation including covalent bonds and thereby forms strong complexes that are not readily susceptible to desorption (Lyngsie, 2013). This adsorption is site-specific: one or two hydroxyl groups of the metal oxide are exchanged with one or two of the oxygen atoms of the phosphate iron, resulting in a monodentate/mononuclear or bidentate/binuclear surface complex, as shown in Figure 2.9. The reaction is considered reversible although the release of absorbed phosphate may in practice be minimal (Klimeski et al., 2012). For adsorption on a solid surface, such as metal oxide, the maximum phosphate retention is achieved when all sorption sites become occupied.

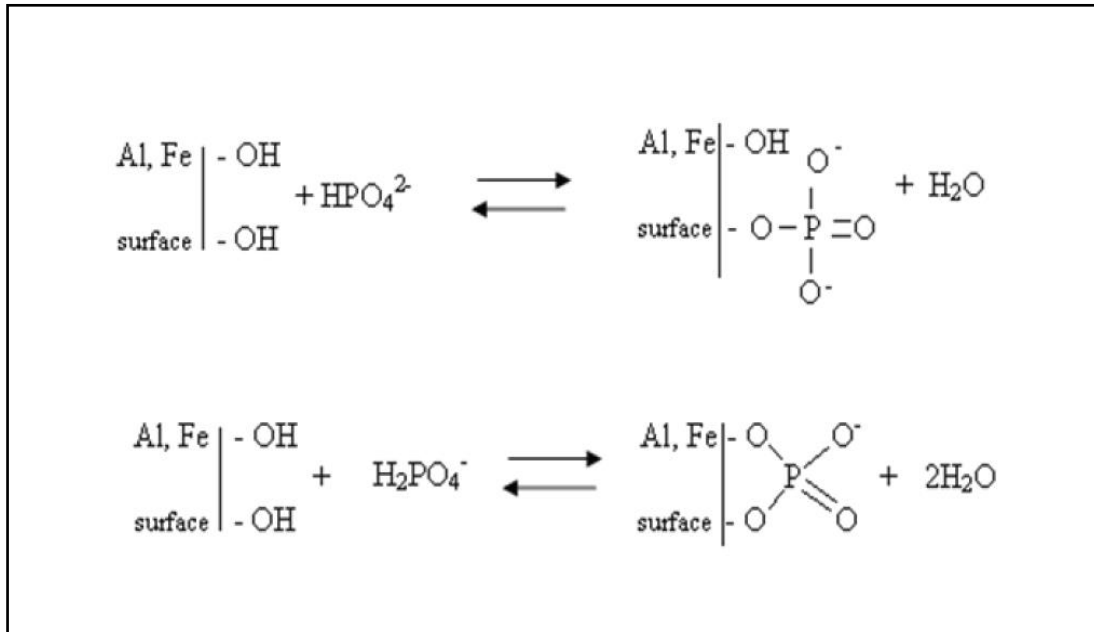


Figure 2.9. Ligand exchange reactions on metals oxide surface (Klimeski et al., 2012)

Permission to use this figure has been granted by the journal editorial office

2.3.5.2 Phosphate sorption to CaCO_3

Phosphate adsorbs to surfaces of CaCO_3 ; this is followed by precipitation of secondary Ca-phosphates. The product precipitating is highly dependent on pH, time of reaction and competitive ions present, both cat- and anions. Phosphate adsorption onto Ca is fairly rapid and completed within 2-3 h (Lyngsie, 2013). Precipitation of Ca-phosphates occurs in phosphate solutions when the solubility product of the mineral is exceeded. With high amounts of solution phosphate (e.g. when using high phosphate concentration) more Ca-phosphate can precipitate and, as the Ca concentration in solution decreases upon precipitation, more Ca will dissolve from CaCO_3 . This will remain ongoing as long as soluble Ca and phosphate are present in concentration exceeding the solubility product of the precipitate.

Precipitation of Ca phosphate can be divided into three phases: induction, rapid crystal growth and maturation in crystal growth (Lyngsie, 2013).

2.4 Factors' influence on the phosphate removal

In this part of the literature review, the factors that influence the removal of the phosphate by filtration process have defined. Many choices were based on these factors to develop the process of the phosphate removal.

2.4.1 Filter media

Physical and chemical forces between the particles of the media and suspended impurities are the key factor to obtain a clean suspension. The media particle size, effluent velocity and suspended particles size are factors which significantly influence these forces (Zamani and Maini, 2009).

Filter media characteristics and its implementation in wastewater facilities is one of the essential design parameters that play vital roles in improving the effluent quality. Many researchers emphasize the significance of the filter media implementation on the efficiency of effluent transfer within the filtration systems. They considered a low-cost method to treat wastewater in comparison with other treatment technologies. Several parameters are applied to study the hydraulic behaviour of effluent inside the filters. However, particle size distribution is one of the important parameters that indicate for the efficiency, reliability and durability of the system. (Rolland et al., 2009).

The filter media selection is a significant process in the filtration technology, in order to acquire the required effluent quality (Yu et al., 2008). Some authors (Valentis and Lesavre, 1989, Kent et al., 1996) have stated, “the media should be resistant to attrition, chemically stable, with high specific surface area and with a low apparent specific weight”.

The efficiency of pollutant removal is affected by the size of the granular media in terms of physical solids removal and available surface area (Smith and Marsh, 1995). The use of large media particles (greater than 6 mm) causes a drop in elimination of solids and nutrients because of the high void spaces and low available area (Stensel et al., 1988). On the other hand, using large media particles increases the required backwashing time, and this will reduce the cost of operating (Costa Reis and Santa’ Anna, 1985, Pujol et al., 1994). Using small media particles (less than 3 mm) leads to enhancing the efficiency of filtration treatment because a greater surface area is available for increasing the chance of contact between the effluent and the filter media particles. However, more repeated and forceful backwashing is required (Robinson et al., 1994). Consequently, it has been recommended that large media particles (greater than 6 mm) could be used for rough impurities, intermediate-size media particles (3-6 mm) for overall treatment and fine media particles (less than 3 mm) for effluent polishing and/or for tertiary treatment (Quickenden et al., 1992).

Sagberg and Berg (1996) mentioned that the shape of the media affects the performance of the filtration process. A comparison between irregular grains media and spherically shaped media revealed that the irregular grains improve the performance better than spherically shaped media, maybe because the size variation

of the void spaces or air bubbles passing through the filter media are broken up, but it probably has a negative effect on backwashing rates.

Roughness of the media is also another important factor that must be taken into consideration. Rough surface media offers more surface area for contact than smooth media.

Physical properties of filter media that include size, shape and porosity significantly affect their hydraulic conductivity and surface reactivity. Consequently, they influence the media's capability for phosphate sorption (Lyngsie, 2013). Filter media acts as a vital factor in phosphate sorption, oxygen substrate mass transfer and is an important influence on the hydraulic characteristics.

2.4.2 pH

Many studies evaluate the properties of metal adsorption and they demonstrated that the adsorption is affected by pH variation (Bennour, 2012). Al/Fe metal oxides are positively charged at low pH and negatively charged at high pH values. As phosphate is an anion, adsorption is greatest at low pH and decreases with increasing pH (Klimeski et al., 2012). At high pH, phosphate adsorbs to surfaces of CaCO_3 ; precipitation of Ca-phosphate is efficient at alkaline pH. Several researchers have studied the influence of pH on phosphate sorption, the findings are tabulated in table 2.1.

Table 2.1. pH Influence on Phosphate Removal

Media type	pH	Phosphate removal	Reference
Nanoscale zerovalent iron	3 to 12	35 -98 mg p/g	(Wen et al., 2014)
high-surface-area Fe/Mn-hydroxide sorbent	4 to 9	25% to 99%	(ZENGE et al., 2008)
Sand	7.70 to 9.57	16.5% to 26.2%	(Del Bubba et al., 2003)
Iron-oxide-coated sand (IOCS-1)	2.4 to 9.5	0.24 to 0.18	(Jianbo et al., 2009)
Iron-oxide-coated sand (IOCS-2)	2.4 to 9.5	0.019 to 0.012	(Wen et al., 2014)

Recent work by Szabo et al. (2008) showed that there is an optimum pH for phosphorus removal, but that the optimum is relatively wide – ranging from pH 5 to pH 7 – with deterioration outside this pH range. At acidic pH, soluble phosphate complexes form and, at higher pH, some soluble iron-hydroxide complexes start to form with a resulting decrease in the phosphorus removal efficiency.

2.4.3 Operational conditions

The variation in the operation process plays a crucial role in the filter performance. Flow characteristics in filtration systems are influenced by the air and liquid input, along with the media (Le Clorec and Martin, 1984).

At the same time, the hydrodynamic characteristics have an effect on the phosphate adsorption. For instance, the contact time between wastewaters and filter media that acts as phosphate adsorbent is highly important to determining the removal efficiency.

2.4.4 Residence time distribution

Residence time distribution RTD is a method that is implemented in continuous flow systems to gain information about the flow behaviour and the mean residence time for particles' transfer. Moreover, RTD is applied to develop the design of the existing treatment facilities and optimize the design of the new treatment systems (Pant et al., 2015). The RTD is represented by the material exit age. A specific amount of tracer is injected into the entering filter stream. Afterward the concentration of the out tracer is measured as a function of time.

2.4.4.1 RTD measurement

The effluent concentration–time curve is represented by the C curve in the RTD analysis. The normalised RTD function, E(t), is obtained by dividing each data point by the area under the tracer concentration curve (Levenspiel, 1972). The function E(t) has the units of time as equation 2.1:

$$E(t) = \frac{c(t)}{\int_0^{\infty} c(t)dt} \quad \text{Equation 2.1}$$

The F curve is another function, which has been defined as the normalised response to a particular input. The concentration of tracer at the outlet is measured and normalised to obtain the non-dimensional cumulative distribution curve F (t), which goes from 0 to 1, as equation 2.2:

$$F(t) = \frac{c(t)}{c_0} \quad \text{Equation 2.2}$$

It is very common to compare RTDs by using their moments instead of trying to compare their entire distributions. The first is the mean residence time MRT; from the

measured RTD curve, the mean residence time of the reactor was determined. The mean residence time is calculated as in equation 2.3:

$$MRT = \int_0^{\infty} t E(t) dt \quad \text{Equation 2.3}$$

Levenspiel (1999) states that the mean residence time is represented by the time t at which 50% of the total integral value recorded has passed. De Souza Jr. and Lorenz (2014) show that the theoretical mean residence time MRT of influent with fixed volume reactor, V , operating with a steady flow rate Q , is given by:

$$MRT = \frac{V}{Q} \quad \text{Equation 2.4}$$

The second moment is taken about the mean time and is called the variance, or square of the standard deviation. It is defined by:

$$\sigma^2 = \int_0^{\infty} (t - tm)^2 E(t) dt \quad \text{Equation 2.5}$$

The magnitude of this moment is an indication of the spread of the distribution; the greater value of this moment the better the distribution's spread will be.

2.4.4.2 Tracer selection

A tracer can be any material used to investigate the physical movement of fluids over the environmental systems; it could be either pathways of surface water or those in the subsurface. Tracers are moved via the same physical pathways and at the same rate as the particles' flow in the fluid paths. The tracers are categorized as inert or conservative species. Tracers can be selected according to their feasibility to assist us to realize the chemical characteristics of a substance in stream paths. 'A specific tracer can be chosen based upon the parameters an investigation aims to study. There is no

‘ideal’ tracer, and therefore choice of tracer will depend upon the ultimate objectives of a tracer test’ (Ward et al., 1998). The types of the tracer can be classified according to their nature and source, such as environmental tracers, they are substances coming from a particular environment and their features allow using them as tracers. They are categorized into two subclasses: natural environmental tracers and anthropogenic environmental tracers. Both natural and anthropogenic environmental tracers are exploited in a same way. Natural environmental tracers result from naturally occurring processes. An example is the use of radon-222 (Ellins et al., 1990, Ellins et al., 1991, Cecil and Green, 2000). The second tracer type is the artificial tracers; they are intentionally discharged into nature during the study of tracers. ‘These may be conservative, to track the movement of surface or subsurface waters, or non-conservative, to study the effects of and potential for sorption, biodegradation and storage within a stream or aquifer system’ (Berryman, 2007). Various substances are available to be selected as artificial tracers, and the selection of an appropriate tracer must be depending on the specific data required from an investigation. An optimum tracer should have the following characteristics: chemically inert, soluble in the mixture and easily detectable (De Souza Jr. and Lorenz, 2014).

2.4.4.3 Injection methods

There are two methods of injecting the tracer: pulse input and step input (Levenspiel, 1999, De Souza Jr. and Lorenz, 2014) as illustrated in Figure 2.10. In the pulse input method, the tracer amount is rapidly injected in a single shot into the path of the fluids that flow into the reactor. The exit concentration is then identified as a function of time. In the RTD analysis, the derived effluent concentration–time curve is indicated to as the C curve.



Figure 2.10. Methods of tracer injection through the reactors

The diagram originally presented here cannot be made freely available via LJMU Digital Collections because of 'copyright'. The diagram was sourced from (Levenspiel, 1999, De Souza Jr. and Lorenz, 2014)

The tracer material across system boundaries can be analysed according to the injection method. For the pulse injection, we chose an increment of time Δt that was sufficiently smaller than the concentration of the tracer, $C(t)$, exiting between time t and Δt was essentially the same. Then the quantity of tracer material, ΔN , leaving the reactor between time t and $t + \Delta t$ was stated as follows:

$$\Delta N = C(t) v \Delta t \quad \text{Equation 2.6}$$

Where v is representing the effluent volumetric flow rate. ΔN is the quantity of substance spent between t and $t + \Delta t$ in the reactor.

2.4.5 Isothermal adsorption models

The equilibrium isotherm utilization is a very significant tool for interpreting the adsorption process in any system. Adsorption isotherm represents the magnitude of a solute that is adsorbed at constant temperature and its concentration in the equilibrium

solution. In addition, the applicability of the adsorption process as a complete operation is assessed through physicochemical data that is provided by the adsorption isotherm model (Yousef et al., 2011). Several isotherm models are obtainable for analysing the data of experimental adsorption equilibrium. In this work, the sorption isotherms determined experimentally were evaluated using the Langmuir model and the Freundlich model, which are widely used to describe P retention isotherms for natural materials. The obtained data of the phosphate equilibrium concentration were fitted to the Langmuir and Freundlich isotherm models, as per the following isotherm equations:

The Langmuir equation:

$$q_e = (Q K C_e)/(1+K C_e) \quad \text{Equation 2.7}$$

Where q_e is the mass adsorbed per mass unit of adsorbent (mg/g), C_e is the equilibrium concentration of adsorbed material (mg/l), Q is the maximum mass adsorbed at saturation conditions per mass unit of adsorbent (mg/g), and K is the empirical constant with unit (1/mg) (de-Bashan and Bashan, 2004).

The Langmuir equation in linear form:

$$1/q_e = 1/Q + 1/(K.Q) \cdot 1/C_e \quad \text{Equation 2.8}$$

The constants K and Q relate to the energy of adsorption and maximum adsorption capacity.

The Freundlich equation:

$$q_e = K_f C_e^{1/n} \quad \text{Equation 2.9}$$

Where q_e is the mass of adsorbed per mass unit of adsorbent (mg/g), C_e is the equilibrium concentration of adsorbed (mg/l), and K_f and n are Freundlich constants, which correspond to adsorption capacity and adsorption intensity, respectively.

The equation can be linearized as below:

$$\log(q_e) = \log[K_f] + \log[1/n C_e] \quad \text{Equation 2.10}$$

2.5 Filter media coating technologies

2.5.1 Overview of literature relevant to coating technologies

Commonly, conventional method for eliminating the metals and metal ions from the wastewater is precipitation of the metals such as hydroxides, oxides, and carbonates. Next step is separating the captured metals by settling, via coagulant aid such as iron hydroxide. This technology has some practical limitations; the limitations could be:

- If the metals are present in complex formula, the precipitation could be ineffective.
- Solubility product limits the lowest accomplishable concentration for metal.
- In some cases, the metals precipitate as small particles; this lead to difficulties in the process of settling them.
- The collection of metals needs large settling basins. Often, sludge thickening process follows the settling operation to concentrate the solids, or by granular media filtering to eliminate the residual particulates from the clarifier overflow.

- Polymeric coagulants and filter acids are frequently required for solids separation to be effective.

Recently, considerable attention has been paid to adsorption as a phosphate removal method. In comparison with other removal methods, adsorption is substantially efficient, has low sludge production, is economical and has the possibility of phosphorus removal at low concentration. (Benjamin et al., 1996) 'Adsorption is the binding of a chemical species at a phase boundary', such as the surface of suspended particles. According to this approach, several researchers have applied a new method in removing the metals and metal ions to avoid the above difficulties of employing metal oxides as powder in treating the wastewater. This method involves coating the metal oxides onto sand surface.

As shown below, some researchers have implemented the media coating technology in different manners according to their own targets. The main goal is to examine the developed media as adsorbent for dissolved metals and as a medium for filtration of particulate metals.

2.5.1.1 MARK M. BENJAMIN, RONALD S. SLETTEN, ROBERT P.

BAILEY and THOMAS BENNETT (1996)

In this work the removal of different metals was investigated by utilizing ordinary filter sand coated by iron oxides. Iron-oxide-coated sand IOCS is the name of the composite media in this research. It was applied as a fixed bed filter for sorption of dissolved metals and filtration of particulate matter simultaneously. Synthetic and actual wastewater with different metal concentrations were examined in this process. The removal of uncomplexed and ammonia-complexed cationic metals (Cu, Cd, Pb,

Ni, Zn), as well as some oxyanion metals (SeO_3 , As O_2) was accomplished successfully.

The media coating process involves two different forms of IOCS. Both forms of IOCS were coated in two stages.

The first stage included

- A solution of 2.5 M FeCl_3 with volume 80 ml was poured on 200 ml of bulk sand (sieved with mesh 20 - 30). Then,
- The mixture heated at 110°C and stirred for 3 hours. This is the time that the mixture looks dry. Then,
- The mixture exposed to temperature 550°C for 3 hours. Finally,
- The sand was cooled to the room temperature naturally in air. The coating looked quite dark at this stage.

The second stage included

- A bulk of hot temperature mixtures with volume of 40 ml was placed in a heat resistant dish, it was mixed with a solution of 80 ml of 2.1 M $\text{Fe}(\text{NO}_3)$ and 0.6 ml of 10 M NaOH for IOCS1 or 80 ml of 2.5 M Fe Cl_3 for IOCS2. Then,
- The mixtures were covered and heated at 110°C for a time from 10 to 14 hours, until they looked to be dry. Then,
- After cooling, the crust that had formed around the grains was broken mechanically, and the sand was sieved.
- The IOCS1 was heated at 110°C for 3 hours again to guarantee that all grains were dry. When IOCS2 was cooled, the coating became quite moist.

**2.5.1.2 Lu Jianbo, Sun Liping, Zhao Xinhua, Lu Bin, Li Yinlei and Zhang Lei
(2009)**

The iron-oxide-coated sand IOCS was assessed for removal of different metals as mentioned in previous work. However, in this research, IOCS was utilized as filter media to evaluate its capability for phosphate removal from aqueous solutions. The work was performed in batch experiments. In this study, IOCS were prepared by two different coating methods in order to obtain IOCS as efficient filter media for phosphate removal. In general, both coating methods have the same procedure as illustrated in the paper of Benjamin et al. (1996). However, there are a number of differences existing between both works. These differences are related to the amount of chemicals that are applied in the coating process as well as the temperature and time of heating. These differences could have a positive influence on the strength of substance coating. The coating process for both methods is illustrated below:

IOCS-1: A mixture of solution which consists of 400 mL of 2.5 M Fe (III) and 1 mL of 10 M NaOH was poured on 800 g of dried sand placed in a heat-resistant dish. After gentle agitation, the mixture was heated for 96 h at 110 °C and then at 200 °C until it appeared to be dry. After cooling, the coated sand was washed with tap water until run-off was clear. Then the coated sand was dried at 110 °C. After the above coating process was completed, the sand was coated again according to the same process, and stored in polystyrene bottles for further use. This kind of coated sand was called IOCS-1.

IOCS-2: 800 g of dried sand was placed in a heat-resistant dish, after soaking in a solution of 400 mL of 2.5 M Fe (III). Then gentle agitation was applied, the mixture was heated at 110 °C for period reach to 96 h then the heating temperature was raised

to 550 °C until the mixture appeared to be dry. Afterwards, the coated sand was left to cool down, and then it was washed with tap water until run-off was clear. Again, the coated sand was dried at 110 °C. After the above coating process was completed, the sand was coated again according to the same process, and stored in polystyrene bottles for further use. This sort of coated sand was called IOCS-2.

2.5.1.3 Li, S., cui, J., Zhang, Q., FU, j., Lian, J. and Li, C. (2010)

As mentioned in the filter media part, the physical properties for the filter media such as size, surface area and porosity play a vital role in the process of contaminant transportation over the treatment systems. Therefore, some researchers focused on development of the physical characteristics of filter media depending on the media coating processes.

Li et al. (2010) used the blast furnace dust BFD as a major substance and clay and sodium silicate were used as additives and mixed together to create a new type of filter media. The researcher used the new media, blast furnace dust clay sodium silicate ceramic particles BCSCP and commercial ceramic particles to treat brewery wastewater in two lab-scale up-flow biological aerated filters BAF to compare and examine their capabilities to work as supporters for biofilm. Especially, to investigate their efficiencies for removal of COD and NH₃-N. BFD is generated from the process of the iron making as a by-product of blast furnace gases. The composition of BFD is illustrated in figure 2.10.

In this study, the factors which were considered in the mixing process for BCSCP preparation were BFD dosage, ratio of clay added, ratio of sodium silicate added, and calcination temperature.

Variable	Level			
	1	2	3	4
BFD dosage (g)	100	150	200	250
Ratio of clay added (%)	5	10	15	20
Ratio of sodium silicate added (%)	4	6	8	10
Calcination temperature (°C)	500	600	700	800

Figure 2.11. The experimental conditions for the preparation of BCSCP

Permission to use this figure has been granted by Elsevier

The researcher applied the additives ration depending on the BFD dosage to investigate the effect of all factors on the properties of BCSCP. Before BCSCP preparation, the large particles and debris of the BFD were removed through the washing it, then they left to dry naturally. Afterward, the BCSCP were prepared as follows: Muller was used to mix the raw materials and then the mixture was transferred into a rotational disk. Water was injected to conglutinate the powdered materials into particles with similar diameter. Then, after the semi-manufactured BCSCP were desiccated, they were diverted to a rotary kiln fired at 600 °C to produce the final product. The optimal preparation conditions of BCSCP were 150 g blast furnace dust, 15% clay and 6% sodium silicate, calcined at 600 °C.

2.5.2 Coating material

Various sorts of low-cost materials have been investigated to act as sorbents for phosphate. Waste materials offer an attractive solution for nutrients treatment by utilizing them as a filter media (Osorio and Hontoria, 2002, Yu et al., 2008). According to Hjelm et al. (2010) bottom ash is considered as one of the most frequently dumped solid residues, thus, bottom ash is available as a free material. Furnace bottom ash FBA is the waste material that was utilized in this experimental work to investigate its

capability for phosphate removal. FBA consist of oxides that tend to retain the PO_4 such as Al_2O_3 and Fe_2O_3 . These oxides are chemically active because the original material (coal) is exposed to high temperature for power generation. According to Chandler et al. (1997), the bottom ashes have a surface area ranging from 3 to 46 m^2/g as measured in several studies by using Brunauer–Emmett–Teller (BET) absorption isotherms.

Coal ash is not a simple chemical compound. It is produced as a consequence of coal burning, especially, in the power generation plants. After burning, a portion of it is caught in the chimneys; this portion is referred to as fly ash. Another portion, which is the non-combustible inorganic residue, is recovered from the bottom grates of the furnaces and is referred to as bottom ash (Kirk et al., 2003). FBA is a coarse ash predominantly consisting of oxides of iron, aluminium, and silica. Plenty of bottom ashes are produced as waste from thermal power treatment. Nowadays, bottom ash is one of the most frequently dumped solid residues (Hjelmar et al., 2010). According to Kirk et al. (2003) bottom ash is generally available for free and is categorized as a waste material. Recently, efforts have been made to reuse bottom ash for construction purposes as a secondary material because its properties are similar to those of the natural aggregates being utilized in construction applications (Di Gianfilippo et al., 2015). A part of the FBA is used as a lightweight aggregate in road construction, products for the construction industry and cement industries, but the majority of the FBAs are disposed in landfills.

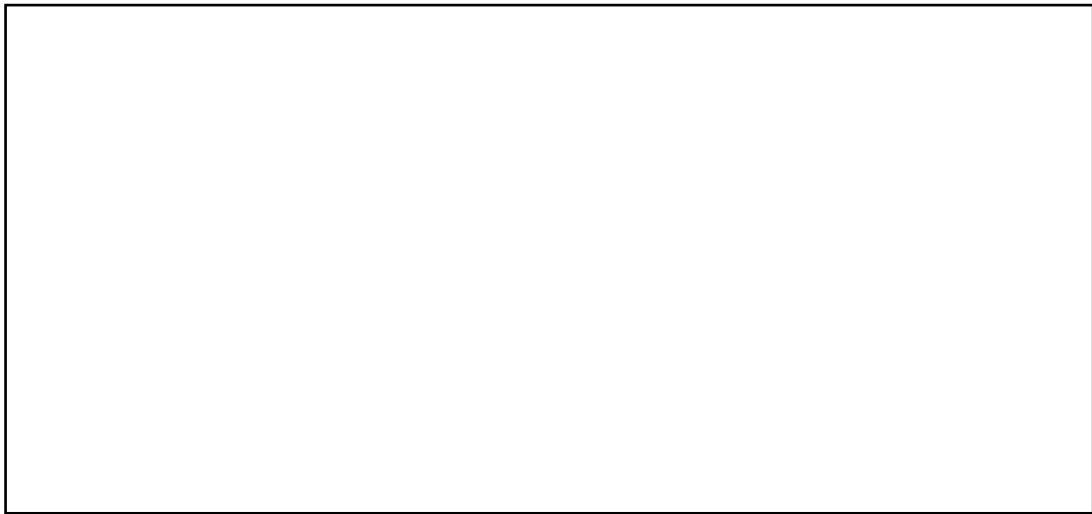


Figure 2.12. Schematic layout of a coal-fired electrical generating station illustrate the production of bottom and fly ash

The diagram originally presented here cannot be made freely available via LJMU Digital Collections because of 'copyright'. The diagram was sourced from (Sear, 2001)

The FBA sample was collected from the Fiddlers Ferry Power Station. It is a coal-fired power station situated in the North-West England between the towns of Widnes and Warrington on the north bank of the River Mersey. The power station imports coal from the Liverpool docks and other ports. Each day, approximately 16,000 tons of coal are burned for power production (Hydro, 2006). So, a large quantity of bottom and fly ash are generated as waste.

2.6 Chapter summary

There is an international and continental tendency to enact legislation that protect the water bodies from the eutrophication phenomenon. Therefore, there is an urgent need to develop the treatment process with regard to phosphorus removal, as a result of the high proportion of phosphorus released from WWTP.

Orthophosphate is the predominant form of phosphorus in wastewater. Recently, several methods are developing for phosphorus removal from wastewater such as physical, chemical and biological treatment. However, many researchers are still searching for the development of these methods or find alternative methods that achieve harmony with environmental and economic requirements. The possibility of applying various treatment types such as biological, physical-chemical or a combination, which makes CoUF as a promising technology in wastewater treatments.

Application of phosphorus sorbing materials PSM offer an attractive solution for treating municipal wastewater. Understanding the contaminants' behaviour and their removal mechanism is providing a supportive and flexible start point towards improving the filtration system performance. The chemical composition of filter media is the key factor of phosphate removal chemically. PSMs can be classified according to their chemical composition; metals, mainly Fe/Al-containing materials, materials containing soluble (Ca and Mg).

Physical properties of filter media particles that include size, shape and porosity have a significant influence on the phosphate sorption and an important influence on the hydraulic characteristics. pH, dissolved oxygen, temperature and operational condition; all these factors should be taken into account because they have a significant effect on the nutrient removal process.

CHAPTER 3 RESEARCH METHODOLOGY

3.1 Chapter introduction

This research is concentrated on characterisation and optimisation the aspects of the continuous upflow filter that improve the efficiency of phosphate removal. In filtration systems the filter media plays the essential role in the treatment process. Consequently, finding a suitable material to act as a phosphate absorber is the priority of this study. A plan was set up to create the structure of the work which achieves the research goal. This chapter is focused on describing the major parts of the research work plan, including the laboratory work and analysis tools that work together to address the central research target.

The research method will be conducted through a sequence of stages as below:

Stage one: An extensive literature review will be administered by collecting the necessary information about the materials that act as filter media, according to their physical and chemical characteristics, availability and cost, to determine the research candidate materials. In addition, the literature review will help to establish the research structure and understand the knowledge gap that needs to be addressed by the research.

Stage two: The selected materials will be subjected to a series of tests to investigate their eligibility to act as phosphate sorption material. As mentioned in the literature review chapter the physical and chemical characteristics of filter media is the key factor that retains the phosphate from the influent. Therefore, properties such as bulk density, specific gravity, porosity, permeability and particles' effective size were studied to identify the materials' physical characteristics, and scanning electron microscopy SEM was performed to give a better understanding of the nature of the

materials' surface. The chemical composition was investigated according to the X-ray fluorescence analyser XRF.

Stage three: This part of the research methodology is directly dependent on the research aim. Specifically, how to set the work steps to introduce the research procedures. The most expected outcome from this stage is obtaining data, which is based on the study aim. This stage included preparing a risk assessment for any part of work which has potential risk, preparing a sampling plan, conducting batch experiments to investigate the materials capability for sorbing and retaining phosphate, constructing a bench scale rig to simulate the filtration process of up flow filter, performing a residence time distribution RTD study to characterize the hydrodynamic aspects of the filtration system, establishing a new coating method for filter media harmonized with the sustainability approach, and investigating the possibility of regeneration the capability of the filter media to retain the phosphate after saturation.

Stage four: The data obtained from the experimental work require analysis tools suitable to the research domain. For example, isothermal adsorption models such as Langmiur and Freundlich model will be applied to interpreting the adsorption mechanism of the material which is utilized in this present study. All data will be analysed mathematically or statistically to reach a conclusion to the research problem.

Stage five: in this final stage, the research findings will be addressed to understand the effectiveness of the research design in problem solution. In addition, it will provide the possible recommendations that allow the researchers to enhance and improve the upflow filtration systems regarding phosphate removal further and further.

A flow chart summarising the research methodology is shown in Figure 3.1.

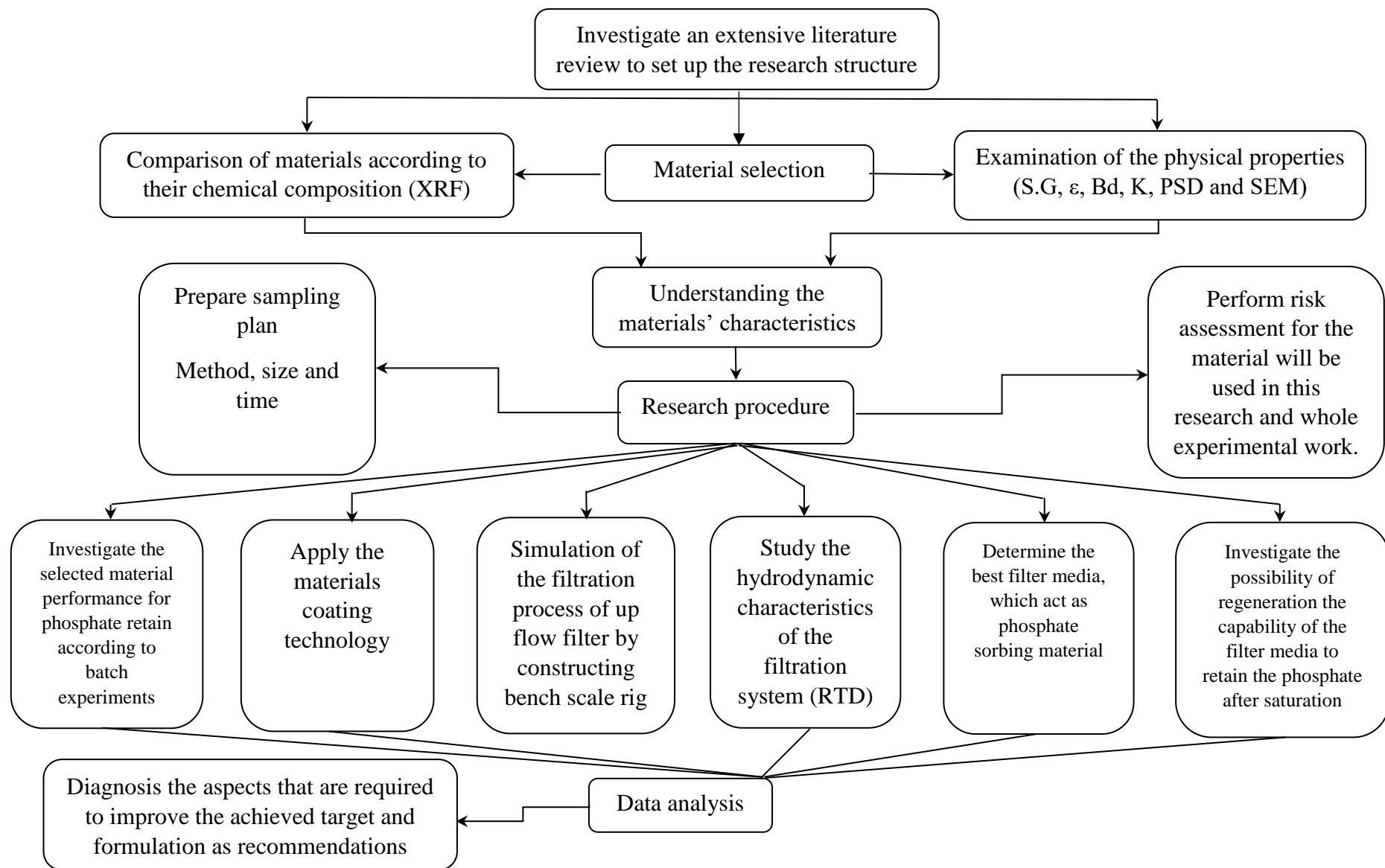


Figure 3.1. Research methodology flow chart

3.2 Material selection

Selection of filter media type is the core of any filtration system. Commonly, in most studies choosing of filter media is based on arbitrary decisions, tradition, or a standard approach. Therefore, the new studies should establish an alternative method to determine the most effective and efficient media (Kawamura, 2000).

Different factors must be considered in the process of material selection. The basic factor is the material's properties; as mentioned previously in the literature review chapter the materials which are expected to retain the phosphate are the materials that basically contain Fe/Al and/or soluble (Ca and Mg). Physical properties of filter media that include size, shape and porosity significantly affect their hydraulic conductivity and surface reactivity. Consequently, they influence the media's capability for phosphate sorption (Lyngsie, 2013). The new challenge for the researchers and industry managers is how to obtain a material which is consistent with a sustainable approach. Consequently, material cost and availability have a direct influence on the process of materials choosing. This present study focuses on the low cost material such as natural material or by-product waste material, to achieve the economic and environmental requirements. Figure 3.2 shows the priority of factors to set up the material selection process.

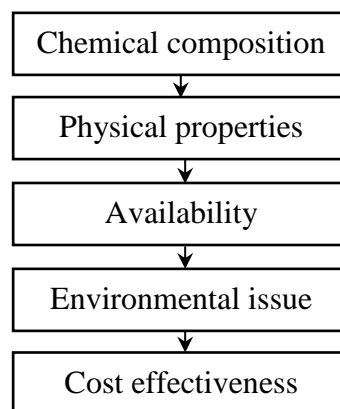


Figure 3.2. Material selection priorities

The material that were subjected to examination of their capability of phosphate sorption are Limestone, Dolomite, Furnace bottom ash FBA and Biomass bottom ash BBA, all these materials available in UK. The limestone is supplied from Omya UK Ltd and the source is the Dowlow quarry, UK; while the dolomite tested was white dolomite, supplied by Specialist Aggregates Ltd, UK. Furnace and biomass bottom ashes were obtained from Warrington power station in North West England.

Although, some materials contain oxides of Fe/Al and soluble oxide of Ca/Mg such as fly ash and ground granulated blast furnace slag GGBS. However, they were discarded from the study because they contain a portion of heavy metals in their chemical composition, which may represent a danger in the quality of treated effluent.

3.3 Investigate the characteristics of research candidate materials

The selection of filter media has been set as the one of the major research aims because it acts as a vital factor in the contaminant removal process. The candidate materials (Limestone, Dolomite, FBA and BBA) will be subjected to a series of experiments to investigate the suitability of their characteristics to the removal process. Based on the research target the below tests will be the major tools to identify the materials' characteristics.

Physical characteristics

- Particle size distribution (PSD)
- Specific gravity S.G
- Porosity (ϵ)
- Bulk density

- Hydraulic conductivity (K)
- Scanning electron microscopy (SEM)

Chemical characteristics

- X-ray fluorescence analyser (XRF)

Hydrodynamic characteristics

- Residence time distribution (RTD)

In this part of research methodology, the data collection instruments will be explained according to their method of working. How to conduct the experiment, sampling and obtaining the results?

3.3.1 Particle size distribution PSD

Particle size distribution is a significant factor in the solid liquid separation process particularly in granular bed filtration (Ben Aim et al., 1997). Moreover, particle size distribution allows better understanding of filter performance and more accurate simulations of filtration models (Kaminski et al., 1997). The particle size distribution is obtained by sieve analysis as shown in figure 3.3.



Figure 3.3. Sieve analysis

A known amount of the sample will be added to a series of different-sized sieves at the top, and then the sieves will be shaken in a vibrator; the sample is segregated onto the different-sized sieves according to the particles' diameter. The weight of the remaining sample in each sieve is measured to determine the particle size distribution. The taken sample size is (200 g) and the sieves arranged from the top to the bottom (3.55, 2.00, 1.18 and 0.60 mm).

Different measurement techniques were applied to measure the particle size of filter media but the sieve analysis is still the simplest, cheapest and easiest of data interpretation methods. In addition, this technique is well-adapted for bulk materials.

3.3.2 Coefficient of permeability K

Permeability is a property of the materials that describes the ease with which a fluid can move through pore spaces or fractures. The K value is highly dependent on the media's intrinsic permeability, this gives a good indication about the contact behaviour between the influent and the filter media. The collected data from the laboratory experiment to find K will be applied in the equation below to find the K Value:

$$K = (Q I) / (t A h) \quad (\text{mm/s})$$

Equation 3.1

Where

Q = quantity of fluid collected (mm³)

I = distance between piezometer tapping (mm)

t = fluid collected time (s)

A = area of sample (mm²)

h = head loss (mm)

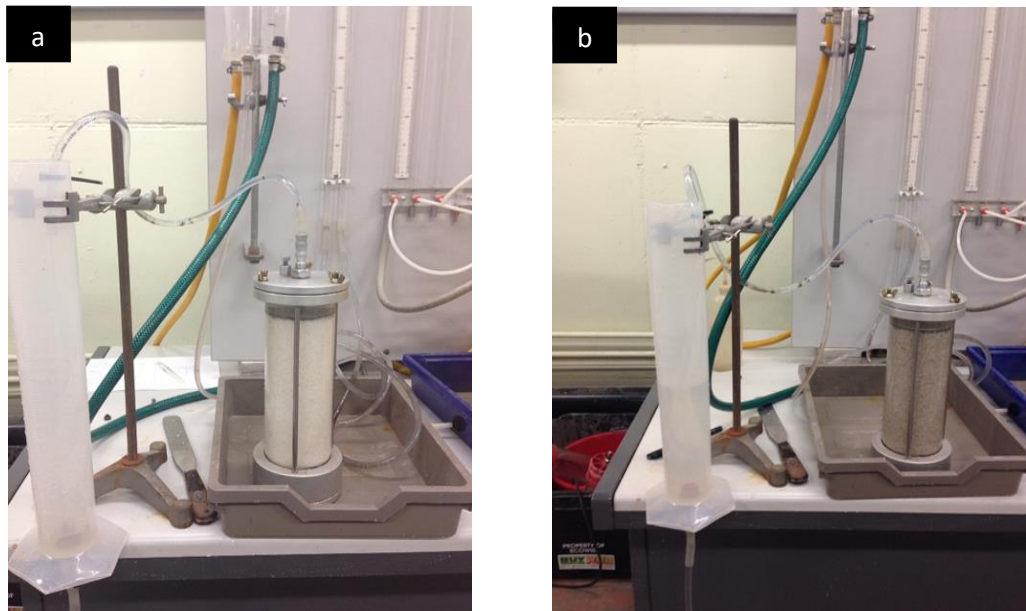


Figure 3.4. Hydraulic conductivity measurement (a) Dolomite (b) Limestone

The constant head permeameter is the test which was accomplished in order to determine the K value. The water is running through the system at a constant flow rate as shown in figure 3.4. A 500 mL of water is collected in a graduated cylinder from the outflow nozzle. The time required to collect the 500 mL of water was recorded in the experiment data sheet as shown in Appendix A. meanwhile the distance between manometer A and B was measured to determine the head loss (h), this value was also

recorded in the experiment data sheet. The experiment was run four times in total for each material to calculate K value. Hence, the average value for the four experiments was used to represent the final K value. The values of parameters such as Q, I and A were constant along the experiments performed, they are 500 ml, 100 mm and 4303 mm², respectively as shown in experiments data sheet in Appendix A.

3.3.3 Specific gravity S.G

The media in upflow filter is cleaned by a simple internal washing system, continuously. Thus, the dynamic movement of the media requires careful attention to the specific gravity of the selected materials. Filter media has a specific gravity of less than one, which caused floating in a bed of filter media (Wagener, 2000). High specific gravity materials are used in multimedia filters. Commonly, the multimedia filters have upper, middle and lower layers of high specific gravity. The duty of the lower layer is to allow high flow rates to carry the impurities deep into the other layers. Engelhardt (2012) presented as shown in figure 3.5 an example which summarizes the general specifications of the filter media in multimedia filter, it is noticeable that the specific gravity for lower layer (High-Density) is > 3.8 .

Filter Material	Uniformity Coefficient	Effective Size	Specific Gravity	Acid Solubility
Silica Sand	< 1.7	0.35 to 0.65 mm	> 2.5	<5%
Anthracite	< 1.7	0.6 to 1.6 mm	> 1.4	<5%
High-Density	< 2.2	0.18 to 0.60 mm	> 3.8	<5%

Figure 3.5. Filter media specifications for multimedia filter

Based on the upflow operation requirement the materials with specific gravity in range more than > 1 and less than < 3 could be useful as a packed material. The gas jar method was applied to determine the specific gravity for the selected materials. According to Equation 3.2 the mass of jar and plate, dry sample and water are

measured to obtain a dimensionless value representing the specific gravity, the method details are illustrated in experiment data sheet in Appendix A.

$$S.G = \frac{M_2 - M_1}{(M_4 - M_1) - (M_3 - M_2)} \quad \text{Equation 3.2}$$

Where

M1 = mass of gas jar and plate

M2 = mass of gas jar, plate and dry sample

M3 = mass of gas jar, plate, sample and water

M4 = mass of gas jar and water

3.3.4 Porosity and Bulk density

Porosity is one of the most important physical characteristics in defining porous media. It is described as the ratio of volume of pore space to the bulk volume of the sample as described in equation 3.3, porosity is a dimensionless quantity.

$$\varepsilon = \frac{V_v}{V_t} \quad \text{Equation 3.3}$$

Where V_v is the volume of void-space (such as fluids) and V_t is the total or bulk volume of material, including the solid and void components. In the same experiment the bulk density for samples was calculated as illustrated in the data sheet of the experiment in the Appendix A. Bulk density represent the ratio of the sample mass to the bulk volume.

3.3.5 Scanning electron microscopy (SEM)

Studying the morphology of the material's surface is crucial in the process of interaction between the material and impurities. Specifically, identifying the shape of

bends and protrusions on the surface that offer more surface area for contact with the influent. The micro-surface characteristics of the filter media were studied by the quanta 200 SEM, as shown in Figure 3.6. Images have been taken of several points on the surface with specific magnification.

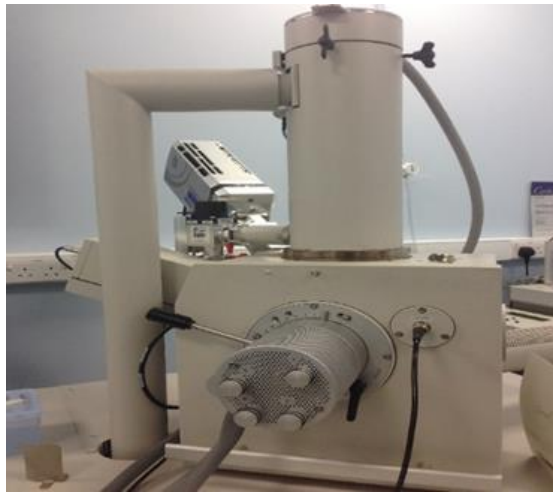


Figure 3.6. Scanning electron microscopy

The SEM analysis Process includes a focused beam of high-energy electrons to produce a range of signals at the surface of a solid sample. In general, the data is obtained by SEM applications over a certain selected area of the surface of the solid specimen, a two-dimensional image is created that shows spatial differences in the material's characteristics especially the material's texture.

3.3.6 X-ray fluorescence analyser (XRF)

The chemical composition of phosphate sorption materials PSMs is the determining factor for the phosphate affinity and capacity. The most efficient PSMs tend to be those that contain Fe/Al hydroxides or easily soluble Ca/Mg compounds.



Figure 3.7. Energy dispersive X-ray fluorescence

The chemical composition of filter media has been analysed by the energy dispersive X-ray fluorescence, Shimadzu EDX 720 analyser, as shown in Figure 3.7. The device performs a qualitative and quantitative analysis to determine the oxides and trace elements in the samples. The analysis process is achieved by exposing the samples to X-ray and then measure the re-emitted characteristics fluorescent X-ray.

3.3.7 Atomic absorption spectrometry (AAS)

Heavy metals such as cadmium (Cd), zinc (Zn), lead (Pb) and copper (Cu) are elements that have a potential toxicity for the environment. Investigation of the safety of the effluent from the heavy metals for some packed materials have been performed by atomic absorption spectrometry AAS. AAS is an analytical tool for determining the elements' concentration. Atomic absorption is such a sensitive technique that it can measure the concentration in samples to parts per billion of a gram. Firstly, a lamp that supplies the right wavelengths to be absorbed by the atoms of the selected sample is fitted. Afterward, the sample is converted into free atoms in the vapour state and a

beam of electromagnetic radiation emitted from the selected lamp is passed through the vaporised sample; the element atoms in the sample absorb some of the radiation. The amount of light which is absorbed is proportional to the number of atoms in the sample. Several samples of known concentration are measured under a specific condition to construct a calibration curve. Then the amount of light, which is absorbed by the unknown concentration of the sample, is compared with the calibration curve and this allows the measurement of the unknown sample concentration.

3.3.8 Residence time distribution (RTD)

The influence of the influent retention time (RT) on contaminant removal has to be identified; RT is also referred to as the influent-to-media contact time (Lyngsie, 2013). The flow dynamics of the research's filtration system was characterised via the measurement of the RTD of the aqueous phase in the lab-scale up-flow filter using a red drain dye (RDD) as the tracer. RTD experiments were carried out in the same mode of operation and at different flow rates.

RTD was measured by injecting a 50 ml shot of tracer (RDD of 2g/l concentration) into the path of influent stream that was pumped to the filters via submersible pumps at time $t = 0$. The tracer concentration, C , in the effluent stream was measured as a function of time. All the experiments were performed at a steady flow state (inlet flow rate = outlet flow rate). The pulse injection method was applied in this experiment. A syringe as a single shot at the flow stream inlet performed the process of injection as it permits for simple interpretation because all the substances enter the reactor at the same time. The process of samples collection was performed by way of collecting from the outlet of the filter column over regular periods. The data was collected at three different flow rates: 0.5, 1 and 1.5 l/min. For each flow rate, the concentration

and amount of tracer remained the same. The HACH LANGE DR 2800 spectrophotometer was used to measure the out tracer concentration. The device measures the RDD absorption amount at wavelength $\lambda = 525$ nm. Afterward, the RDD concentration is determined from the calibration curve as illustrated in the coming chapter. RDD was selected as the tracer to inject at room temperature in the lab-scale filters because it is chemically inert, easily detectable and soluble in the mixture.

3.4 Research procedure

3.4.1 Risk assessment

A series of laboratory experiments were set up to determine the phosphate removal performance of a selected media. Therefore, looking at work activities according to systematic method is required. Risk Assessment is one of the essential parts of the research methodology; includes identifying the risks, which could be expected from the work materials and activities, and suitable actions that are required to control and prevent damage or injury in the workplace. In this present research, chemicals as listed below were used in laboratory work:

- Potassium dihydrogen orthophosphate KH_2PO_4 ; to prepare synthetic phosphate solution.
- Molybdate and amino acid; chemical reagents utilized for phosphate measurement by spectrophotometry.
- Red drain dye RDD; injected as tracer in the filtration system to study the hydraulic behaviour of the system.

A sample of wastewater as well was subjected to risk assessment. In addition, a comprehensive risk assessment is performed for the whole work process to eliminate,

reduce and minimise any expected risks. All prepared sheets of risk assessment were placed in the lab in case of need.

3.4.2 Synthetic influent

Phosphorus in wastewater exists in various forms such as particulate, organic and inorganic Phosphorus. The predominant form is the inorganic Phosphorus; especially, in the form of orthophosphate. Therefore, Potassium dihydrogen orthophosphate KH_2PO_4 is used as the influent solution that was pumped to the filtration system that was set up in this work. The salt was dissolved in deionized water to prepare the phosphate solution. Commonly, the P concentrations in wastewater range from 5 to 10 mg P/l. However, in some cases they can be as high as 20 or 30 mg P/l. The initial P concentration in this work was 10 mg P/l so as to simulate the maximum P concentration in wastewater that is most likely.

3.4.3 Effluent sampling

The effluent samples were collected in plastic containers over the operating time of the experiments. At first the samples were collected every 5 minutes then every 15 min, 30 min, 1, 2 and 4 hr and so on because the sorption rate decreases with time. The collected samples were then filtered with filter paper 0.45 μm and the phosphate concentration is measured.

3.4.4 Phosphate measurement:

The phosphate concentration was measured by the HACH LANGE DR 2800 spectrophotometer, according to the Amino Acid method, which helps to measure the concentration range of 0.2 to 30 mg/l PO_4^{-3} .



Figure 3.8. Spectrophotometer device

The steps of phosphate concentration measurement were as below:

1. Touch Hach Programs. Select program 485 P React. Amino. Touch Start.
2. Fill a 25-mL mixing cylinder with 25 mL of sample.
3. Add 1 mL of Molybdate Reagent using a 1-mL calibrated dropper.
4. Add 1 mL of Amino Acid Reagent Solution. Insert stopper and invert several times to mix (this is the prepared sample). A blue colour will form if phosphate is present.
5. Touch the timer icon. Touch OK. A 10-minute reaction period will begin. Continue with step 6 while the timer is running.
6. Pour 25 mL of sample into a round sample cell (this is the blank).
7. When the timer beeps, place the blank into the cell holder.
8. Touch Zero. The display will show: 0.00 mg/l PO_4^{-3} .

9. Pour the prepared sample into a round sample cell.

10. Place the prepared sample into the cell holder. Results will appear in mg/l PO_4^{3-} .

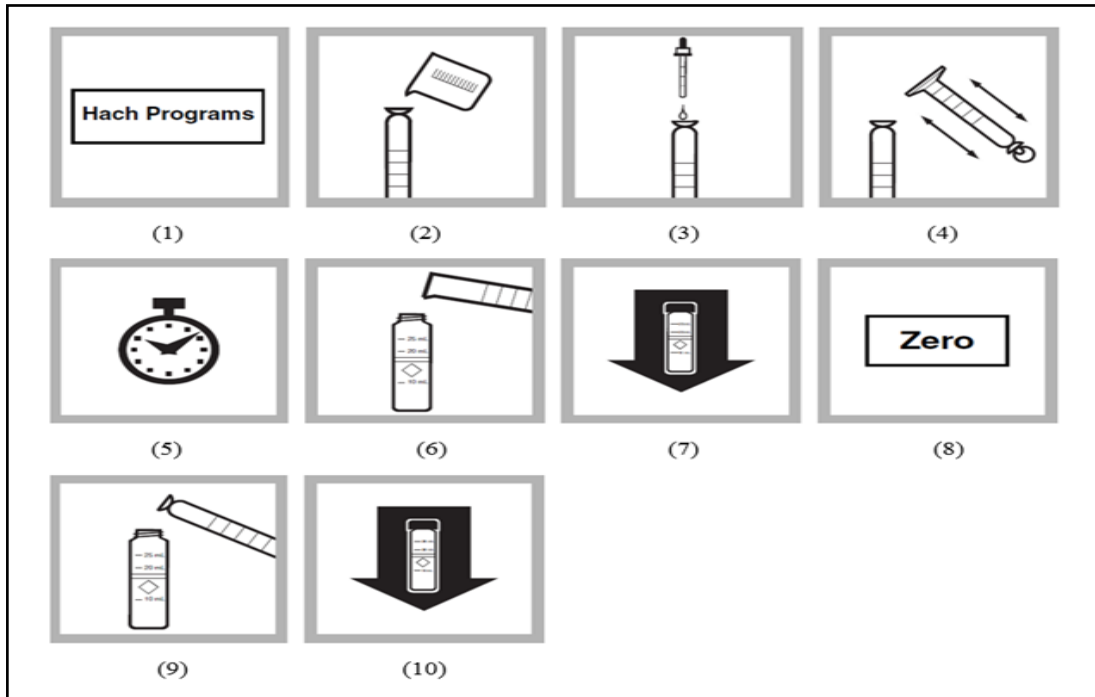


Figure 3.9. Steps of the phosphate concentration measurement; according to the Amino Acid method

3.4.5 Batch tests

Closed batch experiments are rather easy and fast to conduct. They can be used to estimate the first predictions of phosphate retention. In a typical batch experiment, a fixed amount of material is shaken with a fixed amount of a phosphate solution at varying phosphate concentrations. The estimated maximum retention can then be calculated or modelled via the phosphate sorption isotherm. However, batch studies commonly overestimate the performance of the PSM, particularly for precipitation-controlled phosphate retention.

3.4.6 Lab-scale filter

In the present study, a lab-scale filter was set up as shown in figure 3.10. The filter is a cylindrical shape had a diameter of 10 cm and height 45 cm and had an up-flow configuration. The filter was packed with gravel to a height of 10 cm from the bottom to maintain the influent flow smoothly. The filter media was packed over the gravel layer for a depth of 25 cm. Influent was fed into the cylinder from the top centre of the filter by submersible pump placed inside the feed tank. The influent continues to flows downward through the feed pipe placed inside the centre of filter media. Then the influent is introduced into the bottom of the filter bed and distributed inside the filter media during the way out from the filter outlet at the top of the filter. Treated effluent exits through the effluent pipe back again into the feed tank. The aqueous solution is recirculating until phosphate concentration 0.1 mg/l is achieved. The fed influent volume was 8 L and it is pumped at flow rate according to the results of RTD.

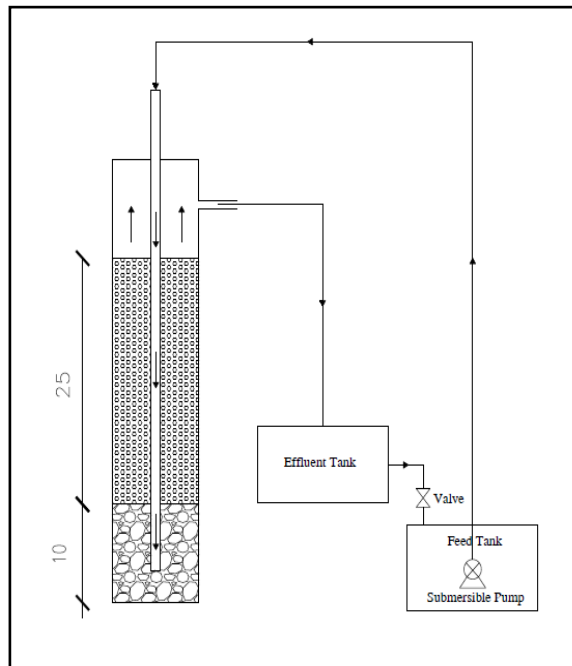


Figure 3.10. Schematic diagram of upflow filter set-up (dimensions unit is cm)

3.5 Data analysis tools

Data analysis methods may vary according to the scientific discipline of the research. In this present research, the analytical procedures are based on applying an experimental modelling and statistical analysis. The analytical tool selection depends on the findings type as illustrated below:

- Experimental analysis: the performance variation of the filter media for phosphate removal has been interpreted according to their physical and chemical characteristics. The results that were obtained from experimental tests such as SEM and XRF will be the key factors that identify the material's characteristic, which is responsible for phosphate removal.
- Modelling analysis: The adsorption mechanism was described according to equilibrium isotherm models such as Langmuir and Freundlich model. Adsorption isotherm models are a tool to determine the magnitude of a solute that is absorbed at a constant temperature and its concentration in the equilibrium solution. In addition, the data provided by the adsorption isotherm model will help to understand the applicability of the adsorption process, especially the maximum phosphate adsorption by the material's surface and the nature of the adsorption process. Langmuir and Freundlich isotherm models are selected in this study because they are commonly used in modelling the adsorption data (Chen, 2015).
- Statistical analysis: part of the research work is to find the relationship between the efficiency of the phosphate removal as a dependent variable and several independent variables, which affect the efficiency of the phosphate removal. Therefore, multi regression procedures have been used as a statistical tool to

determine the influence of each variable on the phosphate removal by the filter media.

3.6 Chapter Summary

Systematic steps for the materials' selection process have been set to avoid the arbitrary, traditional, or standard approaches. Chemical composition, physical properties, availability, environmental issues and cost effectiveness are the factors have been followed in the process of material selection.

The candidate materials have been subjected to a series of experiments to investigate the suitability of their characteristics to the phosphate removal process. The physical properties of the filter media have a significant influence on the hydraulic characteristics of the filtration system and the contaminant mass transfer. Therefore, the physical properties have been characterised according to experiments such as particle size distribution, specific gravity, porosity, bulk density, permeability and scanning electron microscopy. The materials' eligibility for phosphate sorption could be investigated by applying the X-ray fluorescence analyser test to indicate the materials' content from Fe/Al and soluble Ca and Mg oxides.

The safety of the effluent from the heavy metals for some packed materials has been investigated by atomic absorption spectrometry. Meanwhile, the influence of the influent retention time on contaminant distribution inside the filtration system has been conducted by residence time distribution study.

Potassium dihydrogen orthophosphate KH_2PO_4 is used as a source of phosphate in the process of preparation of the synthetic phosphate solution. The phosphate concentration was measured according to the Amino Acid method by utilizing the HACH LANGE DR 2800 spectrophotometer.

Lab-scale filter was set up, it is cylindrical shape has a diameter of 10 cm and height 45 cm and had an up-flow configuration. In this present study the experimental, modelling and statistical analysis are the data analysis tools.

CHAPTER 4 INVESTIGATING THE SUITABILITY OF SELECTED MATERIALS AS PHOSPHATE FILTERS

4.1 Chapter introduction

Recognising the necessity to locate a solution to the pollution caused by phosphate, the employment of reactive filter materials for phosphate removal has in recent years become an attractive method for the treatment of wastewater. Currently, searching for materials with a significant affinity for phosphate is required to achieve the necessary water quality as declared in the EU Water Framework Directive WFD (Kaasik et al., 2008). Based on this ground, many researchers considered the investigation on alternative materials has become essential as one of the sustainable technologies for phosphate removal. According to Johansson Westholm (2006b) these materials can be classified into three groups: natural materials, industrial by-products, and manufactured products. Recently, a large number of Phosphate sorbing materials PSMs have been examined to determine their capability to remove phosphate from wastewater. Most studies have discussed the materials' removal capacity for high phosphate concentrations (Cucarella, 2009).

In this chapter, five materials have been tested with respect to phosphate sorption efficiency for possible use of these materials as filter media. Consequently, high, fast and strong phosphate retention was the test criterion in this investigation. The assessment includes a batch-mode testing of the phosphate removal efficiency. The overall phosphate removal capacity of tested materials is strongly dependent on their characteristics. Considerable attention must therefore be given to the choice and composition of a suitable material in order to ensure optimal phosphate sorption and retention over the long term. However, the physical and chemical characteristics of

the tested materials have been studied in this chapter to determine their suitability as upflow filter media.

In the following chapter an introduction to the different types of phosphate sorption materials PSM's is given, and their sorption reactions.

4.2 Material collection

Based on the scheme which sets up the priorities of filter materials selection as shown in Figure 3.2 in the methodology chapter, limestone, white dolomite, furnace bottom ash FBA and biomass bottom ash BBA have been selected. Considerable attention has been given to the chemical composition of these materials based on the grounds that the most efficient materials for phosphate sorption tend to be those that contain Fe/Al hydroxides or easily soluble Ca/Mg compounds.

According to the previous researches, limestone is a rock whose composition is dominated by Ca; it is expected it contains at least 50% calcium carbonate. Limestone contains a minor percentage of Al, Fe, Mg and other oxides. While, dolomite is known as a calcium magnesium carbonate, the dominated oxides are Ca and Mg. On the other hand, the bottom ash contains little Ca and Mg and it is dominated by Al and Fe compounds. The sand has been used as a filter media for phosphate removal for a long period. Sand has a limited capability for phosphate removal in comparison with other materials but it is applied as one of the standard filter media required for findings comparison. All these materials are available in UK. The limestone is supplied from Omya UK Ltd and the source is the Dowlow quarry, UK; while the white dolomite is supplied by Specialist Aggregates Ltd, UK. Bottom ash was obtained from Warrington power station in North West England. The investigation of low cost materials for phosphate removal has become a significant factor in supporting the sustainable

technologies. Consequently, the materials that are applied in this study are natural materials such as limestone, white dolomite and sand, and waste by-product materials such as FBA and BBA. Accordingly, the manufactured products have been excluded from examination as phosphate sorption material.

The filtration system capacity for phosphate removal is strongly reliant on the filter media sorption characteristic. Therefore, a comprehensive study was conducted to characterise the properties of the selected filter material as described in the next part of this chapter, and in addition to check their validity to act as phosphate sorption material.

4.3 Investigation of the materials characteristics

The physical and chemical properties that describes the material play a crucial role in the mechanism of phosphate removal. Therefore, investigation of the filter media properties is the first step that is applied in examining the suitability of the selected materials for the filtration system. The good filter material must interact rapidly and have a tendency to P sorption and high capacity to P retention. The findings from the study of materials' characteristics will help to figure out the reasons for the good affinity between the filter materials and phosphate ions.

4.3.1 Physical characteristics

4.3.1.1 Particle size distribution analysis PSD

The structure of materials helps to identify their eligibility to act as filter media. Therefore, particle size distribution PSD study was applied to understand the suitability of the particle size of materials to our filtration system. Soil is classified into four constituent parts, one of them sand (sand is any soil particle larger than 0.06 millimetres). Therefore, the selected materials in this study is considered as a sand. Sieve analysis is the method which is applied to determine the particle size distribution of the samples because it is the method that is applied when the particle sizes are larger than 0.075 mm (our samples are classified as a sand). Commonly, the findings that were obtained from sieve analysis represent the percentage of the total weight of the sample that passed through the sieves. As shown in all tables from 4.1 to 4.5 the total weight of the sample for each material which has been subjected to sieve analysis was 700g. A set of sieves were placed from top down in the order of sieve number (4, 6, 10, 16, 30, 50 and pan); then the samples were poured from the top and were then shaken by the vibrator for a period of 10 min. The results of sieve analysis for the sand samples are shown in table 4.1 that the most of the sample mass retained was in sieve number 30; almost 45% from total weight of the particles is at a diameter 0.6 mm. Whereas, a percentage of 24% and 21% from the mass were retained in sieve number 16 and 50 respectively. This means the sand particle size ranged from 0.3 mm to 1.18 mm with plenty of particles at size 0.6 mm.

Table 4.1. The results of sieve analysis for Sand sample

Sieve No.	Diameter (mm)	Mass of sample retained on each sieve (g)	Percent retained (%)	Cumulative retained (%)	Percent finer (%)
4	4.75	0.00	0.00	0.00	100.00
6	3.35	0.00	0.00	0.00	100.00
10	2.00	56.00	8.00	8.00	92.00
16	1.18	168.00	24.00	32.00	68.00
30	0.60	315.00	45.00	77.00	23.00
50	0.30	147.00	21.00	98.00	2.00
Pan		14.00	2.00	100.00	0.00
	Sum =	700			

While the sieve analysis results for limestone have revealed that 56.20% of the particles at size 1.18 mm as illustrated in table 4.2. While, particles size 2 and 0.6 mm represented 20% from the total weight of the sample for each one. However, the limestone has wider particles size range from 0.6 to 2 mm in comparison with sand and larger dominant particle size.

Table 4.2. The results of sieve analysis for Limestone sample

Sieve No.	Diameter (mm)	Mass of sample retained on each sieve (g)	Percent retained (%)	Cumulative retained (%)	Percent finer (%)
4	4.75	0.00	0.00	0.00	100.00
6	3.35	0.00	0.00	0.00	100.00
10	2.00	144.82	20.69	20.69	79.31
16	1.18	393.44	56.20	76.89	23.11
30	0.60	140.62	20.09	96.98	3.02
50	0.30	1.12	0.16	97.14	2.86
Pan		20.00	2.86	100.00	0.00
	Sum =	700			

Table 4.3 shows the results of white dolomite sieve analysis. The particle size 2 mm dominated on the mass of the sample, it is representing a 66.56% of the total weight of the sample. 31.86% from the sample mass was retained in the sieve number 16; this means approximately one third of the sample is at particle size 1.18 mm. The dolomite particle sizes are almost look as if they were a single size according to the sieve analysis; results that revealed a narrow range of particles size ranging from 1.18 to 2 mm.

Table 4.3. The results of sieve analysis for White dolomite sample

Sieve No.	Diameter (mm)	Mass of sample retained on each sieve (g)	Percent retained (%)	Cumulative retained (%)	Percent finer (%)
4	4.75	0.00	0.00	0.00	100.00
6	3.35	0.00	0.00	0.00	100.00
10	2.00	465.90	66.56	66.56	33.44
16	1.18	223.02	31.86	98.42	1.58
30	0.60	4.17	0.60	99.01	0.99
50	0.30	2.91	0.42	99.43	0.57
Pan		4.00	0.57	100.00	0.00
	Sum =	700			

Although, there are different masses retained on sieve 10, 16, 30 and 50 when we performed the sieve analysis for BBA, it is noticeable the largest amount has been retained on sieve 10. Then sequentially the quantity of BBA sample has decreased at sieves 16, 30 and 50 at percentage 28, 12 and 8.5% respectively. The BBA sample offers a wide range of particle sizes in comparison with sand, limestone and white dolomite.

Table 4.4. The results of sieve analysis for BBA sample

Sieve No.	Diameter (mm)	Mass of sample retained on each sieve (g)	Percent retained (%)	Cumulative retained (%)	Percent finer (%)
4	4.75	0.00	0.00	0.00	100.00
6	3.35	14.00	2.00	2.00	98.00
10	2.00	304.5	43.50	45.50	54.50
16	1.18	196.00	28.00	73.50	26.50
30	0.60	84.00	12.00	85.50	14.50
50	0.30	59.50	8.50	94.00	6.00
Pan		42.00	6.00	100.00	0.00
Sum =		700			

The FBA exhibited a wider range in particle size in comparison with all other materials, and there is no dominant size between the retained masses on all sieve. All materials presented a particle size no more than 2 mm except FBA showed large size particles such as 4.75 and 3.35 mm at percentage 6.57 and 27.86 respectively.

Table 4.5. The results of sieve analysis for FBA sample

Sieve No.	Diameter (mm)	Mass of sample retained on each sieve (g)	Percent retained (%)	Cumulative retained (%)	Percent finer (%)
4	4.75	46.00	6.57	6.57	93.43
6	3.35	195.00	27.86	34.43	65.57
10	2.00	158.00	22.57	57.00	43.00
16	1.18	131.00	18.71	75.71	24.29
30	0.60	85.00	12.14	87.86	12.14
50	0.30	55.00	7.85	95.71	4.29
Pan		30.00	4.28	100.00	0.00
Sum =		700			

The sieve analysis has provided the findings, which help to determine the particles' size and the particles' size range, consequently, identifying the surface area of the particle for each material. The particle surface area is a critical factor in determining the rate of reaction between the filter media and pollutants. The smallest particles diameter is the largest surface area. Therefore, if the same amount of each material is packed in the filter system the sequence of the filter media from the largest surface area to the smallest is sand > limestone > white dolomite > BBA > FBA, according to the sieve analysis results as revealed in tables 4.1 to 4.5. Based on sieve analysis particle size distribution curves for all materials were created as shown in figure 4.1. The percentage of passing materials is plotted on the y-axis and particle size or diameter is plotted on the x-axis on the logarithmic scale.

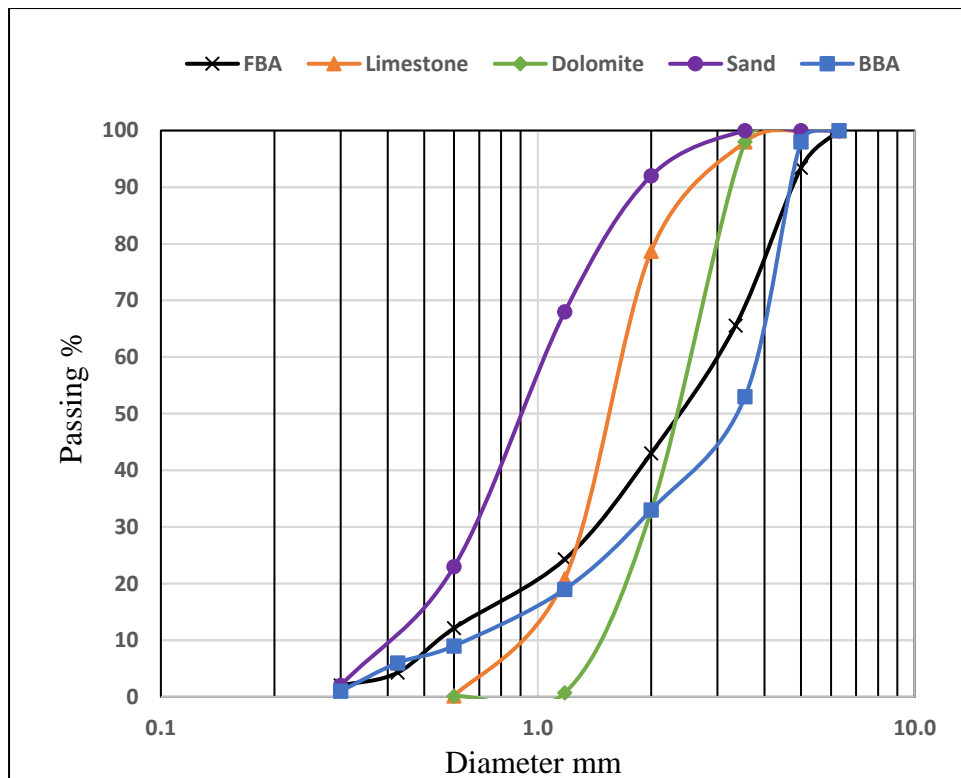


Figure 4.1. Particle size distribution curve PSD

This curves helped to determine the basic parameters of the materials such as uniformity coefficient UC and coefficient of gradation C_c . The values of d_{10} , d_{30} and d_{60} were obtained from the PSD curves and then applied in equation 4.1 and 4.2 as shown below to calculate the UC and C_G .

$$UC = \frac{d_{60}}{d_{10}} \quad \text{Equation 4.1}$$

$$C_c = \frac{d_{30}^2}{d_{10} \times d_{60}} \quad \text{Equation 4.2}$$

Determining the values of UC and C_c as illustrated in table 4.6 is required as a validation process for our selection of the materials in this present study. For the sample at UC value to be greater than 4 and C_c value in the range of 1 to 3 is considered a well graded sample. The UC for sand, limestone and white dolomite are below 4 and the C_c in range 1 to 3; this means they are considered to be poorly graded or uniformly graded. While the UC for BBA and FBA are between 4 and 6 and the C_c in range 1 to 3; this indicated they are well graded materials (mass consists of different ranges of particle sizes).

Table 4.6. The basic parameters that can be determined from particle size distribution curves

Material	Effective Size d 10	d30	d60	Uniformity Coefficient UC	Coefficient of Gradation C_c
Sand	0.43	0.78	1.06	2.45	1.34
Limestone	0.68	1.44	2.12	3.12	1.44
Dolomite	1.18	1.91	2.57	2.18	1.20
BBA	0.68	1.82	3.84	5.67	1.27
FBA	0.58	1.55	3.01	5.150	1.37

The particle size distribution analysis indicates a better surface area for some materials in comparison with the other materials as mentioned above. But the significance of

surface area of the materials is related to other factors which will be investigated later in this chapter. The filter media recirculate inside the upflow filtration system as a result of the internal washing system. Therefore, the uniformly graded materials such as sand, limestone and white dolomite are more appropriate to be packed in the filter than the BBA and FBA.

4.3.1.2 Specific gravity S.G

The media inside the upflow filter systems are exposed to a dynamic motion as a result of the internal washing system. Consequently, the filter media packed in upflow filters should be not very light, which would cause it to float, or heavy that would lead to preventing the media from moving during the washing process. Specific gravity analysis was performed as shown in table 4.7, and it is noticeable that the specific gravity of FBA and BBA are 1.29 and 1.17 respectively. The materials with specific gravity > 1 can be floating even under low flow rate. While material such as FBA and BBA can be floating in the case of high influent flow rate. On the other hand, materials such as sand, limestone and white dolomite with specific gravity 2.57, 2.65 and 2.42 respectively are characterized as a good filter media in term of physical characteristics.

Table 4.7. The physical properties of the material

material	Specific Gravity S.G	Porosity ϵ	Bulk density g/cm^3	Hydraulic conductivity K (m/s)
Sand	2.57	0.36	1.58	0.110
Limestone	2.65	0.46	1.47	0.014
Dolomite	2.42	0.50	1.42	0.020
BBA	1.17	0.73	0.41	0.029
FBA	1.29	0.66	0.47	0.025

4.3.1.3 Porosity

Porosity is the ratio of the fraction of the voids volume to the total volume of the sample, porosity value between 0 and 1. Based on the sieve analysis findings we have two groups of materials. First, well graded materials such as FBA and BBA, and the second group uniformly graded or single size such as white dolomite and to a lesser extent limestone and sand. It is expected that the well-graded materials have the lowest porosity in comparison with uniformly graded materials because some smaller particles can effectively fill the pores. However, the obtained results from the porosity test introduced a different expectation, where the porosity of well-graded materials such as FBA and BBA were 0.66 and 0.73. While the porosity for the materials having less gradation than FBA and BBA, such as sand, limestone and white dolomite, were 0.36, 0.46 and 0.50. The shape of the surfaces for FBA and BBA particles could be irregular, with pores and many bends, which provides large specific surface areas that lead to creating more voids between the material particles, consequently, increasing the materials' porosity.

4.3.1.4 Bulk density

Bulk density is another factor that can help us to understand the expected behaviour of the filter media inside the continuous upflow filtration systems. It can be simply defined as the dry weight of the sample over the volume, which includes particles, and pore space. As mentioned previously the media inside the upflow filter systems are exposed to a dynamic motion as a result of the internal washing system. Therefore, the bulk density of the media is significantly important to maintain the motion of the media inside the filtration system smoothly. According to Cheremisinoff (2002) the bulk density is known as the degree of solids packing or the packing density.

Cheremisinoff (2002) characterized the materials according to their bulk density. Based on literature values, he reported there are three categories as shown in table 4.8. The information that is stated in table 4.8 can be used as a validation tool to determine the suitability of the materials to act as filter media for a specific filtration system.

Table 4.8. Materials characterization according to their Bulk Density

Materials characterization	Bulk density kg/m³
Light	< 600
Average	600 < Bd < 2000
Extra heavy	> 2000

The results of the tests, which were performed to calculate the bulk density for the selected materials, were in g/cm³. Hence, the bulk density values as presented in table 4.7 were converted to kg/m³ to compare them with the bulk density values in table 4.8. The bulk density for sand, limestone and white dolomite was 1580, 1470 and 1420 kg/m³ respectively. This means all materials were considered to have an average weight as their bulk density values lay between 600 and 2000. On the other hand, the FBA and BBA were considered as a light material as the values of bulk density were less 600.

4.3.2 Chemical characteristics

X-ray fluorescence spectrometer XRF was performed to characterize the chemical composition of the selected materials as shown in table 4.9. The key target of this test is to determine if the materials are consisting of the oxides that tend to retain the phosphate ions such as Al₂O₃, Fe₂O₃, CaO and MgO. In addition, to inspect if the materials contained an oxide that indicates a hazardous level of heavy metals.

The results revealed that the limestone and white dolomite consists of a significant percentage of calcium oxide, which reached to 84.162% and 48.807% of the total weight, respectively. Furthermore, they contain no Al_2O_3 and Fe_2O_3 and only contain small amounts of MgO . Therefore, the XRF analysis presented the CaO as the dominant component in the chemical composition of limestone and white dolomite. On the other hand, the FBA and BBA consists of small amounts of CaO and MgO in comparison with limestone and dolomite as indicated in table 4.9. However, both materials consist of an acceptable percentage of Al_2O_3 and Fe_2O_3 . It is noticeable that the FBA and BBA consists of 10.002% and 7.168% of Al_2O_3 and 6.28% and 4.397% of Fe_2O_3 , respectively.

Table 4.9. The X-ray fluorescence analysis for the selected material

Oxides	White Dolomite	Limestone	FBA	BBA
SiO ₂	13.920	14.846	21.297	12.493
Al ₂ O ₃	10.002	7.168
Fe ₂ O ₃	6.28	4.397
CaO	48.807	84.162	1.264	7.615
K ₂ O	0.050	0.140	0.739	2.973
MgO	3.187	0.513	0.655	0.451
Ti ₂ O	0.094	0.093	0.264	0.085
BaO	0.144	0.199	0.197	0.033
SO ₃	0.191	0.181
P ₂ O ₅	0.250	0.25	0.107	0.512
SrO	0.015	0.031	0.042	0.012
MnO		0.029	0.103
ZrO ₂	0.006	0.008	0.015	0.007
Cr ₂ O ₃	0.010
Rb ₂ O	0.003	0.002
ZnO	0.002	0.003	0.003	0.005
NiO	0.003
Y ₂ O ₃	0.002	0.0045	0.002	0.001
CHO	58.897	63.957
CuO	0.012	0.005	0.004
Na ₂ O	8.545	1.333
Cl	0.040	0.040
F	0.050	0.050

Based on the literature review and the results in table 4.9, it is expected that all selected materials have a tendency to remove the phosphate. However, the degree of removal will be various according to the type and amount of components which formed the chemical composition of the materials. The chemical composition for sand was not tabulated in table 4.9 because the XRF analysis of sand showed that the silica is the dominant component in sand formation.

Some of oxides indicate the presence of heavy metals such as ZrO_2 , ZnO and CuO . However, it is noticeable also they represent minor components in the formation of the materials. This will lead to the belief that the solution leaching from the materials is safe. Although, an inspection of the materials' safety was conducted by utilizing the atomic absorption spectroscopy AAS to determine the concentration of heavy metals which was expected to leach from materials.

4.3.3 Surface characteristics

The adsorption mechanism of phosphate ions onto filter media might be proposed as both physical adsorption, which depends on the availability of large specific surface area and porosity of filter media surface, and chemical adsorption, which depend on the chemical composition of filter media. Therefore, characterization of the filter media surface is an essential factor to understand the variation of adsorption capacity for the investigated materials. Scanning electron microscopy SEM was performed to identify and observe the exterior surface morphologies of the selected materials; Images with a magnification of 100 μm have been taken as shown in Figure 4.2. The appearance of many bends pores and protrusions on the surface leads to more surface area for contact with the influent, consequently, better contaminant removal. Figure 4.2 shows the distribution of the protrusions and micro pores on the material's surface.

The figure 4.2a is the image of limestone; it looks to have a rougher surface in comparison with other materials' images because many protrusions with fine diameter are distributed on the large surface area relative to the smooth surface. On the contrary, the smooth surface area for white dolomite, BBA and FBA looks larger than rougher surface area as shown in figure 4.2b, d and e. However, it is noticeable the white dolomite has different size pores and the BBA and FBA have many bends which lead

to increase the specific surface area for them. While the SEM image for figure 4.2c shows the sand surface; its looks to have a somewhat rough surface but comparatively less rough than limestone. In general, the limestone looks to have a rougher surface than the other materials and accordingly a larger specific surface area.

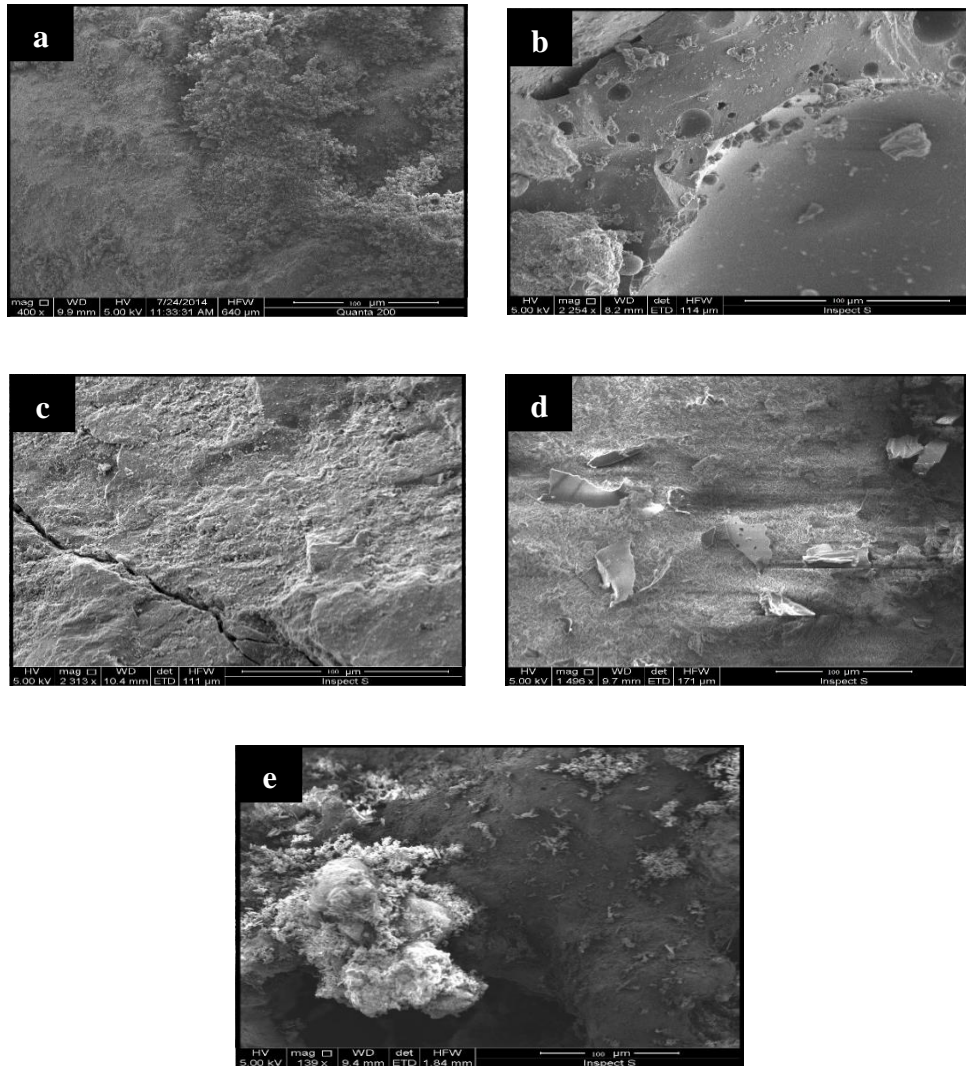


Figure 4.2. SEM comparison of limestone surface (a), white dolomite surface (b), sand surface (c), BBA surface (d) and FBA surface (e)

4.4 Investigating the efficiency of materials for phosphate sorption

4.4.1 Preparation of the phosphate calibration curve for spectrophotometer

The phosphate concentration was measured by HACH LANGE DR 2800 spectrophotometer, according to the Amino Acid method, which helps to measure the concentration range of 0.2 to 30 mg/l PO_4^{3-} . However, this present study seeks to achieve the phosphate removal at the standard limit 0.1 mg/l. It is noticeable that the adopted method for phosphate measuring did not allow measuring the phosphate samples at concentration under 0.2 mg/l. Therefore, a calibration curve for phosphate concentration measurement was created that allows us to measure low phosphate concentration level and to validate the measurement method.

4.4.1.1 Preparation of Standard samples

A number of 10 standard phosphate samples have been prepared at concentration range from 0 to 12 mg/l as shown in table 4.10. Phosphate stock solution was prepared by dissolving a 14.316 g of potassium dihydrogen orthophosphate KH_2PO_4 in 500 ml of deionized water. Consequently, the standard samples were prepared according to further dilution of the stock solution. The next step is preparing the samples to measure in the spectrophotometer; molybdate and amino acid reagent were added to the samples in volume ration 1:25 and the reaction period is 10 min. The colour of samples has been converted to blue, which indicates the presence of phosphate in samples.

4.4.1.2 Wavelength determination λ_{Max}

Before measuring the phosphate, concentration in the spectrophotometer the wavelength λ of absorbance should be determined. Several authors indicate that the concentration of the phosphate can be determined by measuring its absorbance at a wavelength range from 800 to 880 nm by using spectrophotometer (Shyla et al., 2011, Pradhan and Raj Pokhrel, 2013). Three standard samples at phosphate concentration 0.4, 1 and 6 mg/l were measured by spectrophotometer at wavelength range 800 to 880 nm to determine their absorbance. The wavelength was plotted against the absorbance as shown in figure 4.3, to determine the maximum absorbance, which was considered the suitable wavelength for measuring the absorbance of phosphate samples. As illustrated in figure 4.3 the maximum wavelength was found at 830 nm.

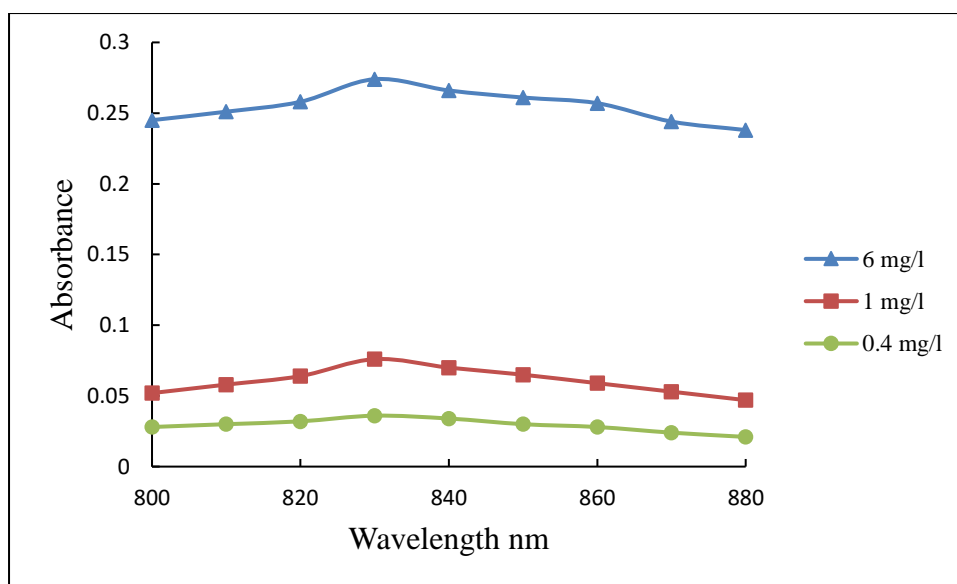


Figure 4.3. Wavelength determination for phosphate samples by utilizing spectrophotometer

4.4.1.3 Create the calibration curve

In order to create the calibration curve, the absorbance of prepared samples was measured at wavelength 830 nm as shown in table 4.10.

Table 4.10. Absorbance of the prepared standard samples

Samples No.	Phosphate concentration mg/l	Abs
Deionize water	0	0
1	0.1	0.019
2	0.4	0.036
3	0.6	0.047
4	0.8	0.051
5	1	0.076
6	2	0.131
7	4	0.221
8	6	0.274
9	8	0.331
10	10	0.437
11	12	0.519

The standard phosphate concentration is plotted against the results of absorbance, then a polynomial trend line plotted at degree 6 as shown in figure 4.4. The equation for polynomial curve and R square were displayed. The R square was 0.9998, this means we gained a good curve fitting for the obtained results. Either the polynomial curve or the equation could be used to calculate the phosphate concentration for the samples in this present study. The Amino Acid method will be utilized as a validation tool for the calibration curve on the term of the experimental work.

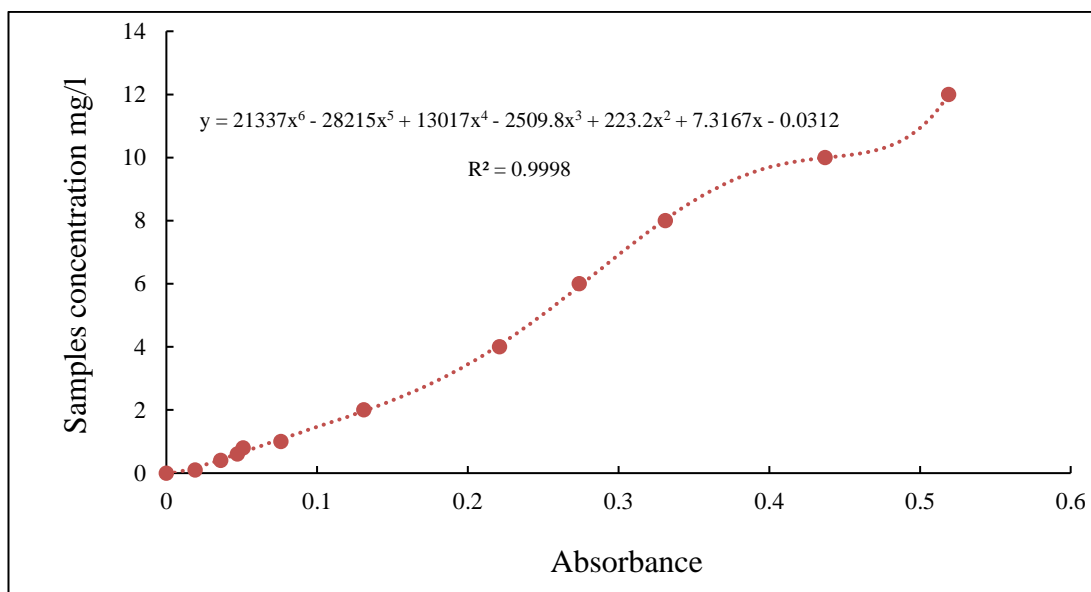


Figure 4.4. Spectrophotometric absorption for phosphate samples at wavelength 830 nm

4.4.2 Batch experiments

Batch experiments were conducted to obtain an initial understanding about the capability of the selected materials to act as phosphate sorbing materials. Specific volumes of the phosphate solution were brought into contact with the masses of the materials in a set of one-litre capacity beakers. The liquid to solid ratio in this experiment was maintained at 1.7 ml to each g, to prevent the material when they soaked in the solution from buoyancy upward. The suspension was shaken at the beginning, and then left to stagnate over the course of the experiment to avoid the effect of mixing on the sorption results. The samples were collected from minor intervals. The collection time was increased with the progress of the experimental time. The samples were filtered through a 0.45 μm filter paper to exclude the suspension particles that may interfere in the scattering of light when applied to the spectrophotometer to secure results that are more accurate.

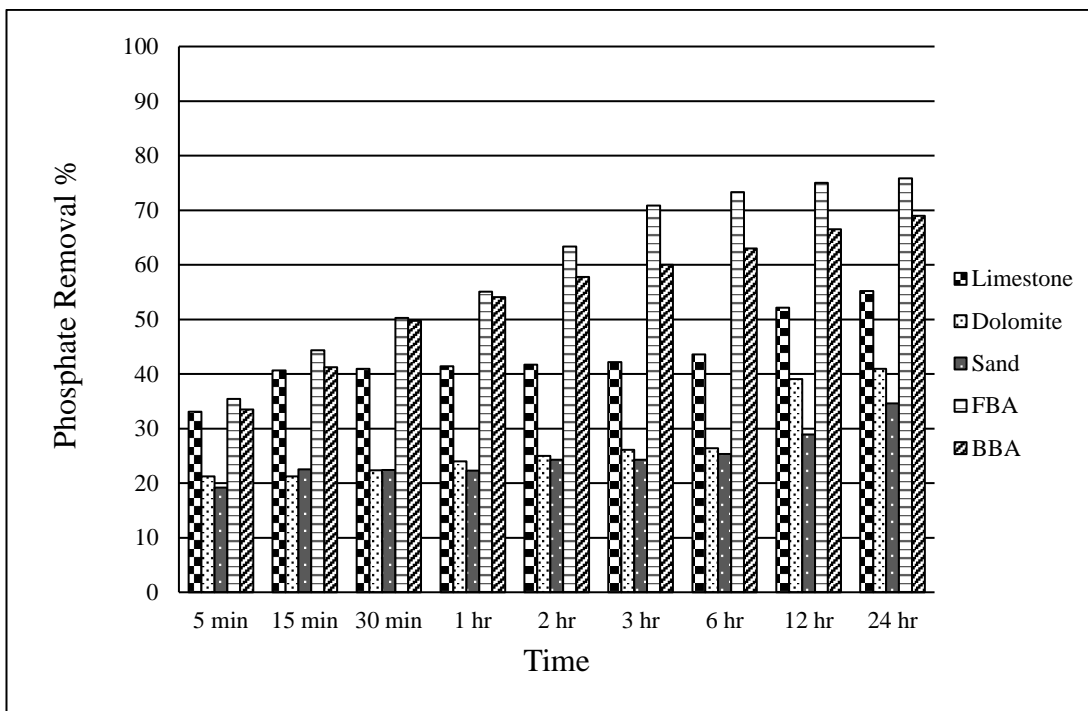


Figure 4.5. Batch experiments results

Compare the phosphate removal by five selected materials illustrated in figure 4.5., the results were obtained from batch experiments. It can be clearly seen that the bar chart presented the FBA and BBA as the most efficient material for phosphate removal over all the time of the experiments. While the other materials show low capability for phosphate removal such as limestone, white dolomite and sand but the limestone looks more efficient than the others. The phosphate removal is measured in percentages.

Overall, it can be seen that all materials correlate with the time at the same pattern. At the beginning of the batch experiments period specifically after 5 min the phosphate concentrations have dropped to 33.08, 21.25, 19.17, 35.42 and 33.50% for the limestone, white dolomite, sand, FBA and BBA, respectively. Over the next time intervals, the removal rate became slower with progress over the duration of the experiments. The experiments were conducted over a period of 24 hours, the final phosphate removal percentages for the FBA and BBA were 75.83 and 69%. On the

other hand, the limestone, white dolomite and sand achieved phosphate removal percentages of 55.17, 40.92 and 34.58%, respectively at the end of the experiments.

Based on the batch experiments results the FBA and BBA were selected for further investigation to make sure they are good phosphate sorption materials. However, FBA and BBA have poor physical properties comparatively to the limestone, white dolomite and sand. While these materials have good physical characteristics but somewhat low affinity to the phosphate.

It could be concluded that the chemical composition of these materials plays a vital role in phosphate sorption. It is obviously the materials, which contain oxides such as Al, and Fe, which presented better phosphate sorption. In addition, the oxides of FBA and BBA are chemically active because the original material is exposed to high temperature for power generation.

4.5 Chapter discussion

The batch experiments results revealed that the materials that consist of oxides of Al_2O_3 and Fe_2O_3 such as FBA and BBA have presented better performance than material consisting of oxides of CaO such as limestone and white dolomite. It might be that the phosphate retention mechanism is playing a key role in enhancing the removal performance. The process of ion exchange caused adsorption of the phosphate on the surface of the materials that contain Fe/Al oxides. While materials rich with soluble Ca, phosphate removal takes place via formation of Ca-phosphate precipitate. Consequently, it is expected that the phosphate removal via material containing Fe/Al oxides are performed faster than formation of Ca-phosphate precipitate to remove the phosphate from the influent in the case of excluding other factors. This approach can be adopted based on the batch experiment results; the materials with Fe/Al oxides have decreased the phosphate concentration at the beginning of experiments faster than at the end. In contrast, phosphate removal via material rich with Ca started at a slow rate then the rate increased in later periods. Although, FBA and BBA have presented an outstanding performance for phosphate removal, they have poor physical characteristics in regards specific gravity, which prevents utilizing them as filter media in continuous upflow filters.

4.6 Chapter summary

This chapter concentrates on investigating the suitability of selected materials to act as filter media in upflow filters for phosphate removal. The materials, which have been selected to investigate their performance for phosphate removal, are limestone, white dolomite, furnace bottom ash FBA and biomass bottom ash BBA. The materials' selection process is based on the ground that the most efficient materials for phosphate sorption tend to be those that contain Fe/Al hydroxides or easily soluble Ca/Mg compounds.

Investigation of the filter media properties is the first step that was applied in examining the suitability of the selected materials for the filtration system. Particle size distribution PSD study was applied to understand the suitability of the particles size of materials to our filtration system. According to sieve analysis the main particle sizes for sand, limestone, white dolomite, BBA and FBA are 0.6, 1.18, 2, 1.18 and 3.35 mm, respectively. The particle surface area is a critical factor in determining the rate of reaction between the filter media and pollutants. The smallest particles diameter is the largest surface area. Therefore, if the same amount of each material is packed in the filter system the sequence of the filter media from the largest surface area to the smallest is sand > limestone > white dolomite > BBA > FBA. Based on the particle size distribution curves, the uniformity coefficient and coefficient of gradation have been calculated. The results revealed that the sand, limestone and white dolomite are considered to be poorly graded or uniformly graded. While the BBA and FBA are well-graded materials. The filter media recirculate inside the upflow filtration system as a result of the internal washing system. Therefore, the uniformly graded materials such as sand, limestone and white dolomite are more appropriate to be packed in the filter than the BBA and FBA.

The specific gravity of sand, limestone and white dolomite are 2.57, 2.65 and 2.42, respectively; this means they have admissible specific gravity to pack in the continuous upflow filters. While the specific gravity of FBA and BBA are 1.29 and 1.17 respectively, they are light materials so might be floating under low influent flow rate. There is a variation in materials' porosity values.

The materials are arranged from highest porosity to lowest as follows: BBA > FBA > white dolomite > limestone > sand. According to the bulk density categories reported by Cheremisinoff (2002) the FBA and BBA are characterized as light materials. While, sand, limestone and white dolomite are characterized as average bulk density materials.

XRF was performed to characterize of the chemical composition of the selected materials. XRF analysis presented the CaO as the dominant component in the chemical composition of limestone and white dolomite. While, FBA and BBA consist of an acceptable percentage of Al₂O₃ and Fe₂O₃.

SEM was performed to identify and observe the exterior surface morphologies of the selected materials. Based on visual judgment the limestone surface morphology looks more complex than other materials because many bends and protrusions with a fine diameter are distributed on the surface.

Calibration curve for phosphate concentration measurement was created that allows us to measure low phosphate concentration level and to validate the measurement method which utilizes the HACH LANGE DR 2800 spectrophotometer to measure the phosphate samples' absorbance. Moreover, the suitable wavelength of measuring the absorbance of phosphate samples was found to be 830 nm.

Batch experiments were conducted to obtain an initial understanding about the capability of the selected materials to act as phosphate sorbing materials. The batch

experiments results revealed that the FBA and BBA are the most efficient material for phosphate removal over all the time of the experiments. While the other materials such as limestone, white dolomite and sand showed poor removal performance comparatively to FBA and BBA. It might be that the outstanding performance of FBA and BBA is related to their chemical composition. Especially, they are consisting of an acceptable percentage of Al_2O_3 and Fe_2O_3 . Poor physical characteristics of both FBA and BBA prevent them being utilized as filter media in continuous upflow filters. The efficiently phosphate removal by FBA and BBA, and the good physical characteristics of limestone, white dolomite and sand lead to a decision to apply coating technology. FBA and BBA will be the coating dosage, which covers the support media such as limestone, white dolomite and sand. FBA and BBA are the source of phosphate removal, and limestone, white dolomite and sand will be utilized to enhance the physical properties of the new created filter materials. More details about applying the coating technology and adopting the best coating filter material is illustrated in the next chapter.

CHAPTER 5 FILTER MEDIA COATING TECHNOLOGY

5.1 Chapter introduction

The simplest definition for the coating process is a covering that is applied to the surface of an object (Grainger and Blunt, 1998). Recently, considerable attention has been paid to applying the coating concept in developing a new type of filter media to obtain an efficient phosphate removal. In this study, some coating technologies have been illustrated in the literature review chapter. The coating technology was considered in this study because of two main reasons. Firstly, to obtain a new coating method which is more consistent with the sustainability approach. Secondly, based on the examination of the chemical and physical characteristics for selected materials applying the coating technology is required to develop the characteristics to act as efficient phosphate filter media.

The decision of creating new filter media was implemented by coating the FBA or BBA over the limestone or white dolomite or sand. The new product is characterized by containing Al_2O_3 and Fe_2O_3 (capable to retain the PO_4^{-3}) and developed physical characteristics such as specific gravity (to prevent media from floating) and obtain high surface area (Increase the contact chance with influent).

The coating process needs a binder to create a bonding between the coating dosage (FBA and BBA) and support media (limestone, white dolomite and sand). Ordinary Portland cement OPC is the binder, which is utilized in this work because it is easy to activate as a binder, the water is the catalyst of binder activation. OPC for general purpose is the type of OPC that used in this study because it is good for early strength

development, cheap and available. While, the other types of OPC are intended for specific purposes.

This chapter includes the implementation of the coating technique and illustrates the characteristics of the new products. The process of coating aims to develop the physical characteristic of FBA and BBA, and at the same time to maintain the amount of Al/Fe oxides in their composition. The new physical and chemical characteristics will be the base that interprets the capability of new filter materials to act as phosphate sorption materials. Batch experiments have been conducted to seek out new filter materials, which achieved a significant phosphate removal. A lab-scale upflow filter was constructed to simulate the efficiency of new filter media inside this system as one of the main research targets. The final decision in adopting the created filter materials is dependent on the results that were obtained from the lab-scale filter.

5.2 Materials bonding mechanism

As a result of OPC hydration, a calcium hydroxide has been released which reacts with the coating dosage to produce a bonding between the mixture materials by creating calcium-silicate hydrates (C-S-H). The availability of high amounts of calcium and silicate in the composite material lead to the formation of the calcium-silicate hydrates (C-S-H) the predominant binder. On the other hand, the released calcium hydroxide reacts with other coating dosage oxides to produce hydrates depending on the amount of the oxide such as calcium-aluminate hydrates. Many researchers illustrated that, in the presence of moisture, a chemical reaction takes place between the aluminium oxides and calcium hydroxide at ordinary temperatures to form compounds having cementitious properties. The cementitious behaviour of the coating dosage is beneficial to increase the bonding between the composite materials but in the same

time, it is reducing the availability of the Al_2O_3 and Fe_2O_3 , which are necessary to retain the phosphate during the treatment process.

5.3 Filter media preparation

The FBA and BBA was ground in a 2L capacity grinder with pestle and mortar as shown in figure 5.1 for 10 min to render them as a fine powder. The support media were washed to remove any fine particles and debris, which may affect the mixture bonding, and then dried naturally in air. Six mixtures were prepared to produce six composite materials; three of them are created by adding FBA as coating dosage to the support media (limestone, white dolomite and sand), the rest are created by adding the BBA as coating dosage to the same support media.



Figure 5.1. Grinder with pestle and mortar, 2L capacity

The preparation process has been performed as follows: the coating dosage, OPC and support media were mixed in a Hobart 5 L capacity bench mixer as shown in figure 5.2 as a dry mixture for 2 min. Then water was added during mixing process and the

bench mixer kept mixing for 4 min; then the mixture was left in sealed plastic sheets for 28 days for curing as shown in figure 5.3.



Figure 5.2. Bench mixer, 5 L capacity



Figure 5.3. Samples of new-coated materials

The mixture has been kept at room temperature 20 C° and moisturized regularly to protect it from loss of moisture. Consequently, the OPC will build cementitious bonds between the mixed materials to obtain the final product. Coating dosage, binder, water

ratio and curing time are the factors considered in the new filter media preparation. The mixtures were produced as one mass; a gentle crushing was applied to obtain the filter media as particles.

The ratios of materials added depend on the quantity of support media. Based on an extensive literature review, the OGE (2008) reported that the suggested OPC quantity for modification or stabilization of the soil ranged between 4% and 6% from the dry weight of the soil. Therefore, OPC at a quantity 5% of the dry weight of the support media was added for the first investigated mixtures. While the coating doses were added at a quantity 50% of the dry weight of the support media because this quantity covered all the mass of the support media during mixing process. In addition, the water ratio depends on the blended quantity of the coating dosage and OPC because both materials having a cementitious property when activated by adding water. Many authors stated that the water/OPC ratio was within a range of 25 to 50% (Tarun et al., 1992, Wong and Buenfeld, 2009). In this present study, 35% was used as the water ratio; it approximately represents the average of the familiar range of water/OPC ratio. According to the construction industry, the most cementitious materials requires 28 days to cure and reach 100% of its strength (Barger, 2013). Therefore, 28 days was used as a curing age in these experiments.

5.4 Composite materials characteristics

5.4.1 Physical properties

The physical properties of new composite materials have been investigated to understand the development of materials characteristics which are achieved by the coating process. The given data in table 5.1 presents the new physical properties of six

new filter media that were produced after the coating process. As mentioned previously, the FBA and BBA are the coating materials and the limestone, white dolomite and sand are the support media. Therefore, the new composite materials are named as shown in table 5.1; first character represented the support media and the rest represented the coating dosage.

Table 5.1. The physical properties of new composite material

material	Specific Gravity S.G	Porosity ϵ	Bulk density g/cm³	Hydraulic conductivity K (m/s)
SFBA	2.67	0.39	1.52	0.110
LFBA	2.75	0.52	1.40	0.014
DFBA	2.51	0.56	1.59	0.020
SBBA	2.63	0.40	1.54	0.029
LBBA	2.70	0.50	1.43	0.025
DBBA	2.46	0.54	1.60	0.022

It is noticeable that the specific gravity for all new materials became approximately the same specific gravity of the support media with slight differences in comparison with table 4.7. The porosity values are also slightly changed in comparison with porosity values in table 4.7. The porosity of new materials has been increased; it might be as a result of the change in the material's surface morphology after the coating process. It is expected that bends and protrusions will be formed as a result of the coating process, and this will lead to the generation of more voids that increase the material's porosity. Furthermore, the bulk density has decreased for all materials as illustrated in table 5.1; this result might also support the idea of voids creation as a results of the formation of bends and protrusions.

Generally, the physical characteristics of all new media have approximately the same features as the support media with a slight increase in porosity and decrease in bulk density.

5.4.2 Chemical properties

X-ray fluorescence spectrometer XRF was performed to characterize the chemical composition of the newly created materials as shown in table 5.2. One of the most significant issues in the process of creating new filter media is to maintain the presence of specific oxides. Especially, the Al_2O_3 and Fe_2O_3 because these oxides are responsible for retaining the phosphate.

In comparison with the chemical composition of FBA and BBA as shown in table 4.9; the amount of Al_2O_3 and Fe_2O_3 were reduced for all new products because the reaction of coating materials with the calcium hydroxide that is released from OPC hydration will consume these oxides to produce cementitious compounds. It is noticeable that the amount of Al_2O_3 and Fe_2O_3 for the support materials, which were coated by FBA is higher than the materials coated with BBA. It might be related to the original amount of these oxides in FBA and BBA before the coating process. Therefore, the initial expectation is that SFBA, LFBA and DFBA will present better phosphate removal than SBBA, LBBA and DBBA according to the findings revealed by the XRF.

Table 5.2. The x-ray fluorescence analysis for the new created media

Oxides	SFBA	LFBA	DFBA	SBBA	LBBA	DBBA
SiO ₂	40.780	43.631	45.452	36.520	28.154	31.642
Al ₂ O ₃	5.623	6.520	6.894	3.633	2.217	2.841
Fe ₂ O ₃	5.539	6.051	5.702	2.924	2.286	2.826
CaO	6.548	10.477	7.864	24.737	42.878	29.626
K ₂ O	1.794	1.843	1.892	4.742	4.596	5.033
MgO	4.276	4.811	5.053	1.329	1.202	1.364
Ti ₂ O	0.986	0.976	1.290	0.435	0.342	0.448
BaO	0.104	0.111	0.120	0.147	0.129
P ₂ O ₅	0.250	0.250	0.250
SrO	0.098	0.045	0.044
MnO	0.034	0.030	0.032	0.176	0.185	0.201
ZrO ₂	0.023	0.025	0.026	0.013	0.014	0.014
ZnO	0.022	0.023	0.024	0.012	0.018	0.014
Y ₂ O ₃	0.007	0.007	0.007	0.004	0.005	0.004
CuO	0.010	0.010	0.012	0.007	0.009	0.010
Na ₂ O	1.131	1.177	1.219	1.148	1.249	1.327
Cl	0.040	0.040	0.040	0.040	0.040	0.040
F	0.050	0.050	0.050	0.050	0.050	0.050

5.4.3 Surface characteristics

This part of the research is aimed to investigate the surface morphology of the new created filter media according to the analysis of SEM. Figure 5.4 shows the SEM images that have been taken at magnification 50 μm for all materials. As illustrated previously there are three support media; before coating a1 limestone, b1 white dolomite and c1 sand. They have been coated by two coated dosage FBA and BBA; the FBA was generated a2 LFBA, b2 DFBA and c2 SFBA. While BBA was generated a3 LBBA, b3 DBBA and c3 SBBA. In comparison between the surface shape of the materials before and after coating process many changes have occurred. Based on visual judgment the SEM images of the coated limestone (LFBA and LBBA) were

presented as uneven and heterogeneous nature more than other materials, specifically the coated white dolomite (DFBA and DBBA).

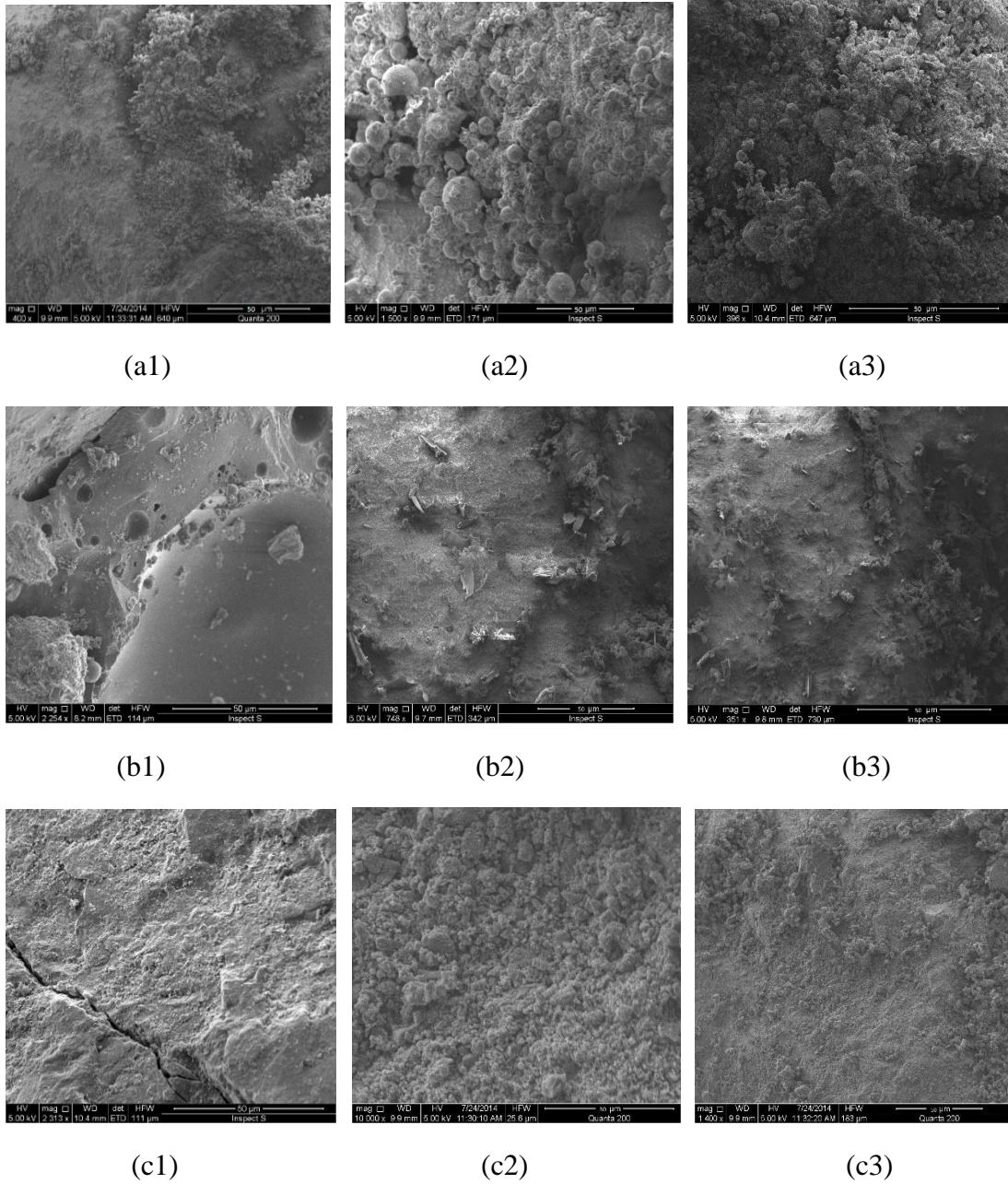


Figure 5.4. SEM comparison of material surface before and after coating, (a1) limestone, (a2) LFBA, (a3) LBBA, (b1) white dolomite, (b2) DFBA, (b3) DBBA, (c1) sand, (c2) SFBA and (c3) SBBA.

The new shape and nature of the surfaces of LFBA and LBBA proposed a creation of a better specific surface area as a result of the coating procedure. This might be related to the nature of the limestone surface which formed many bends and protrusions. Consequently, it supports the formation of the coating dosage on its surface to appear in the shapes as revealed in SEM images a1 and a2. In comparison according to the sort of coating dosage, it could be recognized that the materials coated by FBA as shown in SEM images a2, b2 and c2 offered more heterogeneous surface nature than the same materials when coated by BBA as shown in images a3, b3 and c3. Therefore, it is expected that the materials which were coated by FBA will introduce better phosphate removal as they offer a large specific surface area which provides good contact with phosphate ions.

Based on the results that were revealed by the SEM image as shown in figure 4.6 it can be initially stated that the limestone represented a good support media in comparison with sand and white dolomite. While the FBA showed a good agglomeration on the surface of the support media much better than BBA.

The next part of the study is focusing on analysis of the images that were obtained from SEM according to the MATLAB 16a program to validate our judgment on the nature of the surfaces of the new created materials by an analytical tool.

5.5 SEM image processing

Various approaches were employed for characterizing the SEM images, one of these image analysis methods is the visual inspection as performed in a previous part of this present study. Recently, image-processing methods represent a significant tool in identifying and characterization of different materials in the waste water industry. MATLAB is a powerful tool in the image analysis procedure (Mesquita et al., 2010,

Mesquita et al., 2011). MATLAB 16a was adopted as an analysis program to describe the surface morphology of the new created materials. The image processing codes were created as listed in Appendix B. Each two coated materials with same support media were displayed in the same code to illustrate the agglomeration difference between the coating dosages.

Determining the brightness contrast for the SEM images is the key factor to identify the morphology variation between the surfaces of newly created materials. Therefore, histograms were constructed for each SEM image because they represent the brightness distribution of the image. Consequently, the image that has the largest pixel sum represents the material of the most heterogeneous surface.

The stage of image pre-processing includes converting the image into grayscale, the preferred format for image processing. The second stage is segmentation of the bright field grayscale image; this will help to identify the surface morphology of the materials as shown in figures 5.5 to 5.7. The brightness that appears after image segmentation represents the boundaries of the bends and protrusions. The images of SFBA and SBBA as shown in figure 5.7 looks brighter than the other materials' images after applying image segmentation. However, it is difficult to issue a final decision about the materials' surface morphology depending on the result of image segmentation because there is a variation in the intensity of the brightness that reflects the actual contrast of the coating dosages over the surface of the support media. A histogram was constructed for each image to illustrate intensity vs frequency as shown in figures 5.5 to 5.7. Intensity is represented by the brightness value variation; whereas the frequency is the number of pixels for each intensity. There are 256 different intensities along the intensity axis for all images, and so the histogram will graphically display 256

numbers showing the distribution of images' pixels over the intensity values. As shown in figure 5.5 the variation of frequency of LFBA and LBBA images looks more than the variation of frequency of DFBA and DBBA in figure 5.6 and SFBA and SBBA in figure 5.7. According to the pixels sum of each histogram the LFBA image content 1931264 pixels as the highest pixels number amongst the other images. While the pixels sum for the other materials were 180141 for the LBBA, 1145773 for SBBA and about 965632 for the DFBA, DBBA and SFBA.

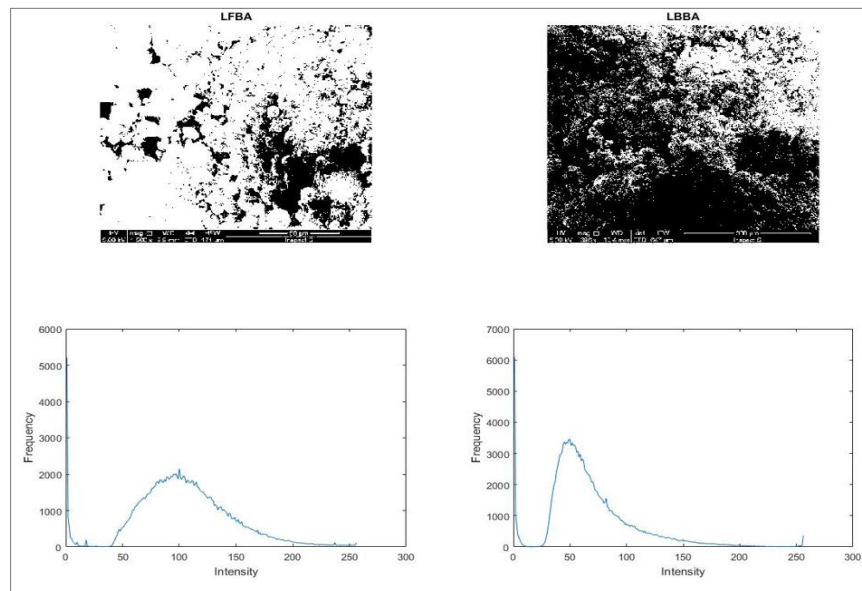


Figure 5.5. SEM image processing analysis for LFBA and LBBA

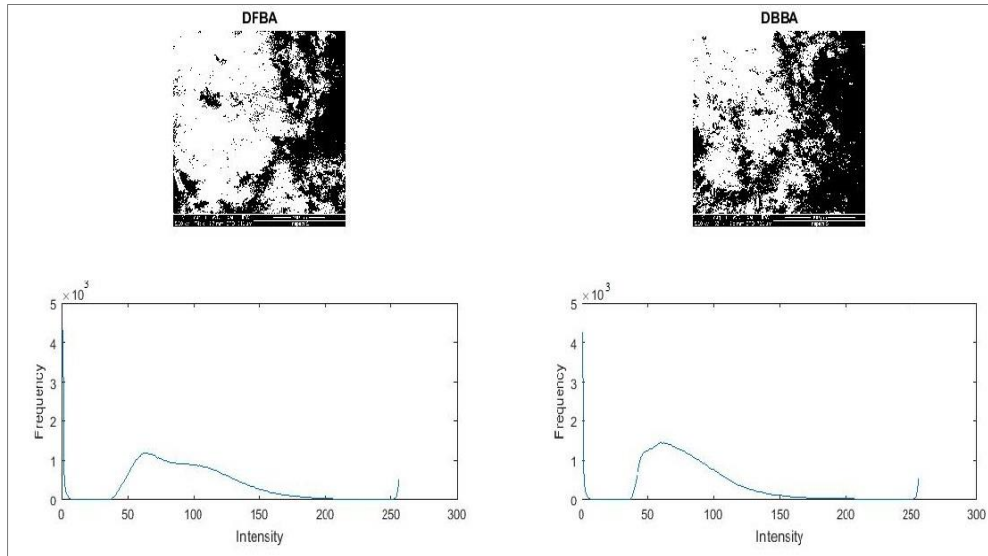


Figure 5.6. SEM image processing analysis for DFBA and DBBA

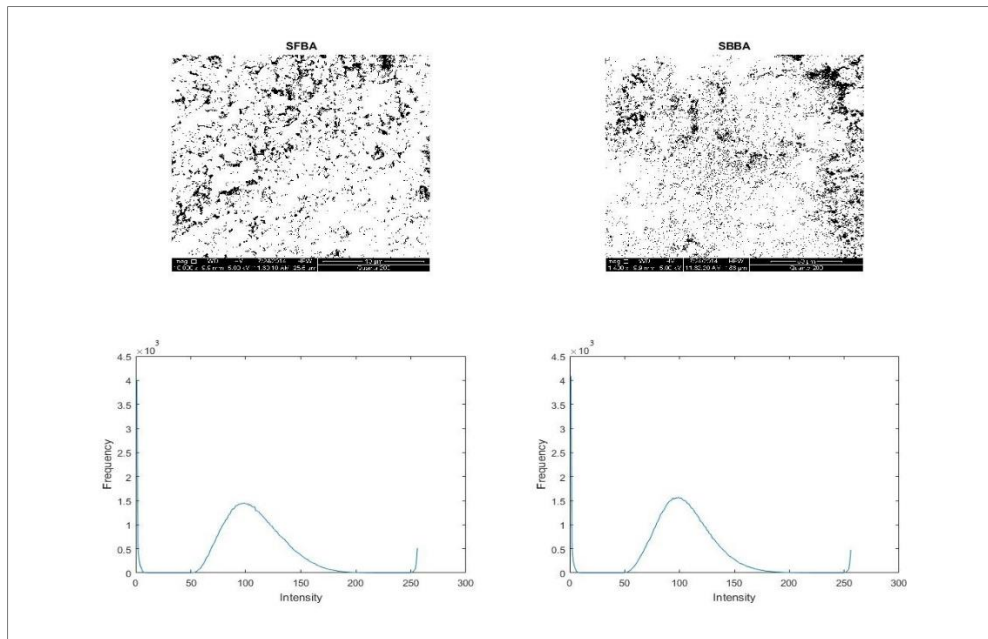


Figure 5.7. SEM image processing analysis for SFBA and SBBA

The results that were obtained from image processing analysis can provide a graphical and numerical finding, which can be adopted in validation of the visual inspection of SEM images. The conclusion of visual inspection proposed that the coating dosage over the limestone such as LFBA and LBBA showed more complex surface than the other materials and this agreed with the results, which were obtained from image analysis; where these materials recorded the highest pixels sum 1931264 and 180141

for LFBA and LBBA, respectively. According to the visual inspection, the SEM images presented the FBA as the coating dosage which agglomerates over all support media better than BBA. On the other hand, this result is consistent with the image processing for LFBA and LBBA, but for DFBA and DBBA the sum of frequency for brightness values was the same, and the SBBA presented highest pixels sum in comparison with SFBA, where pixels sum for SBBA and SFBA were 1145773 and 965632, respectively.

5.6 Investigating the efficiency of new materials for phosphate sorption

Batch experiments were carried out again to determine the phosphate sorption by the new created filter media. In the current experiments, the same experimental conditions for uncoated materials were applied; the initial sample concentration was 10 mg P/l over 24 hr (experiment time). The results of phosphate removal for all new created materials are illustrated in figure 5.8.

Based on the bar chart description for phosphate removal a drastic drop in phosphate concentration just after 30 min for all materials is evident. Specifically, the SFBA indicated fastest removal; it reached up to 56% from the initial phosphate concentration. SFBA continues to present a significant performance for phosphate removal over the course of the experiment but it is clear that the affinity of phosphate into LFBA shows up after 1 hour to indicate that the LFBA became more efficient than SFBA. The LFBA achieved 81% removal, whereas SFBA removed 78% of the phosphate after the same time. Then the LFBA dominated on phosphate removal until the end of the experiment to emerge as the most efficient material capable of removing the phosphate in comparison with the other materials, which were tested. The final phosphate removal for LFBA and SFBA were 97% and 95%, respectively. The final

phosphate removal for LFBA and SFBA was 97% and 95%, respectively. Moreover, the SBBA showed a good phosphate removal but slightly lower than LFBA and SFBA. However, the difference in efficiency was decreased; where SBBA achieved final removal 94%. The other materials which were tested such as LBBA, DFBA and DBBA showed a good phosphate removal also; where the final removal for these materials reached to 88%, 81% and 80%, respectively. Finally, LFBA, SFBA and SBBA were considered the most efficient materials according to the phosphate removal level which they have achieved.

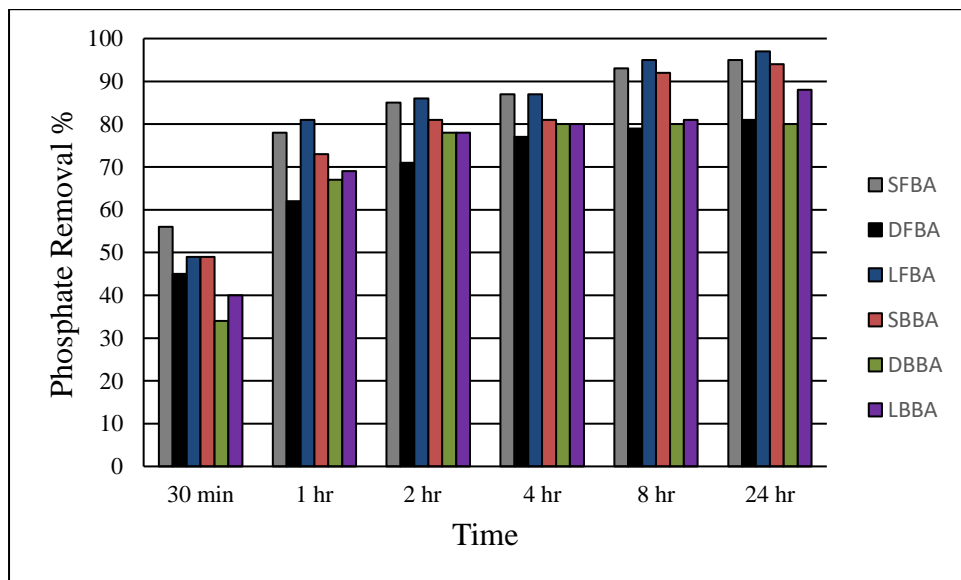


Figure 5.8. Batch experiments results for coated materials

In general, the coated materials have a significant tendency to remove the phosphate at higher concentrations more than lower concentrations. It is noticeable that the removal rate at the beginning was very high; for the first 30 min of experiments it reached up to 0.186, 0.15, 0.163, 0.163, 0.113 and 0.133 mg P/l/min for SFBA, DFBA, LFBA, SBBA, DBBA and LBBA, respectively. While, for the second 30 min the removal rate became lower than at the start; it was 0.073, 0.056, 0.106, 0.08, 0.11 and 0.096 for the same materials order. Furthermore, in comparison between the phosphate

removal percentage after 8 hr and 24 hr there is no significant difference in spite of the large difference in time.

Figure 5.9 illustrates the difference in phosphate removal between the best-selected coated and uncoated materials. The batch experiment results for FBA and BBA, which were obtained from figure 4.5 have been compared with the most efficient coated materials LFBA, SFBA and SBBA. Although, the FBA and BBA are the main coating dosage for the coated materials, the coated materials presented outstanding performance for phosphate removal in comparison with the FBA and BBA performance over the course of experiments. This might be related to the new surface attributes of the coated materials because the FBA and BBA were ground as a powder then coated over the selected materials, which increased the specific surface area of the new materials, consequently increasing the chance of contact between liquid phase and solid phase, which reflected positively on removal performance.

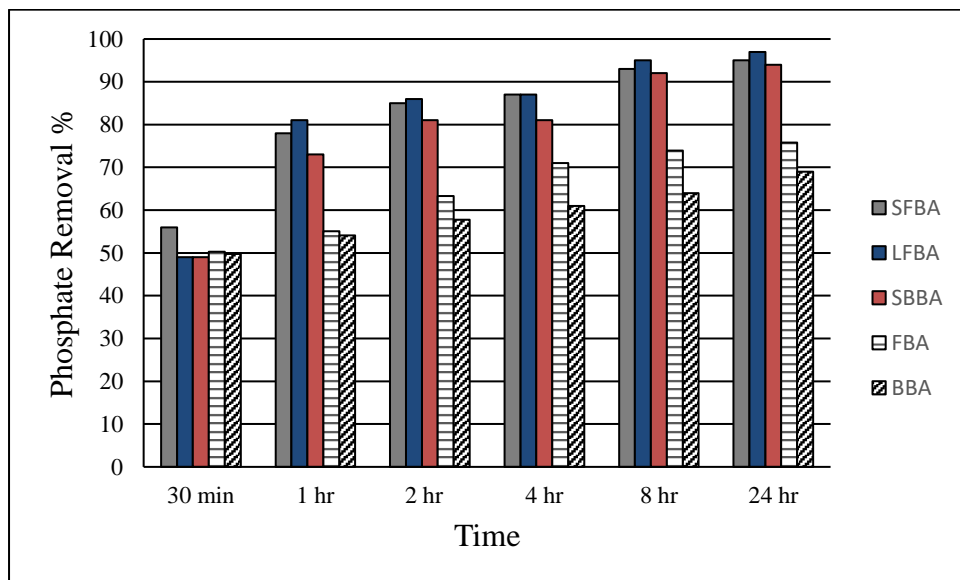


Figure 5.9. Phosphate sorption comparison between coated and uncoated material

5.7 Lab-scale filter

Previously, the coated materials were investigated according to batch experiments to obtain an initial interpretation about their efficiency for phosphate removal. In this current study, a lab-scale upflow filter was constructed (the system configuration is illustrated in the research methodology chapter) to investigate the efficiency of the coated materials after packing them inside the system. Implementation of phosphate removal based on utilizing lab-scale upflow filter is to simulate the efficiency of packed filter media inside this system as one of the main research targets. In addition, there are several important aspects for phosphate removal were not considered in the batch experiment. The most significant aspect is the influent transfer inside the filter media, which illustrates the contact between the impurities and the surface of filter media. Therefore, it is expected that the packed materials in upflow filter will present outstanding performance for phosphate removal in comparison with the batch experiments results. This part of the study was implemented to determine the optimal flow rate that will be set up for the constructed upflow filter and finally determine the most efficient coated materials amongst the LFBA, SFBA and SBBA which were selected from the batch experiments.

5.7.1 Study of influent transfer inside lab-scale filter

The evaluation of the hydraulic characteristics of the filter media in the filtration regime leads to an understanding of the reaction between the influent and filter media structure. The residence time distribution RTD experiments were conducted to analyse the hydraulic behaviour for the influents inside the up-flow filter rig and this will help to determine the optimum influent flow rate that should be taken into consideration in system design. In general, good dispersion could be achieved at low flow rates but the

aim of this study is to identify the maximum flow rate, which could achieve an admissible influent dispersion inside filter materials. Consequently, achieve treatment of the largest possible influent quantity and in the same time maintain the interaction time between the entering solution and filter materials.

The study was implemented via the measurement of RTD of the aqueous phase in the lab-scale up-flow filter using a red drain dye RDD as the tracer. RTD experiments were carried out in the same mode of operation and at different flow rates for each filter media, which was subjected to this test.

5.7.1.1 Packing filter media

The surface characteristics of the filter media can have a significant effect on the influent residence time. In the present study, LFBA, SFBA and SBBA were used as the filter media due to their feasible characteristics in phosphate removal.

5.7.1.2 Tracer selection

The tracer should be chemically inert, easily detectable and soluble in the mixture [10]. Therefore, the red drain tracing dye RDD was subjected to tracer test by exposing the filter materials (LFBA, SFBA and BBA) to the tracer to estimate any potential adsorption. The mass of filter materials was 20 g; it was placed in a 1 litre glass beaker, and almost covered by RDD at concentration 2 mg/l. The beakers were covered from outside by aluminium foil to prevent the influence of light. Based on the suggestion of Cobos-Becerra and Gonzalez-Martinez (2013) the filter materials were exposed to the tracer for 48 hr. There is no alteration in the colour for all the filter materials and the concentration of RDD did not change during the course of the test, leading to the conclusion that the RDD is not adsorbed by the LFBA, SFBA and BBA.

5.7.1.3 Determine RDD wavelength λ_{Max}

Before the beginning of the RTD study, the suitable wavelength of the tracer should be determined. The RDD concentration will be measured by the HACH LANGE DR 2800 spectrophotometer; according to the device's catalog, it is able to measure samples' absorbance at wavelength range 340 to 900 nm. Therefore, this wavelength range was selected to investigate the best wavelength that measures the RDD concentration. A 4 g of RDD powder was dissolved in 0.5 liter deionized water to obtain a stock solution at concentration 2 g RDD/l. Samples at 4 ml volume were taken from stock solution and their absorbance was measured at wavelength range 400 to 900 nm to identify the maximum absorbance value. The results revealed that the maximum absorbance occurred at wavelength 500 nm as shown in figure 5.10.

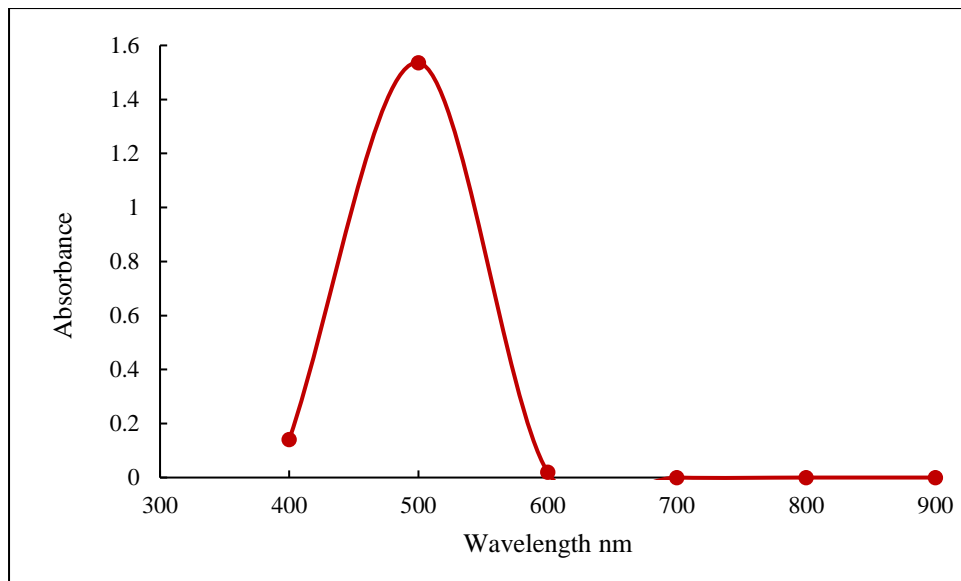


Figure 5.10. Determination of the best wavelength for absorbance of RDD samples, first attempt

To achieve a more accurate result, the test was repeated at narrower wavelength range depending on the finding of the first attempt. This time the samples were tested at wavelength range 450 to 550 nm at each 25 nm over this range. The second attempt results are presented in figure 5.11; the maximum absorbance occurred at wavelength 525 nm. Hence, this wavelength was adopted to measure the absorbance of RDD samples by the HACH LANGE DR 2800 spectrophotometer.

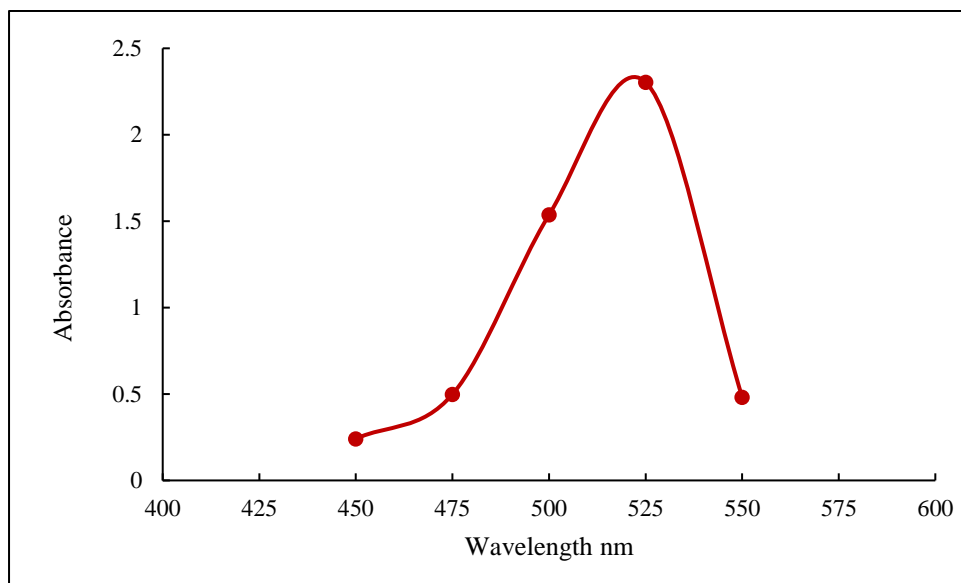


Figure 5.11. Determination of the best wavelength for absorbance of RDD samples, second attempt

5.7.1.4 Calibration curve of tracer concentration

In this part the calibration curve for the spectrophotometer device has been prepared to provide the concentration of the RDD samples, which will be obtained from the RTD study. In order to create calibration curve, 55 RDD samples with different concentrations (varying between 0 mg/l to 2000 mg/l) were used to find the corresponding spectrophotometric absorbance at wavelength 525. The obtained absorbance of the samples was plotted against their standard concentrations; then a polynomial trend line plotted at degree 6 as shown in figure 5.12. The equations for

polynomial curve and R square were displayed. The R square was 0.9961, this meant we obtained a good curve fitting for the RDD results. Both the polynomial curve and the equation could be used to calculate the RDD concentration for the samples in the RTD study.

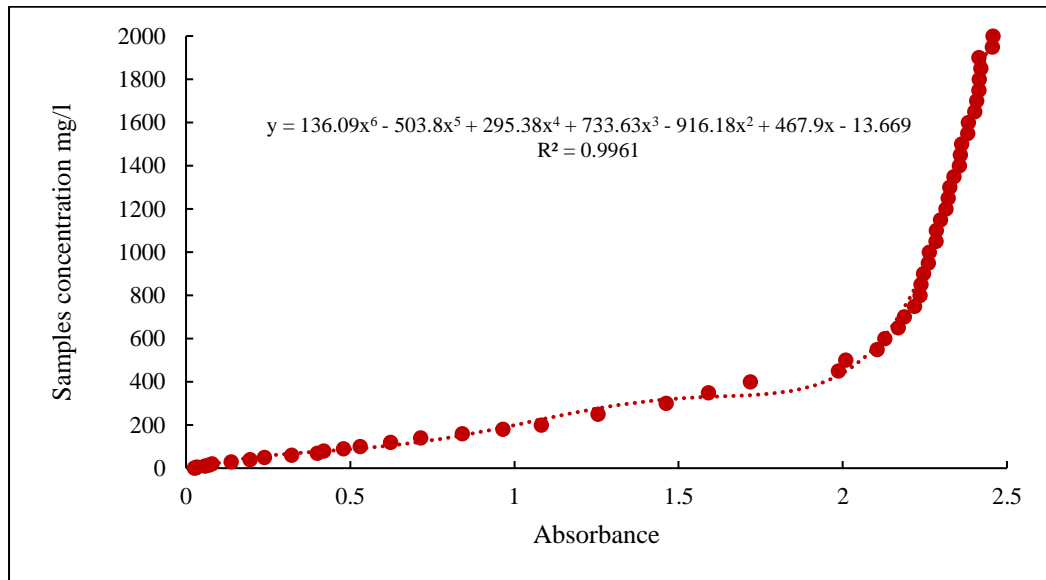


Figure 5.12. Spectrophotometric absorbance values at 525 nm that correspond to known concentrations of RDD

5.7.1.5 Residence time distribution RTD

As explained previously the RTD was measured by a 50 ml shot of tracer (RDD of 2g/l concentration) into the path of the influent stream that was pumped to the filters via submersible pumps at time $t = 0$. The tracer concentration, C , in the effluent stream was measured as a function of time. The depth of the packed materials in the filter rigs is a significant factor in the study of the hydraulic behaviour of the influent inside the wastewater treatment facilities. The depth of all packed materials was found to be 25 cm.

The experimental findings were analysed according to the moment method to determine the optimum flow rate for good influent dispersion during their transfer

through the selected packed materials. Equation 2.1 was applied to obtain the RTD curves as illustrated in the Figures 5.13 a-c.

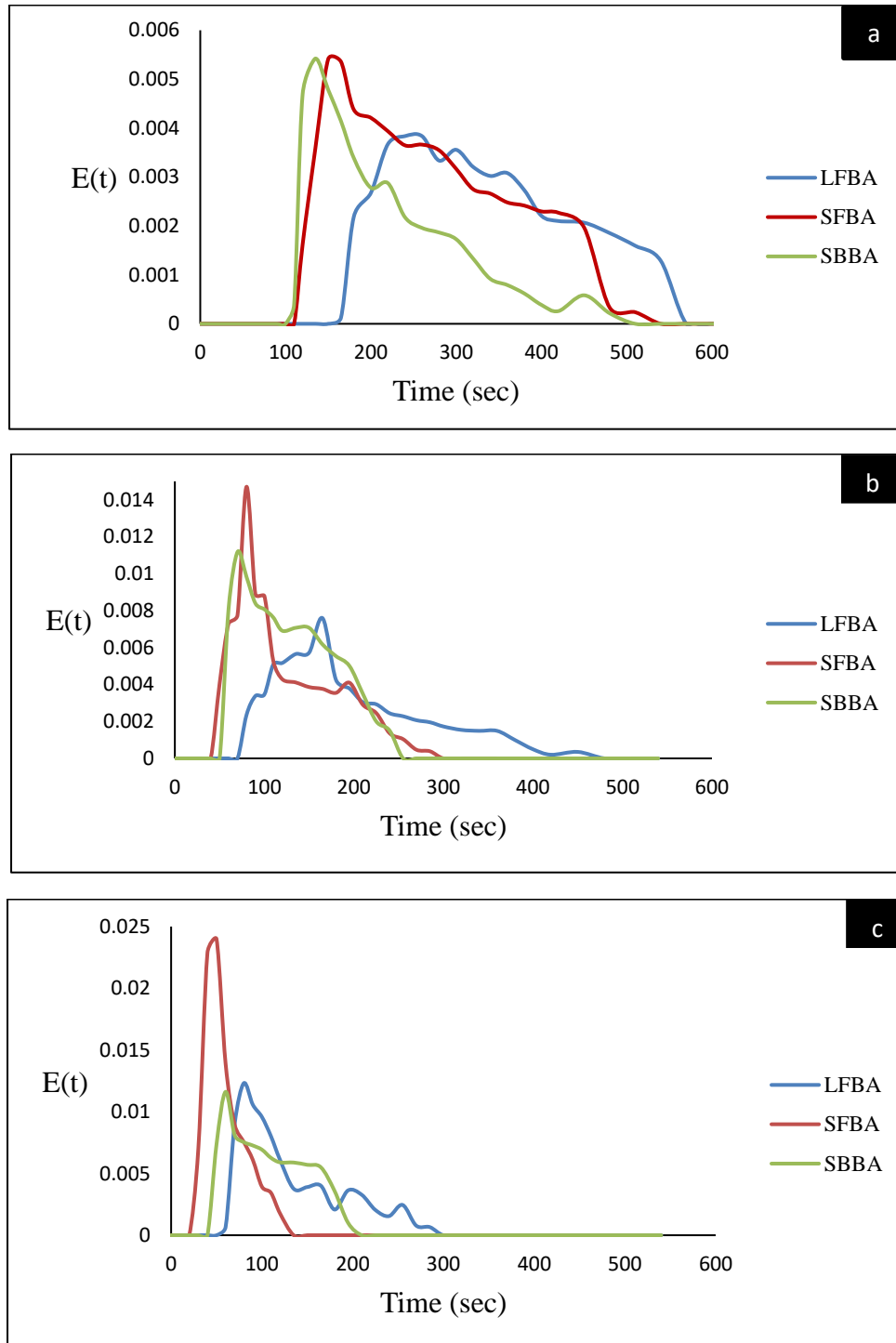


Figure 5.13. The residence time distribution curves for LFBA, SFBA and SBBA at different flow rates: (a) 0.5 l/min; (b) 1 l/min; (c) 1.5 l/min

The tracer totally passed through all filter materials during 410 to 440 sec at flow rate 0.5 l/min as shown in figure 5.13a. Comparatively, the tracer needed approximately 420, 210 and 250 sec for LFBA, SFBA and SBBA, respectively to pass through the filter media completely when the flow rate was 1 l/min as is clear in figure 5.13b. On the other hand, large quantities of the tracer exited from the filter materials in a short time at flow rates 1.5 l/min as presented in Figure 5.13c. Furthermore, the position of the peaks for the tracer that passed across the SFBA and SBBA appeared early in all the flow rates which were implemented compared with the position of the peaks for the tracer passed across the LFBA. When the flow rate increased, the time of peak appearance decreased between all filter materials. Fazolo et al. (2006) stated that the long tails present in the RTD curves referred to the dead zones or stagnations. In the present study, the RDD tracer was injected into the water path. Therefore, the influent did not include any solid particles that would create a dead zone. No long tails appeared in the RTD curves as shown in Figures 5.13 a-c, and the entire tracer was recovered.

The results revealed a good tracer distribution along filter materials at flow rate 0.5 l/min. comparatively; LFBA indicated a better tracer concentration distribution over the time than SFBA and SBBA when the flow rate increased. However, the filter materials presented good influent distribution over the flow rates 0.5 and 1 l/min. However, the tracer distribution drastically decreased when the flow rate increased to 1.5 l/min because of a large quantity of substance exit from the filter system in a short time.

5.7.1.6 Mean residence time MRT

It is very common to compare RTDs by using their moments instead of trying to compare their entire distributions. The mean residence time MRT is a significant moment in RTD study; from the measured RTD curve, MRT of the filter materials were determined. MRT is calculated according to equation 2.3 as illustrated in the literature review chapter. This equation will allow gaining a numerical value for the MRT that will help in comparing the retention time inside the filter materials. The values of MRT for all the filter materials are illustrated in table 5.3; the results suggested that the chance of tracer reacting with FBA was more than that for SFBA and SBBA over all flow rates.

Table 5.3. Process parameters and the MRT values for all filter materials

Run No.	Filter diameter (mm)	Flow rate (l/min)	Hydraulic loading rate (m/h)	MRT (min)		
				LFBA	SFBA	SBBA
1	100	0.50	3.8	6.24	5.18	5.24
2	100	1.00	7.6	3.35	1.61	1.69
3	100	1.50	11.4	2.24	0.69	0.75

Based on the results that were revealed by the RTD's curves and the MRT the flow rate at 1 l/min and below could be adopted as flow rate for these materials because it achieved a good tracer retention time and distribution. While the flow rate above this range is caused poorly distribution inside the filter media.

5.7.2 Investigating the filter materials efficiency

Laboratory made phosphate solution was pumped into the upflow filtration system; then the phosphate removal rate was investigated when the LFBA is the packed media. Under the same experimental conditions, the SFBA and SBBA were packed in the filtration system to determine which filter media presented a better treatment performance amongst them. The samples were collected during continuous flow cycles. The time per cycle was approximately 8 min, and the experiment was run several times to make certain which filter media will show outstanding performance for phosphate removal.

From the obtained results for LFBA, the phosphate removal rate is about 96% and 100% for cycles 1 and 2, respectively. It is noticeable there is a drastically reduced phosphate amount at the first cycle as shown in figure 5.14.a. The phosphate removal was achieved completely after the next cycle. On the other hand, SFBA exhibited the same phosphate removal pattern of LFBA. After one cycle, 88% of phosphate was removed and 97.5% of the total phosphate had been removed after the second cycle. The total removal was achieved at the third cycle. The third material to be tested is SBBA, the phosphate removal pattern for SBBA looks the same as the pattern of previously tested materials. Furthermore, it is clear the removal rates for SBA were lower than other filter materials as shown in figure 5.14.a. The removal rates were 0.75, 90.3 and 96% for cycles 1, 2 and 3, respectively. However, the phosphate was removed completely after the fourth cycle.

In comparison with the results of the first two cycles, the phosphate concentration has decreased sharply by all filter materials as shown in figure 5.14.a, and LFBA presented the best phosphate removal. The experiment was carried out for two more runs as

shown in fig. 5.14.b. and c to observe if there are any changes happening in the removal rate pattern. The similarity in removal behaviour for LFBA and SFBA was due to the fact that the limestone and sand surface have been coated by the same coating material FBA; this mean they are almost having the same chemical characteristics for their surface that contribute to the retention of phosphate. SBBA showed lower phosphate removal comparatively to LFB and SFBA as shown in figure 5.14.a to c. This indicates that the material which has been coated by FBA presented better phosphate retention than the material coated by BBA. Based on the results of the XRF as shown in table 5.2, the FBA contained slightly more Al_2O_3 and Fe_2O_3 than BBA. Hence, the chemical characteristic is considered the core factor in the process of phosphate removal. LFBA has achieved a complete phosphate removal in shorter periods than SFBA. It might be the physical characteristics for limestone which have the positive impact to introduce the LFBA as the more efficient filter media. According to the SEM images as shown in figure 5.4 the LFBA offered a larger total surface area to contact with influent than the other materials.

Based on the finding above, the LFBA presented an outstanding performance for phosphate removal. Therefore, it has been selected to be introduced as filter media for phosphate removal in upflow filtration system.

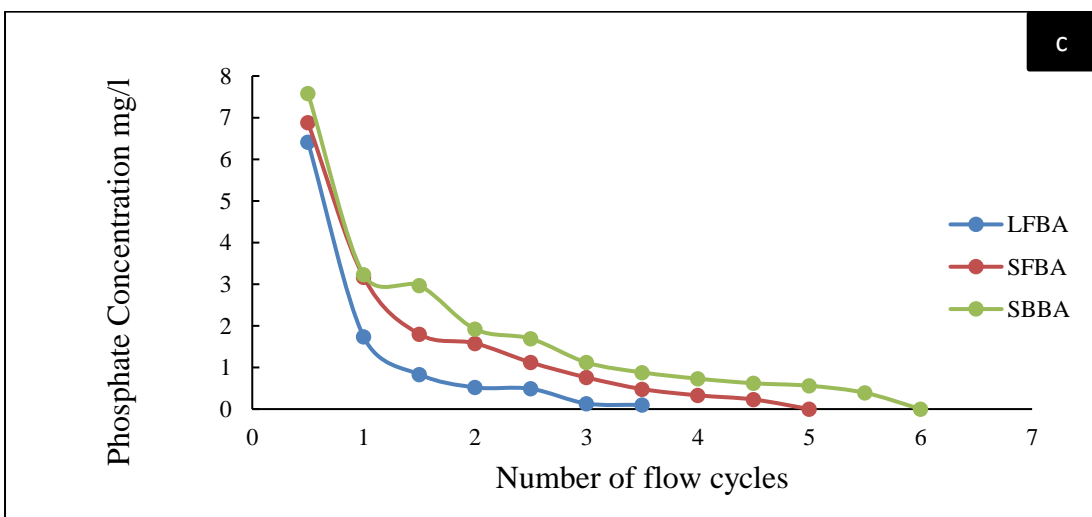
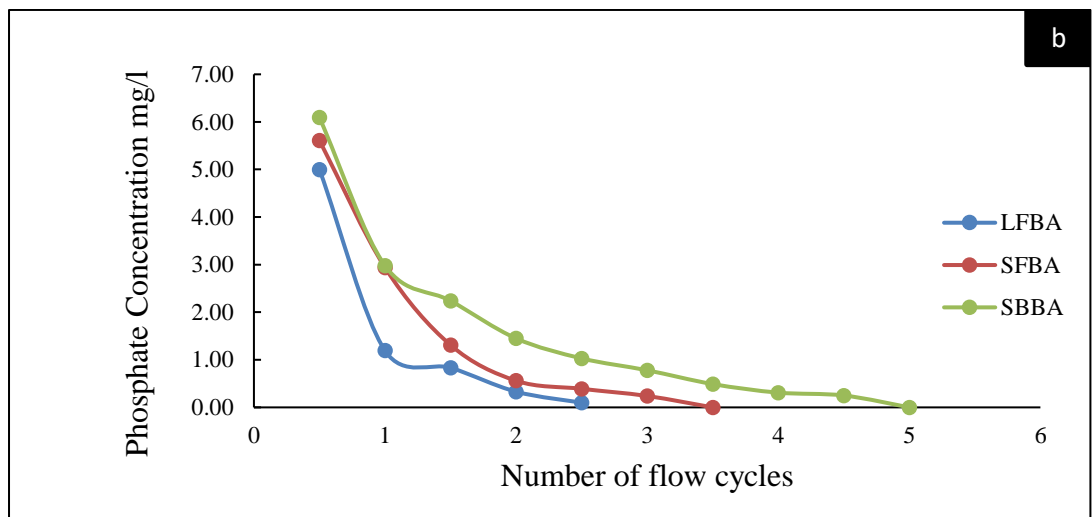
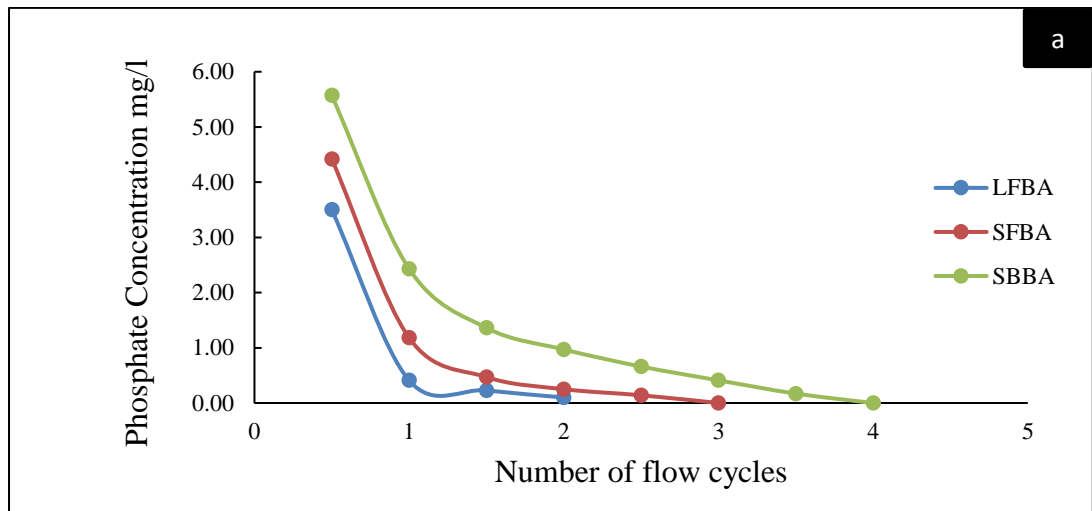


Figure 5.14. Investigate the efficiency of the filter materials for phosphate removal

5.8 Safety examination

Some researchers indicate that the bottom ash and fly ash, which are produced from power generation plants, contain several heavy metals such as Pb, Zn, Cd and Cu. However, bottom ash releases fewer heavy metals than fly ash (Mangialardi et al., 1998). Nevertheless, the fly ash and bottom ash are utilized for the adsorption of heavy metal contaminants in water and wastewaters (Gupta and Torres, 1998). According to the XRF analysis, which was obtained for LFBA as shown in table 5.2, it consists of BaO, P₂O₅, SrO, MnO, ZrO₂, ZnO, Y₂O₃ and CuO. All these oxides are available with minor weight percentages. However, before embarking on the study of the validity of LFBA for phosphate removal from wastewater treatment an inspection for materials' safety was conducted. Atomic absorption spectroscopy AAS was utilized to determine the concentration of heavy metals which were expected to leach from LFBA and SFBA. The results revealed that the concentrations of leaching samples for heavy metals such as Zn, Cd and Cu are very low and approaching zero. While the Pb concentration was 0.005 mg/l, according to the Environmental Protection Agency, the EPA level for Pb in water delivered to users of public drinking water systems is 0.015 mg/l (EPA, 2016). Consequently, LFBA is safe to introduce as filter media for phosphate removal.

5.9 Adsorption isotherm study

Several isotherm models were utilized in analysing the data of experimental adsorption equilibrium to interpreting the adsorption mechanism. In this work, the sorption isotherms determined experimentally were evaluated using the Langmuir model and the Freundlich model, which are widely used to describe phosphate

retention isotherms for natural materials; both models are described in detail as shown in the literature review chapter.

5.9.1 Batch technique and adsorption Isotherms

Batch experiments were conducted to obtain the required data for isothermal models. Phosphate solutions were brought into contact with different FBA masses at various temperature ranges (10, 20 and 30°C) to identify the variation of phosphate sorption behavior by LFBA according to isothermal models. The temperature was controlled by placing the flasks in a water bath. The suspension was shaken at constant speed (100 rpm) for 2 min merely to allow all the surface area to come in contact with solution ions then left to stagnate over the course of the experiment to avoid the effect of mixing on the sorption results. In the previous batch experiments, the LFBA mass was 23 g and the volume of solution was 40 ml to achieve material/solution ratio at 1/1.7. So, to obtain the required data for isothermal models, the amount of solution was kept at 40 ml and the LFBA masses were changed to 16, 23, 30 and 37. All samples were filtered through a 0.45 µm filter paper to exclude the suspension particles that may interfere in the scattering of light when applied to the spectrophotometer. All experiments were carried out in duplicate, and the average value used. An additional flask containing 40 ml of phosphate solution was run as a blank over all experiments.

5.9.2 Adsorption isotherm models

The behavior of phosphate adsorption at different temperatures is illustrated in figure 5.15, which represents the function of equilibrium of phosphate concentration (C_e) vs. mass of adsorbed per mass unit of adsorbent (q_e). The results

revealed a similar pattern of phosphate adsorption by LFBA at different experimental temperatures. However, the adsorbed phosphate at 20°C looked much better than the adsorption at 10 and 30°C. Moreover, the lowest value of adsorbed phosphate at 20°C (0.025 mg P/l) seemed to be higher than the adsorption at 10 and 30°C.

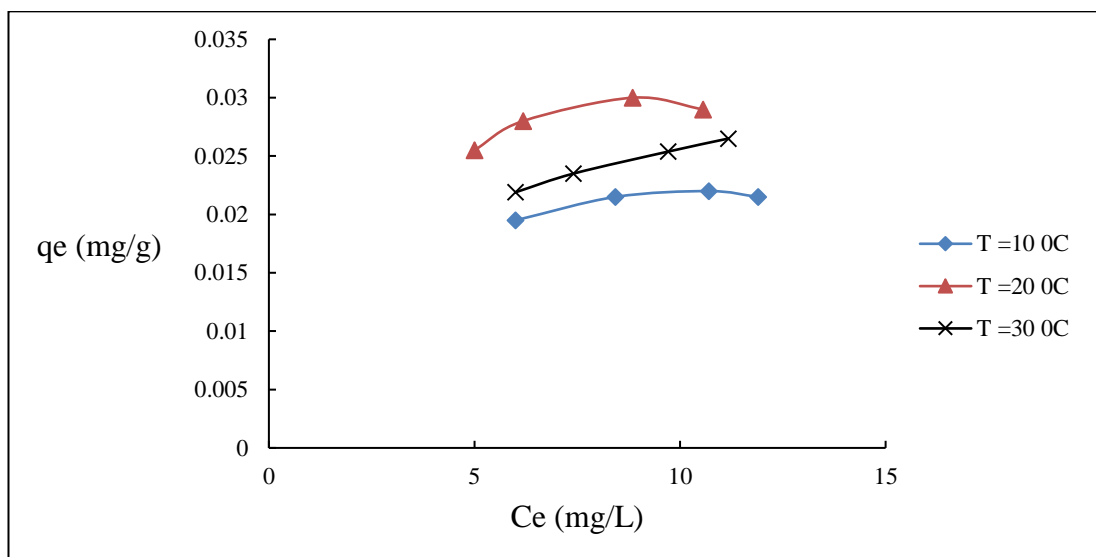


Figure 5.15. Adsorption isotherms of phosphate on LFBA

Langmuir and Freundlich isotherm models were applied to describe the distribution of ions between the liquid phase PO_4^{3-} and the solid phase LFBA. The linear form of the Langmuir equation is represented in equation 2.8 leading to the redrawing of the adsorption isothermal relationship as the inverse of equilibrium concentration $1/C_e$ vs. the inverse of the mass of adsorbed per mass unit of adsorbent $1/q_e$, as shown in figure 5.16.

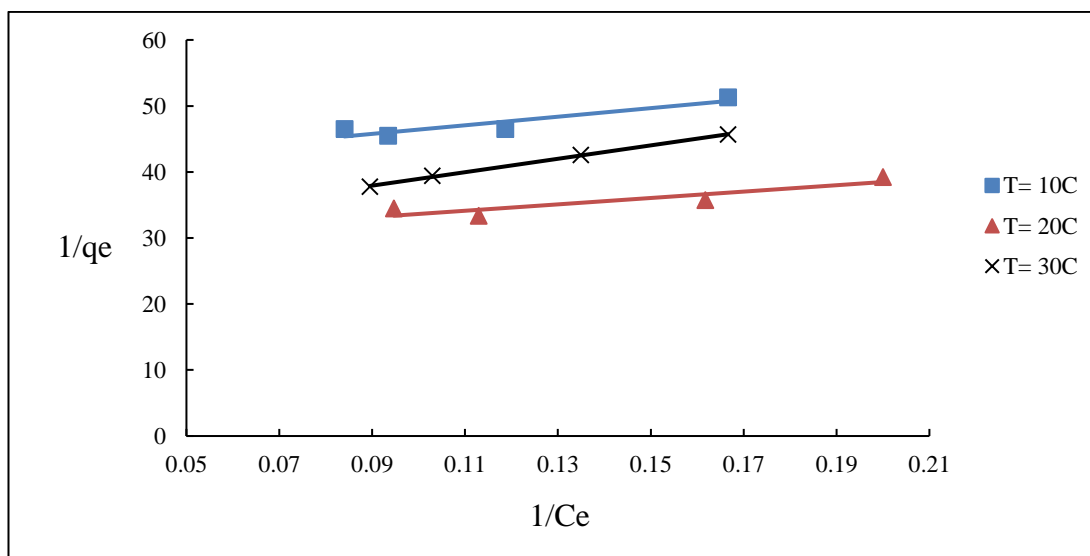


Figure 5.16. Langmuir isotherm model (1/Ce vs. 1/qe)

The determination of the maximum phosphate adsorption by the LFBA surface indicated the LFBA saturation point. The constant (Q) in the Langmuir equation represents the maximum adsorption by the surface. This constant was obtained from the interception of the plot in figure 5.16. As shown in Table 5.4, the maximum adsorption capacity for LFBA at 20°C can be estimated as 0.035 mg/g. This result indicates that the LFBA had a higher affinity for PO₄⁻³ at 20°C in comparison with the values at 10 and 30°C, where the maximum adsorption capacity was 0.02 and 0.03 mg/g, respectively.

Table 5.4. Langmuir and Freundlich isotherm models' parameters for PO₄-3 adsorption on LFBA

Temperature (°C)	Langmuir				Freundlich		
	Q	K	R ²	R _L	K _f	n	R ²
10	0.020	0.7	0.69	0.11	0.013	7.77	0.64
20	0.035	0.6	0.83	0.12	0.020	5.58	0.75
30	0.030	0.3	0.77	0.22	0.011	3.75	0.69

The coefficient R^2 has indicated that the phosphate adsorption by LFBA gives a good fit with the Langmuir model as seen from the values of regression coefficients presented in table 5.4. The data well obeyed the Langmuir model at 20°C where the R^2 value was 0.83. The slope of the plot of $1/q$ vs. $1/C$ gives the value of constant K . The K and the initial phosphate concentration (C_i) were applied to estimate the affinity between the PO_4^{3-} and LFBA using a constant called separation factor or equilibrium parameter (R_L) (Yousef et al., 2011), which can be expressed as follows:

$$R_L = \frac{1}{1 + K C_i} \quad \text{Equation 5.1}$$

The values of R_L between 0 and 1 indicate favorable adsorption while R_L values over 1 indicate unfavorable adsorption. The values of K are illustrated in Table 5.4. These parameters were used to calculate R_L values; from Table 5.4, the R_L values were found to be 0.11 to 0.22, which identified the favorability of phosphate ion to adsorb onto LFBA.

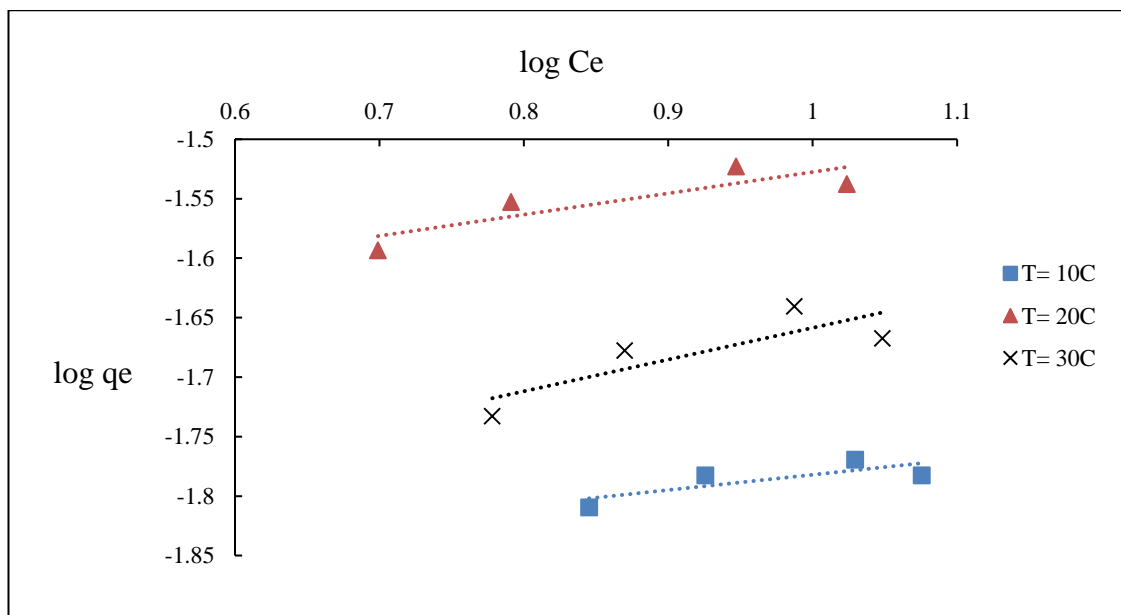


Figure 5.17. Freundlich isotherm model (log Ce vs. log qe)

The Freundlich isotherm is another model that was applied in this investigation. The Freundlich constants K_f and n were calculated from the intercept and slope of the straight line as shown in Figure 5.17. The n values of the range of 2–10 represented good adsorption (de-Bashan and Bashan, 2004). As shown in table 5.4, the values were found to be in a range of 3.75–7.77. The Freundlich constant K_f was found to be related to the adsorption capacity. The adsorption capacity at a temperature of 20°C was found to be better than the other values obtained at other temperatures. Based on the findings of the isothermal models, LFBA has a good affinity for PO_4^{3-} ions, and its adsorption capacity decreased with the increase or reduction in the optimal temperature (i.e., 20°C).

5.10 Chapter discussion

The decision to apply coating technology has been made due to the efficient phosphate removal by FBA and BBA, and the good physical characteristics of limestone, white dolomite and sand. Utilizing solid materials in coating technology is significant to develop the physical characteristics of newly created filter materials. While materials such as FBA and BBA are the source of phosphate removal in coating technology. Coating them as grounded materials will lead to increase the chance of contact between them and the influent. Hence, increasing the filter materials efficiency. Limestone coated by FBA (LFBA) has presented better phosphate retention than other prepared coated materials when they are employed as a filter media in upflow column tests. The main reasons for LFBA effectiveness can be described according to the SEM and XRF findings. Based on identifying and observing the exterior surface morphologies of the created coated materials via SEM, limestone surface morphology looks more complex than other materials because there are many bends and

protrusions with a fine diameter distributed on the surface. Additionally, FBA contains a higher percentage of Fe/Al oxides than BBA according to XRF analysis.

5.11 Chapter summary

The coating process included coating the solid materials such as limestone, white dolomite and sand by powder materials such as FBA and BBA. Utilizing solid materials such as limestone, white dolomite and sand in coating technology is important to develop the physical characteristics of new created filter materials. Materials such as FBA and BBA are the source of phosphate removal in coating technology. Coating them as ground materials will lead to an increase in the chance of contact between them and the influent. Hence, increasing the filter materials' efficiency. Ordinary Portland cement OPC is the binder, which is utilized to produce a bonding between the mixture materials; the water is the catalyst of binder activation. The bonding between the mixture materials occurred as a result of hydration of OPC. The hydration process caused the release of calcium hydroxide, which reacts with the mixture materials to produce a bonding by creating calcium-silicate hydrates (C-S-H). The physical characteristics of all new media have approximately the same features of the support media with a slight increase in porosity and decrease in bulk density. According to the results of XRF, the amounts of Al_2O_3 and Fe_2O_3 were reduced for all new products because the reaction of coating materials with the calcium hydroxide that is released from OPC hydration will consume these oxides to produce cementitious compounds.

Based on visual inspection of SEM images, the materials, which have been coated by FBA, offered a more heterogeneous surface nature than the same materials when coated by BBA.

MATLAB 16a was adopted as the analysis program to describe the surface morphology of the new created materials. This method of image processing analysis

helps in providing a graphical and numerical finding, which can be adopted in validation of visual inspection of SEM images.

Depending on the batch experiments, results the LFBA, SFBA and SBBA were considered the most efficient materials when they achieved a significant phosphate removal. These materials have been adopted to investigate their removal efficiency when they are packed in lab-scale filter.

RTD experiments were conducted, and it has been identified that 1 l/min is the maximum flow rate that could achieve an admissible influent dispersion inside filter materials.

LFBA presented an outstanding performance for phosphate removal in comparison with other materials, which were also tested in the lab-scale filter. Therefore, it has been selected to be introduced as filter media for phosphate removal in upflow filtration system.

The coating technique which was introduced in this chapter provided a sustainable solution to be adopted in wastewater treatment; specifically, phosphate removal. This coating method has achieved the sustainability approach by utilizing waste materials as a source of phosphate removal and a minor percentage of OPC as a binder. Consequently, achieving recycling of waste materials, and reducing energy consumption because most coating technologies utilized heat source as a coating binder.

Four factors have a key impact on the characteristics of the produced filter media; quantity of coating dosage, OPC ratio, water ratio and curing time. The mixture ratios were determined depending on previous review and laboratory judgment. In the next chapter, an optimization process has been conducted to determine the optimal mixture percentages, which achieve best phosphate removal.

CHAPTER 6 OPTIMIZATION OF COATING PROCESS

6.1 Chapter introduction

Recently, many researchers and industrialists have been trying to move on to develop their products via follow a various optimization strategies, which can achieve the highest feasible efficiency for the products (Zbicinski et al., 2006). In general, the optimization process includes developing any aspects that contribute directly in the production process. The optimization process can help to make the product most cost effective or achieve the highest performance; by maximizing the factors which have a positive influence and reducing the factors which have a negative influence. The cost should be taken into consideration when maximizing the desirable factors in the optimization process to attain the highest positive outcomes. The chapter provides an overall description of the optimization process that focuses on developing the quantities of additives in the process of forming the LFBA to select the mixture that achieves best phosphate removal. The optimization process is considered as a core part in most engineering activities. However, in many situations, the optimization is performed by trial and error. In this current case, the conditions and quantities that contribute to the formation of the LFBA such as water ratio, OPC, coating dosage and curing time have been suggested based on information extracted from the literature review. Therefore, the optimization process in this case has a start point to maximize and minimize these conditions and quantities to ensure a better mixture can be found for phosphate removal by LFBA.

The second part in this chapter concentrates on constructing a predictive model based on the experimental results that were obtained from the investigation of the optimal filter media. The model describes the behaviour of phosphate removal via LFBA, by

translating the experimental results into an equation. This model will help to understand the influence of the factors, which contribute to the formation of the LFBA independently, or as a combination, on the capability of the LFBA to remove phosphate. In addition, the model allows us to predict the removal outcomes when applying the factors in conditions and quantities that were not measured experimentally.

6.2 Obtain optimal filter media

The essential step in the process of creating the new filter media is adding a combination of chemicals such as FBA and OPC to establish a bonding between them and the supporting material (limestone). The proposed chemicals' quantities are responsible for the nature of the chemical and physical properties for the produced media. In addition, the chemicals' reaction depending on the quantity of added water and curing time. In this part of the research, all factors that have a key impact on the final production of filter media were subjected to an investigation to introduce the most feasible mixture which achieved better phosphate removal. The optimization process started with water, OPC, FBA ratio and curing time respectively. The factors examination was considered in this sequence according to the order of utilization of the factors in the process of LFBA formation.

6.2.1 Optimization process

According to the findings of the lab-scale filter experiments in the previous chapter, the LFBA was presented as the most efficient mixture for phosphate removal. The first LFBA mixture consisted of 50% FBA and 5% OPC of the dry weight of limestone, 35% water ratio of FBA and OPC mixture and the curing time was 28 days. Therefore,

these percentages will be altered to enhance the performance of LFBA in terms of phosphate removal. Table 6.1 shows the experimental conditions applied to obtain the optimal created filter media.

Table 6.1. Optimization process the factors which influence on the efficiency of created mixture for phosphate sorption

Variables Test No.	FBA dosage %	Binder (OPC) %	Water ratio %	Curing time (days)
Water ratio				
1	50	5	25	28
2	50	5	35	28
3	50	5	45	28
4	50	5	55	28
Binder (OPC)				
5	50	2.5	a	28
6	50	5	a	28
7	50	10	a	28
FBA dosage				
8	30	b	a	28
9	40	b	a	28
10	50	b	a	28
Curing time				
11	c	b	a	7
12	c	b	a	14
13	c	b	a	28

^a Selected optimum water ratio.

^b Selected optimum binder dosage.

^c Selected optimum FBA dosage.

* The weight of limestone in all the tests is 1500 g.

6.2.2 Water ratio

The study starts with water ratio because it is the catalyst for the additives' reaction to form the final composition of LFBA. In other words, added water is the start point of

the process of creation of the LFBA. Based on a wide literature review the quantity of added water should be taken into consideration because it affects the workability of the binder. The water ratio is extremely sensitive for additives' reaction. Thus, the low added water quantity negatively affects the formation of the final product characteristics. While, if water quantity exceeds the required value, a segregation of material occurs and this will lead to influence on the strength of bonding between the materials greatly. In the last test regarding determining the efficiency of supporting material, the applied water ratio was 35%. For the optimal water ratio, the other factors were kept the same and the water ratio applied at 25%, 45% and 55% of the dry weight of FBA and OPC. The results that are presented in figure 6.1 revealed that the water ratio at 35% tends to be the optimal ratio.

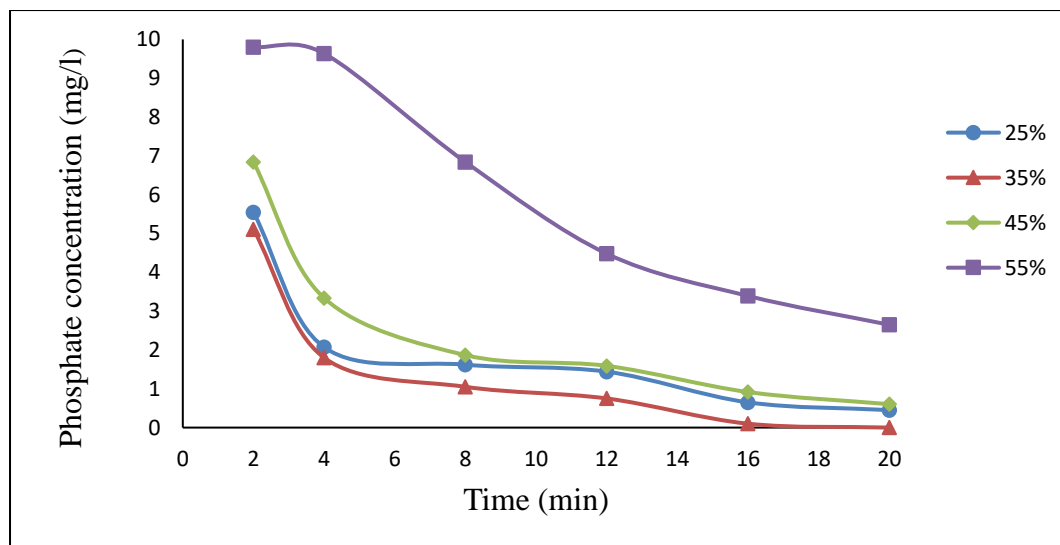


Figure 6.1. Effect of water ratio on the removal of phosphate

Reduction of the water quantity to 25% caused a drop in the capability of filter media to treat the phosphate. At the beginning, a slight difference occurred in phosphate concentration between water ratio 25% and 35%; but the difference increased during the experiment time. Specifically, after 4 min. On the other hand, increasing the water amount to more than 35% leads to a minor reduction in mixture removal efficiency as

shown for the results of water ratio 45% and 55%. Comparatively, there was a minor reduction in removal efficiency when the water ratio was set at 25% and 45%. However, a significant drop happened when the water ratio was 55%. This indicates that the water ratio over 45% is totally undesirable, and water ratio 35% is still the most favourable and will be adopted in the following experiments.

6.2.3 OPC ratio

Increasing the OPC amount in the mixture will positively affect the strength of the materials' bonding, consequently, achieving a successful coating process. On the other hand, it negatively affects the chemical composition of new filter media. Especially, the availability of Al_2O_3 and Fe_2O_3 , which are responsible for the phosphate capture from the influent. In more details, hydration of OPC increases significantly in the presence of pozzolanic material (Thomas, 2007, Dunstan Jr., 2011). Previously, the FBA was identified as pozzolanic material. Therefore, decreasing the OPC ratio is important to avoid further hydration, which could alter the effective properties of FBA. The following change was carried out on the OPC ratio to determine the amount of OPC required for achieving the optimal phosphate removal. Two mixtures were prepared at water ratio 35% and OPC ratio at 2.5% and 10% of the dry weight of the limestone, respectively. The findings of both mixtures were compared with the first mixture (5% OPC ratio) as shown in figure 6.2.

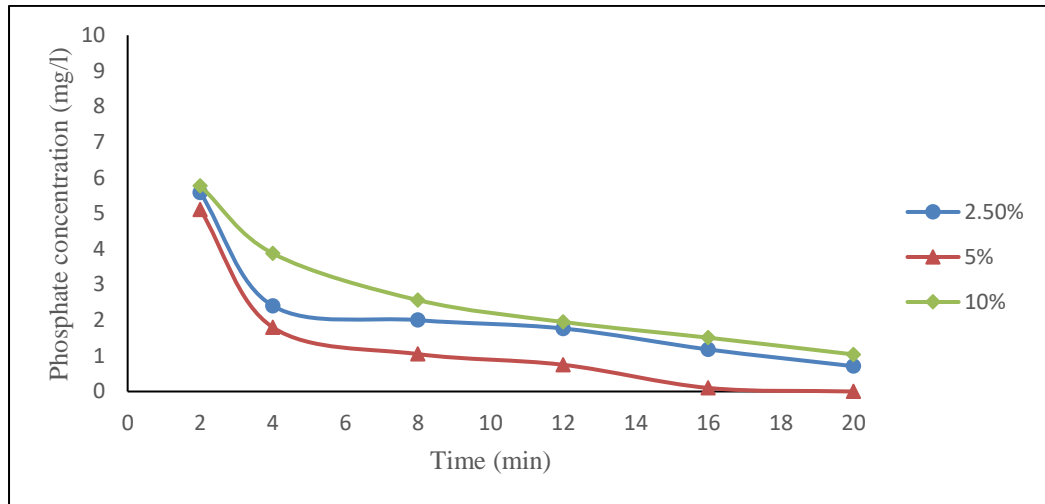


Figure 6.2. Effect of OPC ratio on the removal of phosphate

It is observed that the phosphate concentrations for all mixtures were drastically reduced after 2 min. Then after a further 2 min, the difference in phosphate removal starts to increase. The mixture ratio 5% achieved better phosphate removal over the course of experiment in comparison with other OPC ratios. While minimising the OPC ratio to 2.5% caused a minor drop in phosphate concentration, and increasing the OPC ratio to 10% led to a reduction in the removal performance more in comparison with an OPC ratio of 5%. The results showed that the alteration in OPC ratio is very critical for the LFBA characteristics because the outcomes were not correlated to any increase or decrease in the quantity of OPC. Reducing the binder ratio to 2.5% might cause weakness in bonding between the binder and materials of the mixture which leads to a reduced chance of the FBA (source of phosphate removal) to bond over the limestone surface. Increasing the OPC ratio to 10% has a negative influence on removal performance also because of increasing the formation of cementitious bonds and this will reduce the availability of Al_2O_3 and Fe_2O_3 . The experimental results introduced the OPC at 5% as the preferable ratio to maintain the phosphate removal and the bonding strength of mixed materials.

6.2.4 Coating dosage

FBA is the main material for the coating process because it is representing the core material that forms the surface's morphology in the fabrication process of LFBA. The goal of optimizing FBA is to produce a coated media while maintaining the same chemical composition as at the start before fabricating the new media. Therefore, the optimal quantity of OPC was identified firstly because it has a direct effect on the FBA characteristics.

The optimum amount of FBA is determined correspond to the OPC ratio because the reaction between them generates the final form and properties for the new filter media. Previously, the optimum OPC ratio was already determined at FBA ratio 50% of the dry weight of the limestone. During the filter media preparation, an amount of the mixture of FBA and OPC has been lost as a result of crushing media to obtain the filter media as particles. Therefore, FBA ratio was investigated at under 50% to reduce the loss of FBA. Two mixtures were prepared at optimal water ratio and OPC ratio 35% and 5%, respectively, and FBA dosage 30% and 40%. Figure 6.3 shows the filter media at FBA ratio 40% tends to be efficient at approximately the same level as when the FBA ratio is 50%. While, when the FBA ratio was reduced to 30% the phosphate removal efficiency was decreased.

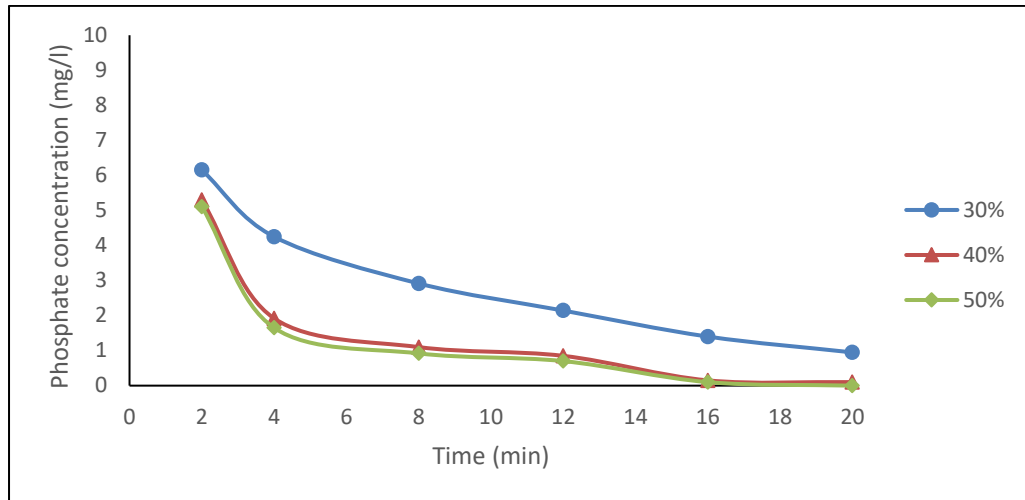


Figure 6.3. Effect of FBA dosage on the removal of phosphate

Although, FBA is a waste material and available for free, controlling the percentage used in the mixture is useful in terms of environmental and economic issues. The optimum amount of FBA that can be used in the filter media mixture is significantly impacting on reducing the waste that results from crushing the mass of mixture to obtain the final product form. According to the experimental results utilizing FBA ratio at 40% maintains the phosphate removal efficiency and reduces the quantity of FBA, which is applied in the coating process.

6.2.5 Curing time

Controlling the rate of moisture loss during the OPC hydration is very necessary. In order to obtain the required strength which achieves the binding between materials of the mixture. According to the construction industry, the OPC requires 28 days to cure and reach 100% of its strength (Barger, 2013). Therefore, all previous tests were applied at 28 days to cure the mixtures. Studying the influence of curing time on the new filter media helps to determine the actual required preparation time. Several researchers studied the OPC curing at different periods. For example, [1] studied OPC curing at (1, 3, 7, 14, 28 days). While, [2] extended the investigation of OPC curing

for (90, 180, 365 days). Curing must be undertaken for an acceptable period to achieve the potential strength of the mixture contents, whereas excessive curing time may lead to unnecessary delays. In this current study, the performance of phosphate removal for the LFBA was tested at curing time 7 and 14 days. Then the results were compared with mixture removal performance of samples which had been cured for 28 days as shown in figure 6.4.

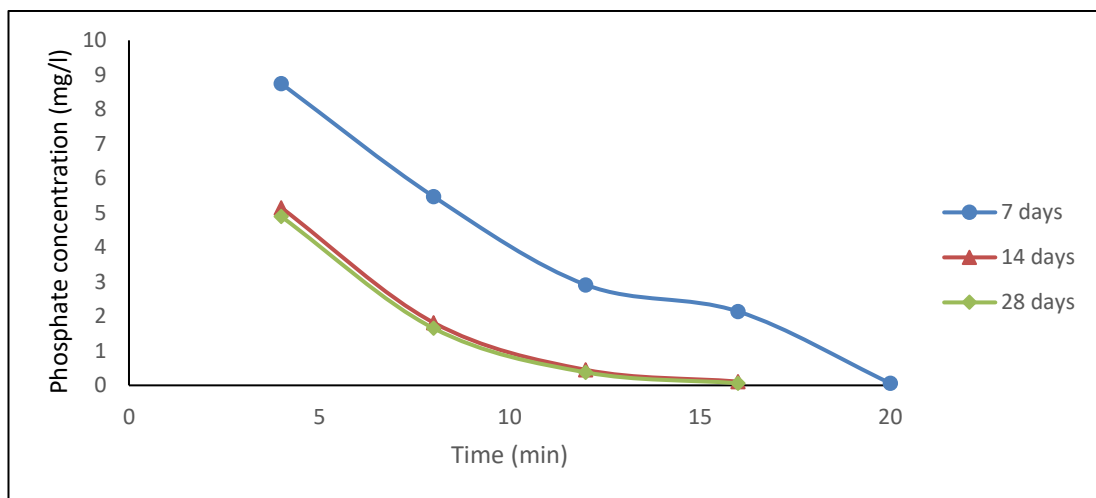


Figure 6.4. Effect of curing time on the removal of phosphate

The filter media at curing time 7 days presented a low phosphate removal efficiency compared to filter media at 14 and 28 days. While the removal efficiency at 14 and 28 days looks approximately the same. According to the results, the portion of OPC that is added to the mixtures is recommended to be cured for a minimum period of 14 days to achieve the adequate reaction between the mixed materials. The pozzolanic characteristics of FBA contribute to the development of the strength of the mixture; it works as secondary reaction to accelerate the materials' binding, consequently, reducing the curing time. It isn't necessary to extend the investigation for longer curing time than 28 days because the mixture gained the similar characteristics at curing time 14 and 28 days.

Finally, it could be concluded that the filter media, which includes 35% water ratio of the dry weight of OPC and FBA 5% OPC and 40% FBA of dry weight of limestone and 14 days curing time, presented outstanding performance and suitability for economic and environmental approaches.

6.3 Multiple regression technique

The previous part of this study calls attention to the fact that the phosphate removal via LFBA is affected by the factors which contribute in forming the LFBA such as water ratio, OPC, coating dosage and curing time. The process of obtaining the most efficient filter media was performed by optimizing the factors consecutively. In order to investigate the combined influences of these factors on phosphate removal using LFBA, an empirical model was required to illustrate these relationships; a statistical model that allows examination of how multiple independent variables are related to a dependent variable. Once it identifies how these multiple variables relate to the dependent variable, we can take information about all of the independent variables and use it to make much more powerful and accurate predictions. Based on these considerations and the obtained experimental data, a statistical model was developed by applying the principles of multiple regression technique, using SPSS23. In addition, the statistical significance of each individual factor and its contribution to the predication of the removal efficiency were calculated.

Multiple regression is a very advanced statistical tool and it is extremely powerful when trying to develop a model for predicting a wide variety of outcomes. The outcomes of the multiple regression allow making predictions about variables based on available knowledge about involved variables. In this study, multiple regression is used to model the relationship between phosphate removal as a dependent variable

and time of removal, water ratio, OPC, coating dosage and curing time as independent variables. Every value of these independent variables is associated with a value of the dependent variable. More specifically, multiple regression analysis helps to understand how the typical value of the dependent variable changes when any one of the independent variables is varied, while the other independent variables are held fixed.

6.3.1 Assumptions of multiple regression model

(Pallant, 2005) reported that to construct a reliable multiple regression model, many assumptions are required to be considered such as sample size, multicollinearity, outliers, significance of independent variables and coefficient of determination. Sample size is the assumption that can be determined before constructing the model and the rest of the assumptions can be calculated from the model outcomes.

6.3.1.1 Sample size

The multiple regression analysis is a complex tool and not appropriate for small sets of data as the results obtained cannot then be generalised to other sets of data (Pallant, 2005). Therefore, addressing the minimum desired sample size is a significant issue. Knofczynski and Mundfrom (2008) stated that the interest of researchers using the multiple regression as a powerful statistical analysis tool led to a call to address the required sample size which produces a reliable model. While, (Maxwell, 2000) mentioned that “sample size will almost certainly have to be much larger for obtaining a useful prediction equation than for testing the statistical significance of the multiple correlation coefficient” (p. 435). Several researchers provided some guidelines to the minimum sample size needed for accurate predictions, Tabachnick and Fidell (2001)

recommended to consider the following formula to calculate the required sample size to perform the multiple regression analysis:

$$N > 50 + 8 * IVs \quad \text{Equation 6.1}$$

Where N and IVs are the sample size and number of independent parameters respectively. Obviously the minimum size of the required sample relies on the number of independent variables. In this current study, the number of IVs are five. According to the suggested formula by Tabachnick and Fidell the minimum size of the required sample N is 90. The obtained experimental data from the optimization process provides a sample size 100. Hence, the sample size looks appropriate to apply in constructing a multiple regression model comparative to the value of the minimum size of the required sample.

6.3.1.2 Multicollinearity MC

The reliable multiple regression model is based on data that have little or no multicollinearity. MC take place when the IVs are not independent from each other. More specifically, MC represent the high correlation amongst the IVs. Appearance of MC negatively influences on the multiple regression because it affects the determinations regarding individual predictors (Pallant, 2005). There are different MC diagnostic factors that can help to detect the existence of MC in the data such as correlation matrix, tolerance, Variance Inflation Factor VIF and condition Index. In this current model, the detection of MC was carried out by measuring tolerance and VIF.

The tolerance measures the impact of one independent variable over all other independent variables; the tolerance is calculated with an initial linear regression analysis. Tolerance is estimated as:

$$T = 1 - R^2$$

Equation 6.2

Where T is the tolerance and R^2 is the coefficient of determination. The low value of tolerance suggests that the variable under investigation is nearly a typical linear combination with the other independent variables. Thus, it is better to exclude it from the regression model. Based on this consideration all variables which are engaged in the linear relationship will have a low tolerance. Consequently, MC may be a significant issue preventing construction of a reliable model. According to the recommendations of some researchers, with a tolerance at level less than 0.2 the MC might be appearing in the data. While, Tabachnick and Fidell (2001) reported that the minimum acceptable level of tolerance is 0.1 and when the tolerance level is less than 0.01 the MC appears in the data certainly.

Variance inflation factor VIF is another factor to diagnose the MC. The VIF is defined as:

$$VIF = 1/T$$

Equation 6.3

VIF is always greater than or equal to 1. (Pallant, 2005) stated that the values of VIF greater than 10 indicates the existence of MC.

After running the model, the results of table 6.2 allow us to inspect the existence of MC in the applied data.

Table 6.2. Tolerance and VIF values for each independent variable

IVs	Collinearity Statistics	
	Tolerance	VIF
Time of removal	1.000	1.000
Water ratio	0.950	1.053
OPC	0.983	1.018
Coating dosage FBA	0.855	1.169
Curing time	0.878	1.138

All IVs indicate tolerance levels greater than 0.2, where the minimum tolerance level achieved by coating dosage was at value 0.855 and the maximum tolerance level achieved by time of removal was at value 1.000. On the other hand, the VIF values were between 1.018 and 1.069. All VIF values are consistent with VIF definition because they are over 1; and at the same time less than 10. In comparison between the considerations and obtained data regarding the MC diagnostic factors, there is no MC existence in the utilized data. Consequently, there is no strong linear relationship between IVs.

6.3.1.3 Outliers

An outlier is a data point that is distant from the other points; Barnett and Lewis (1995) define an outlier to be ‘an observation or subset of observations which appears to be inconsistent with the remainder’ (p. 7). Outliers can be produced from different sources such as errors or the inherent variability of the data.

The outcomes of the multiple regression technique are highly sensitive to the existence of outliers. Therefore, it is essential to inspect for outliers to mitigate their negative influences on the model outcomes. Searching for extreme values should be a fundamental part in the process of initial data screening. Based on this consideration Pallant (2005) states that the collected data must be screened to remove such extreme points. The preferable outlier detection methods are usually selected due to their simplicity (Franklin et al.). ‘Most outlier detection methods use some measure of distance to evaluate how far away an observation is from the centre of the data’ (Franklin et al.). The presence of the outliers in the used data can be detected by calculating the Mahalanobis distances MDs and compare them with the critical values

listed in Table 6.3; any data point with MD greater than the critical value is considered as an outlier (Pallant, 2005).

Table 6.3. Critical values for the MDs (Pallant, 2005)

Number of IVs	2	3	4	5	6	7
Critical value	13.82	16.27	18.47	20.52	22.46	24.32

As previously identified, our model includes five IVs. Therefore, the obtained data points with MD are compared with critical value 20.52 as illustrated in table 6.3. The highest point that was obtained from analysing the data according to MD is 9.59; it is much lower than the critical value. Hence, there is no indication on existence of outliers in the data.

Tabachnick and Fidell (2001) define the outlier in multiple regression, as a data point with standardised residual SR greater than 3.3 or less than -3.3. Based on this definition investigating the outliers according to the SR is another attractive tool for checking the outlier existence. The pattern of the residual plot is shown in figure 6.5; all the residuals were distributed in the domain between 3.3 and -3.3.

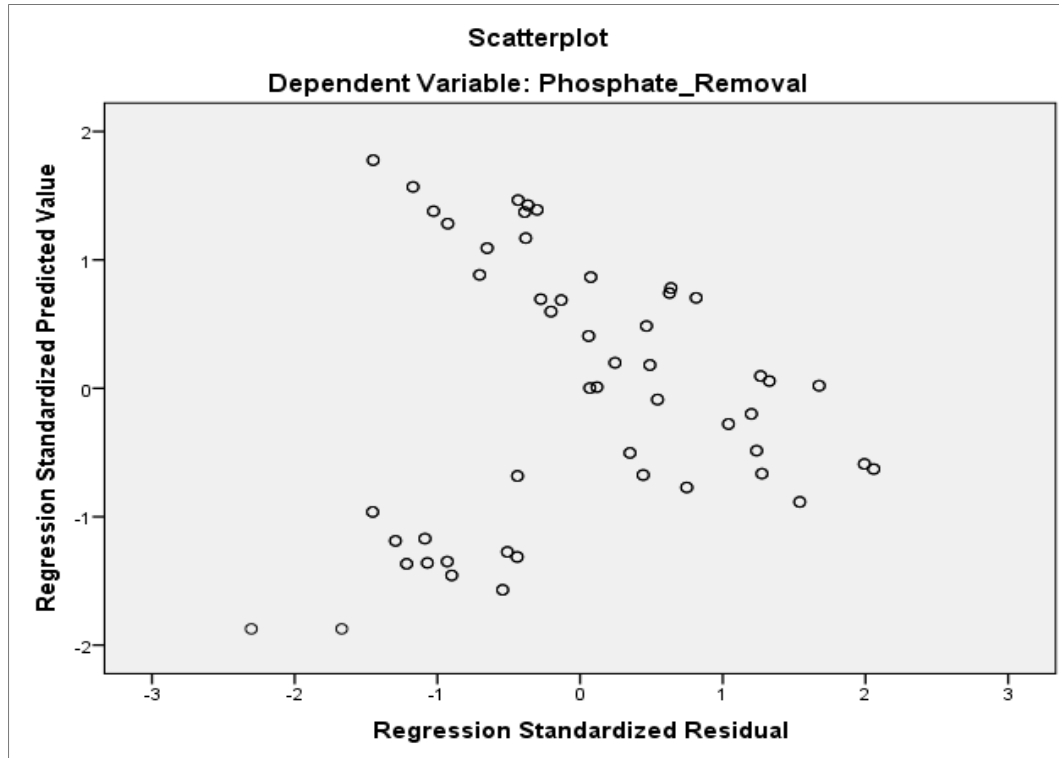


Figure 6.5. Plot of regression standardised residual

Again, there is no outlier existence in the data according to the SR plot. Finally, it can be estimated there are no outliers which have considerable impact upon the regression solution.

6.3.1.4 Normality of data

The linear regression analysis requires all variables to be approximately normally distributed. The normal distribution can be expressed as the data peak in the middle and is symmetrical about the mean. Data does not require to be exactly normally distributed to obtain a reliable regression model but approaching the data from normal distribution reflects positively on the regression solution. Non-normal data distribution can distort the relationships between the variables and reduce the model significance. There are several useful ways to check the assumption of normality such as histogram, normal P-P plot, skew and kurtosis. Histogram and normal P-P plot are two graphical methods which were performed as shown in figure 6.6 to assess the data normality.

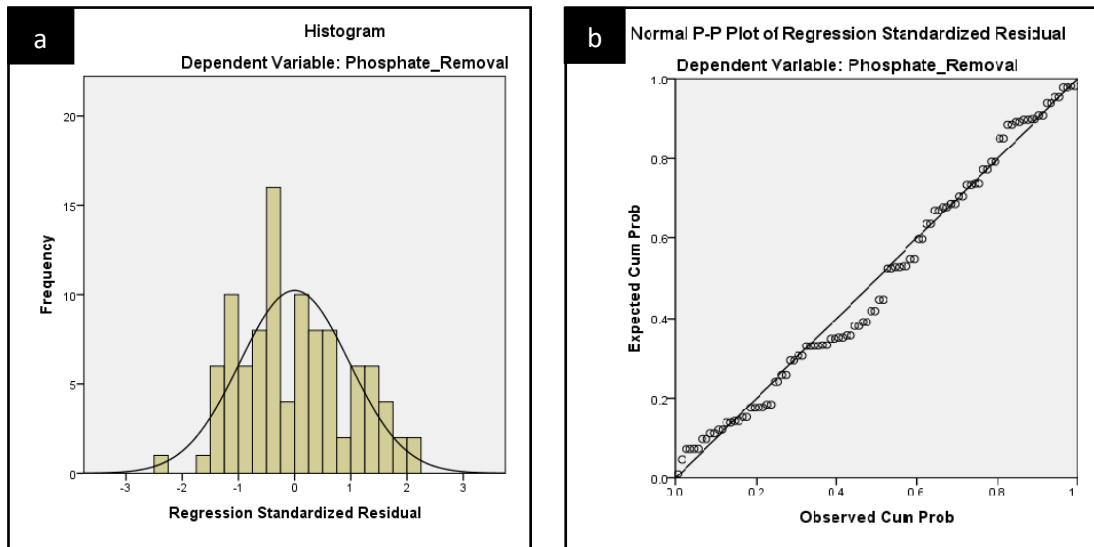


Figure 6.6. Data distribution for all variables, (a) data histogram (b) normal P-P plot

The histogram in figure 6.6a produces a smooth normal curve; the data peak in the middle and symmetrical. Moreover, the normal P-P plot in figure 6.6b also showed normal data distribution because the data is scattered close to the line and there are no clear data points coming away from the line. Based on the results of both graphs the normality can be assumed for this data.

6.3.1.5 Linearity and homoscedasticity of residuals

The aim of the linearity assumption is to identify the relationship between the dependent variable and IVs; if it is linear or not. On the other hand, homoscedasticity describes that the variance of error is the same across all values of the IVs.

The SR plot as shown in figure 6.5 indicates a symmetric residual distribution above and below the zero value and the variance is approximately constant across all IVs. Therefore, the linearity and homoscedasticity might be achieved in this data.

6.3.1.6 Evaluating the model

The purpose of this crucial step is to investigate the ability of the suggested model to explain the variation in the dependent variable (Pallant, 2005). The coefficient of determination R^2 is an efficient tool to achieve this purpose because R^2 shows how much of the experimental data is explained by the model. R^2 value is always between 0-1: the higher the R^2 , the better the model fits the experimental data (Tabachnick and Fidell, 2001).

The regression results comprise a table called model summary as shown in table 6.4; this table includes the value of R^2 .

Table 6.4. Model summary

Model	R	R Square	Adjusted R Square	Std. Error of the Estimate
1	0.875	0.766	0.753	12.63440

R^2 for this model is 0.766, which means that the IVs can explain about 76.6% of the change in dependent variable. This single summary number explains how strong the relationship is between all the IVs and the dependent variable in this model. R^2 at this value allows establishing the confidence in prediction of the dependent variable depending on the IVs.

6.3.2 Model parameters

This part of outcomes is concerned with the parameters that form and describe the model. This includes all the predictors, which make a considerable contribution to predicting phosphate removal. Table 6.5 presents all the model coefficients, which form the final multiple regression as an equation, especially β coefficient that represents the numerical values of individual contribution for each predictor.

Table 6.5. Coefficients of multi regression model

model	Unstandardized Coefficients		Standardized Coefficients	t	Sig.
	β	Std. Error	Beta		
Constant	64.140	10.480		6.120	
Time	3.048	0.179	0.852	17.056	0.000000
Water ratio	-0.675	0.173	-0.200	-3.898	0.000182
OPC	-0.850	0.728	-0.059	-1.166	0.0024600
Coating dosage	0.104	0.204	0.028	0.513	0.0060900
Curing time	0.058	0.190	0.016	0.302	0.0076300

The IVs represent the model's predictors as shown in the first part of the table, and each predictor is associated with β value, which forms the model equation as the following:

$$P = \beta_0 + \beta_1 T + \beta_2 WR + \beta_3 OPC + \beta_4 CD + \beta_5 CT \quad \text{Equation 6.4}$$

Where

P = phosphate removal percentage

T = time of removal

WR = water ratio

OPC = binder

CD = coating dosage FBA

CT = curing time

β_0 = model constant

$\beta_1, \beta_2, \beta_3, \beta_4$ and β_5 = individual contribution of each predictor

When entering the β values in the equation 6.4, the multiple regression model for our case become as following:

$$P = 64.140 + 3.048 T - 0.675 WR - 0.850 OPC + 0.104 CD + 0.058 CT \quad \text{Equation 6.5}$$

The values of β coefficients give an indication on the relationship between the outcomes of phosphate removal and the predictors based on if the β values are positive or negative. Obviously, the water ratio and OPC have a negative relationship with model outcome whereas a positive coefficient represents a positive relationship between the rest of the predictors and model outcome.

The standardized coefficients or Beta coefficient help to determine the independent variable that has the most influence on the dependent variable. It does not matter if the value is negative or positive because the higher absolute value of the beta coefficient represent the independent variable that has the stronger effect on the model outcome. According to Beta coefficient values in table 6.5, the variables, which contribute to the formation of the LFBA, have influence on phosphate removal as following: time of removal > water ratio > OPC > coating dosage > curing time.

The influence of each independent variable on the model construction is assessed by determining its statistical significance Sig.; which indicates whether this IV makes a statistically significant contribution to the suggested model or not (Pallant, 2005). Any IV with a Sig. greater than 0.05 can be neglected from the model as it does not make a significant contribution (Field, 2008). It is observed that all variables have Sig. less than 0.05. Therefore, the final model will include all variables, which were entered to construct this model.

Based on the description of all the model assumptions and parameters; the model as illustrated in equation 6.5 will be adopted to predict the phosphate removal in the case of changing the amount of any variable which formed the LFBA as filter media for improving the phosphate removal efficiency.

6.4 Chapter discussion

Four factors have a key impact on the characteristics of the produced filter media; quantity of coating dosage, OPC ratio, water ratio and curing time. At the beginning, the mixture ratios were determined depending on previous review and laboratory judgment. Afterward an optimization process was conducted to determine the optimal mixture percentages, which achieved best phosphate removal. The sequence of factors examination was considered according to the order of the factors in the process of LFBA formation. These factors represent the cornerstone of formation of the LFBA. Therefore, optimizing their quantities is essential according to the considerations below:

- Increase the OPC amount in the mixture will positively affect the strength of the materials' bonding. On the other hand, it negatively affects the chemical composition of new filter media. Especially, the availability of Al_2O_3 and Fe_2O_3 , which are responsible for phosphate capture from the influent. The presence of pozzolanic material such as FBA caused a significant hydration for OPC.
- The water ratio is extremely sensitive for additives' reaction. Thus, the low added water quantity negatively affects the formation of the final product characteristics. While, if water quantity exceeds the required value, a

segregation of material occurs and this will lead to an influence on the strength of bonding between the materials.

- During the filter media preparation, the unbound FBA is lost as a result of crushing media to obtain the filter media as particles. Therefore, determining the required FBA amount is important in terms of reducing the loss of FBA.
- Controlling the rate of moisture loss during the OPC hydration is very necessary. In order to obtain the required strength which achieves the binding between materials of the mixture.

The combined influences of factors which contributing to forming the LFBA on phosphate removal have been studied according to a statistical model. At the beginning, the data validity was checked based on several assumptions. All assumptions indicated that the data could generate a trustworthy model. The statistical model indicates that all factors make a significant contribution in phosphate removal. Although there is a difference in factors' significance, the model suggested that all factors should be taken into consideration to obtain a successful model.

6.5 Chapter summary

Water ratio, OPC, coating dosage and curing time are factors that have key impacts on the final production of LFBA; they were subjected to an optimization process to introduce the most feasible mixture which achieved better phosphate removal. The optimization process includes maximizing and minimizing the percentage of each factor and fixing the other factors' percentages. The suggested ratios in the optimization process are based on the first LFBA mixture composition which was suggested according to the literature review, the composition consists of 50% FBA and 5% OPC of the dry weight of limestone, 35% water ratio of the FBA and OPC mixture and the curing time 28 days. Hence, they were selected as reference values. The sequence of factors' examination was considered according to the order of utilization of the factors in the process of LFBA formation. Consequently, the process started by examination of the water ratio then OPC, coating dosage, and finally curing time.

The results of the optimization process revealed the composition of LFBA that presented an outstanding performance of phosphate removal consists of 35% water ratio of the dry weight of OPC and FBA 5% OPC and 40% FBA of dry weight of limestone and 14 days curing time. Obviously, the reference values of the ratios of water and OPC showed better performance than the changed values. While, the quantity of coating dosage and the curing time was reduced to 40% and 14 days because LFBA at these values gained the similar characteristics that maintain the phosphate removal efficiency at same level as higher values.

A statistical model has been constructed based on experimental results in order to check the combined influences of factors which contribute to forming the LFBA on

phosphate removal. Multiple regression technique was adopted to create this model. Several key assumptions about the variables used in the analysis have been checked such as sample size, multicollinearity, outliers, significance of independent variables and coefficient of determination to make sure of the reliability of the multiple regression outcomes. All assumptions indicated that the data could generate a trustworthy model. The coefficient of determination R^2 for this model is 0.766, which means that the IVs can explain about 76.6% of the change in phosphate removal. Beta coefficient is one of the model parameters that determine which independent variable has the most influence on the model outcomes. According to obtained values of Beta coefficient, the variables, which contribute to the formation of the LFBA, have influence on phosphate removal as following: time of removal > water ratio > OPC > coating dosage > curing time. The significance is another important model parameter; their outcomes indicate that all IVs makes a statistically significant contribution to the suggested model. Therefore, the final model takes into consideration all variables, which were entered to construct this model.

CHAPTER 7 EVALUATING THE LFBA SUITABILITY FOR FIELDWORK

7.1 Chapter introduction

Assessment of the suitability of LFBA as a filter material for phosphate removal requires consideration of several factors such as material longevity, possibility of performance regeneration, cost, phosphate removal from real wastewater and removal performance according to change of the filter scale.

The lifetime of the filter materials is the most crucial aspect that requires to be clarified because it helps to determine the possibility of their application in the field scale facilities. The lifetime of LFBA was tested via feeding a phosphate solution into a filter for several sessions; then measuring the effluent concentration at the end of each session. It is certain that the efficiency of LFBA will decline with time due to the accumulation of phosphate ions on the LFBA. However, the LFBA acceptability as a filter media depends on how much time is required to reduce the LFBA performance below the necessary removal limit. Certainly, the longer that period of saturation means that LFBA can be presented as an efficient filter media. In addition, a long lifetime of the filter media reflects positively on the cost because it reduces the frequency of changing the filter bed.

Regenerating the performance of LFBA after adsorption enhances its practicality in wastewater treatment. The possibility of reusing the LFBA to remove the phosphate via regeneration of the saturated sites on the LFBA surface will positively affect the economic feasibility of the process. The regeneration process will increase the lifetime of LFBA and maintain the continuity of the treatment process. Based on these consideration, the reusability of LFBA was determined by conducting a desorption

experiment via washing the LFBA through a high pH solution at different concentrations and washing methods.

The cost is a significant factor that should be taken into consideration to estimate the suitability of utilizing the LFBA in fieldwork. Sometimes we can obtain materials with high removal efficiency but their preparation costs are very high. Therefore, the cost of LFBA preparation has been studied in this chapter, and it has compared with the cost of other coated materials.

In this present study, synthetic phosphate solutions were utilized as the phosphate source during the course of experiments to follow the safety and health conditions in laboratory work. In this stage, the performance of LFBA to remove the phosphate from real wastewater has been investigated. In addition, an experiment was conducted to test the LFBA efficiency at different filter heights when the wastewater is the source of phosphate to present an overview on the influence of changing the filter scale.

Finally, a comparison between the LFBA performance and other filter materials in related researches has been conducted.

7.2 Filter media longevity

Estimating the filter media longevity for phosphate removal is significant for evaluating the financial feasibility of active filter technology. Determining the filter media longevity is considered as a key design parameter in the filtration process because it links the magnitude of phosphate removal to the filter size and cost. Simply, determining the filter media longevity can be achieved by assessing the removal efficiency over time. Several operating runs were performed by pumping influent with volume 8 L and concentration 10 mg P/l over a mass of 1500 g from the LFBA packed

in the upflow filter to obtain the required experimental results for checking the LFBA longevity. Each run ended when the final effluent reached the desired effluent limit of 0.1 mg P /l and then a new run started with influent concentration 10 mg P/l. The outcomes of the experimental work are applied in the following mass balance equation to estimate the PO_4^{-3} sorption:

$$q_e = \frac{(C_i - C_e) V}{m} \quad \text{Equation 7.1}$$

Where C_i and C_e are PO_4 initial and effluent concentration (mg/l), respectively and V (L) is the volume of phosphate aqueous solution treated during the experiment and m the mass (kg) of the filter material.

The number of runs was determined depending on the outcomes after each run. The experimental work was stopped after 23 runs because the required time to reach the desirable phosphate removal became very long. The capability of phosphate removal over all runs is shown in figure 7.1. As expected the first runs achieved a rapid phosphate removal in comparison with later runs.

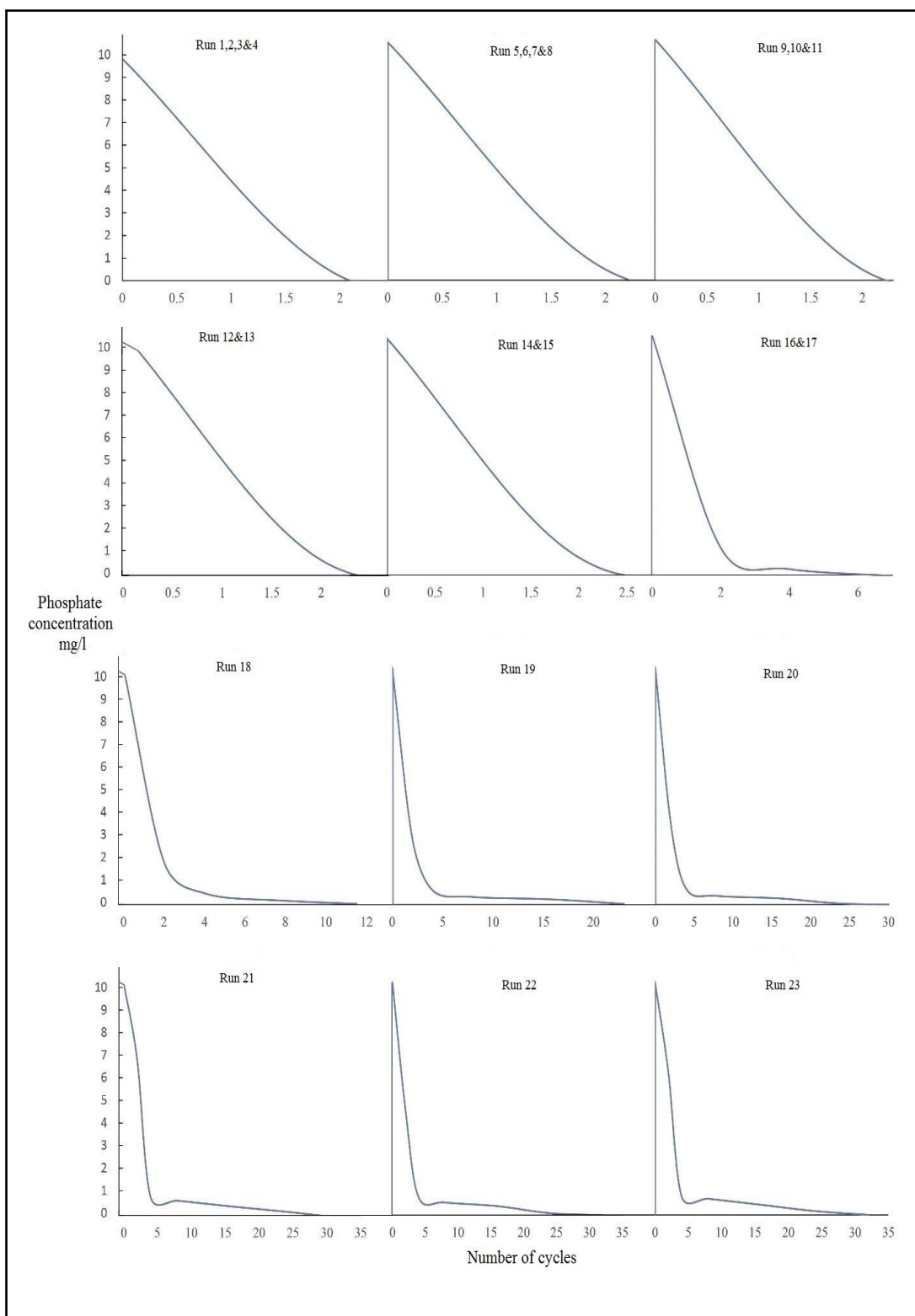


Figure 7.1. Phosphate removal via LFBA over the operating sessions

The first 4 runs showed the same removal pattern and approximately 2 cycles as removal period. The next runs also presented the same removal pattern for several runs such as 5, 6, 7 and 8 together and 9, 10 and 11 together. Afterwards, the number of runs that exhibited the same removal pattern decreased until each run presented its own pattern of removal. Most researchers determine the filter materials' longevity by measuring the saturation point (concentration of influent = concentration of effluent). In this current study, the LFBA did not reach the saturation point. However, the decision to stop pumping the phosphate solution into the lab-scale filter was taken because the treatment time was increased. Long-term treatment is incompatible with economic considerations for example approximately 30 cycles were required to achieve the total removal as illustrated in the run number 23.

According to the equation 7.1, the phosphate sorption rate is 0.053 mg P/g LFBA for each 8 L of phosphate solution reached the required effluent limit of 0.1 mg P/l. Based on that all the runs achieved the required phosphate limit along the term of the experiment. Therefore, the phosphate sorption rate is steady at 0.053 mg P/g LFBA. In comparison between the first and final run there is a large difference in treatment period. However, 97% of the phosphate concentration is removed after 5 cycles in the final run. These results indicate that the phosphate removal occurred rapidly along the experiment progress, especially when phosphate concentrations were more than 0.3 mg P/l (97% from the total phosphate concentration). While the removal became very slow when the phosphate concentration became lower than 0.3 mg P/l. The findings revealed that the LFBA has a positive and useful lifetime because its saturation is significantly slow.

7.3 LFBA regeneration

During the phosphate treatment, many sites on the LFBA surface started to be saturated with phosphate ions, this led to minimizing the removal efficiency. In this study, the regeneration process is employed to activate the LFBA efficiency for phosphate removal again. In addition to increasing the filter material efficiency there are many other reasons that makes the regeneration process important because of their significant impact on the wastewater industry. Regeneration of filter media provides a safe and controlled treatment process that leads to decreasing the need for media replacement; this reflects positively on the treatment process in terms of cost and time taken. Commonly, the filter material regeneration is considered an economical and environmentally friendly solution for the wastewater treatment.

The performance of PSMs is significantly influenced by a wide pH range. Al/Fe metal oxides are positively charged at low pH; and negatively charged at high pH values. As phosphate is an anion, adsorption is greatest at low pH and decreases with increasing pH (Klimeski et al., 2012). Jianbo et al. (2009) investigated the phosphate desorption efficiency from iron-oxide-coated sand IOCS with increasing contact time at various concentrations of NaOH solution. He reports that the desorption efficiency was higher than 80% at 60 min and reached 90% at 160 min. Based on these considerations, the PSMs which contain Al/Fe metal oxides could be regenerated by an alkali solution. Therefore, the decision to regenerate the LFBA is implemented by washing it with an alkaline solution to avoid the efficiency reduction and recover the phosphate that have been removed. Jianbo et al. (2009) focus on measuring the phosphate desorption efficiencies at different NaOH solution concentrations without illustrating the approach in the process of selecting these concentrations. Moreover, according to an extensive search in the literature review there is no indication that the researchers

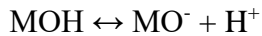
suggested methods to wash the filter materials for the purpose of recovering the captured ions from their surfaces. In this present study, the technique of measuring the point zero charge PZC is applied to determine the required pH value of the washing solution to regenerate the LFBA. Determination of the PZC for LFBA helps to avoid the random selection of the pH of the washing solution. Consequently, reducing the experiment time, material consumption and providing a scientific basis in regard to the pH selection of the washing solution. In addition, two methods were adopted for washing the LFBA for the purpose of recovering the phosphate and regenerating the LFBA efficiency; the methods are continuous and intermittent washing. Based on the outcomes of each method, the method that contributes effectively to regenerating the LFBA will be adopted.

7.3.1 Point zero charge PZC

In this section, an overview on the PZC will be introduced such as its hypothesis, work mechanism and the methods of measurement to understand the significance of measuring the PZC in the process of determining the pH of LFBA washing solution. ‘The point of zero charge (PZC) is the pH of the suspension at which the net charge on the surface of an insoluble oxide/ hydroxide is zero’ (Mahmood et al., 2011b). This means the sum of all the surface positive charges balances the sum of all the surface negative charges. PZC has made a significant contribution to surface characterization of metal oxides/hydroxides (Bourikas et al., 2005). In the aqueous environment the PZC is considered one of the factors that plays a vital role in locating how potentially harmful ions can be adsorbed by metal oxide/hydroxides.

Insoluble metal oxides/hydroxides are an important category of inorganic ion exchangers because they act as sorbents for soluble impurities. Most of the metal

oxides are amphoteric (Anderson et al., 1981); and their surface dissociation may be represented schematically as follows:



Where M is representing the solid surface. The amphoteric behaviour of the surface of metal oxides allows the surface to develop either a positive or a negative overall electrical charge. In the case where the pH of a solution is at lower values than the desired for reaching the PZC, most sites over the surface of the metal oxides develop a positive charge (the oxide behaves as an anion exchanger). In contrast, when the solution is at pH values higher than the PZC, a negative charge is developed over the surfaces of the metal oxides (the oxide behaves as a cation exchanger) (Cardenas-Peña et al., 2012). Mixed oxides can have both exchange types, depending on the relative pKa values of the different surface sites (Ibanez et al., 2007).

Several studies have determined the value of PZC for different metal oxides/hydroxides (Kosmulski, 2006, Naeem et al., 2007, Mahmood et al., 2011a). The findings of these studies reveals different PZC values for the same oxide. Moreover, the findings show that a particular sample of a metal oxide/ hydroxide never has a constant PZC value (Kosmulski, 2006). The values of PZC are often divergent; for example, the PZC of aluminium oxide varies from 6.5 to 10 based on the sort of aluminium oxide. This variation was attributed to the differences in the origin of samples and PZC measurement methods need to be taken into consideration for these contradictions. Many methods are applied to determine the PZC such as fast titration, salt addition, mass titration, and ζ potentiometry.

7.3.2 Measuring the PZC of LFBA

The surface of LFBA is formed from furnace bottom ash and OPC as illustrated in previous chapters. According to the chemical composition analysis, these materials contain Fe/Al oxides, and they are responsible for capturing the phosphate ions from the influent. Based on the literature review as mentioned in the previous section, the PZC of Fe/Al oxide should be obtained at alkaline pH value. However, measuring the pH variation of LFBA samples at acidic pH was performed to follow the standard methods in measuring PZC, and avoid any misleading outcomes. The salt addition method has been applied to determine the PZC of LFBA because it is simple, accurate requires a small quantity of material as compared to other techniques. According to this method, the PZC value of any material is determined by mixing this material with a solution able to set off an ionic exchange with this material. Therefore, the LFBA sample was mixed with KH_2PO_4 to simulate the LFBA reaching net charge during the process of phosphate removal. In addition, the ratio of each LFBA sample to the solution was 1.7; utilizing the same ratio in batch experiments will present more realistic results.

Based on these considerations, 23 g of LFBA sample and 40 ml of KH_2PO_4 were mixed in different reaction flasks. 10 samples were prepared at an initial pH value of 2, 3, 4, 5, 6, 7, 8, 9, 10, or 11. The pH of the solutions was adjusted by adding either hydrochloric acid HCl or sodium hydroxide NaOH. Each flask then was agitated in a shaker bath for 24 h. After settling, the final pH of each suspension was measured by pH-meter model HI 2210. In order to better characterize the ion exchange between the LFBA and the solution, the solution was investigated at three different temperatures 10, 20, 30 C. An additional flask containing 40 ml of phosphate solution was run as a

blank over all experiments to monitor any adverse effects on the quality of the experiment's performance.

The initial pH values of the solutions were plotted against ΔpH (the difference between initial and final pH after settling). The initial pH value at which ΔpH is zero was considered the PZC of LFBA. Figure 7.2 illustrates the values of ΔpH against each initial pH value at three different temperatures.

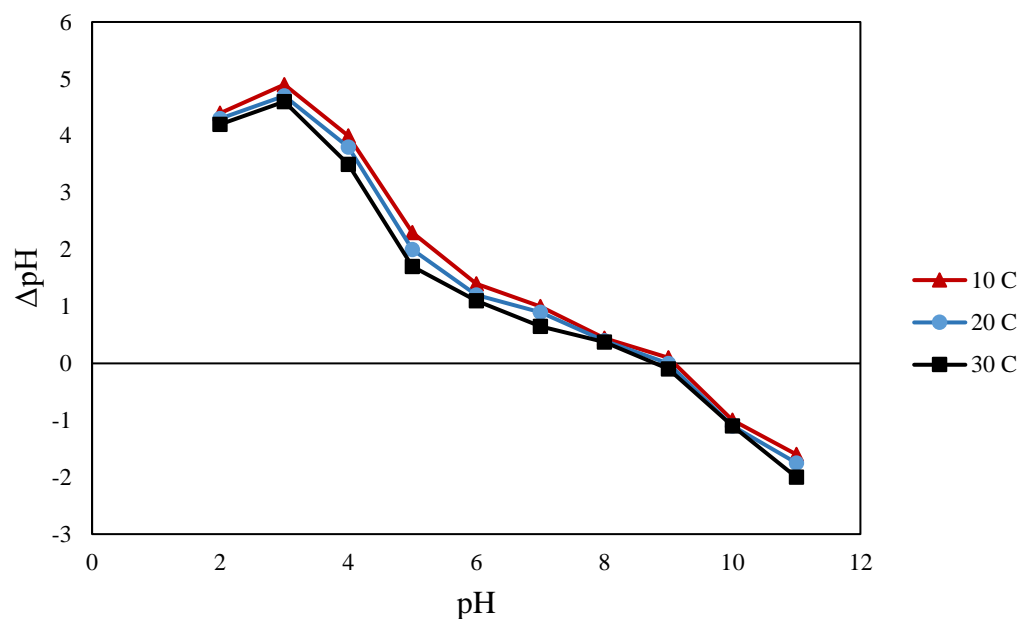


Figure 7.2. ΔpH versus initial pH of LFBA at different temperatures

The results revealed that the initial pH at range from 2 to 8 indicate positive values of ΔpH with a maximum value at pH 3. While, the values of ΔpH at initial pH 10 and 11 indicate negative values. It is noticeable that ΔpH was zero when the initial pH was around 9 for all investigated temperatures. It can be concluded from the findings of the PZC test, the LFBA has an amphoteric behaviour (develops positive charge when pH values less than 9 and acts as anion exchanger and develops negative charge over pH over than 9 and acts as cation exchanger). Therefore, the decision to regenerate the

LFBA has been implemented by washing the LFBA with solution at pH over 9 for desorption of the captured phosphate ions.

7.3.3 Process of washing LFBA

The washing method and pH value of the washing solution should be taken into consideration to achieve the desirable regeneration for LFBA. According to the results of the previous section, the phosphate desorption from LFBA occurred when the pH solution become over 9. Therefore, two solutions were prepared with adjusted pH values at 9.5 and 10 by adding NaOH to deionized water. The decision was taken to test the phosphate desorption efficiency by utilizing washing solutions at these pH values, to avoid any adverse effects which can be happen because of high alkalinity. Therefore, there is no tendency to increase the pH of the washing solution over 10. On the other hand, the contact between the surface of the LFBA particles and washing solution is an essential issue to attain better phosphate desorption. Consequently, continuous and intermittent washing have been suggested as washing methods to achieve the regeneration process. The proposed quantity to be pumped as washing solution into the lab-scale upflow filter, is 8 L. The continuous washing method includes pumping the solution into the filter at flow rate 1 l/min. The same washing quantity in continuous washing has been utilized in the intermittent washing method; but the washing solution is pumped intermittently. The washing solution is pumped into the filter in doses over time; each quantity being in contact with the LFBA for a specific period. The washing solution quantity and washing time for both methods was the same to avoid any changes which could influence the results. Consequent, the findings of the washing process efficiency will only be based on the washing method.

7.3.4 Measuring the efficiency of LFBA after regeneration process

At the beginning, the washing period was determined by soaking specific masses of LFBA in washing solution pH 9.5 and 10. The ratio and method of contact between the LFBA mass and washing solutions is the same batch experiment, which was applied previously in measuring the phosphate sorption. The method was batch experiment and the ratio was 1 LFBA / 1.7 washing solution. The LFBA samples were soaked in the washing solution from 5 min to 2 hours. Afterwards, batch experiments (at same previous experimental conditions) were conducted to investigate the samples' performance for phosphate removal after regenerating them via washing solutions by bringing them in contact with phosphate solution at concentration 10 mg P/l for 24 hours. Figure 7.3 illustrates the phosphate removal efficiency via LFBA samples versus washing time of these samples by solutions at pH 9.5 and 10.

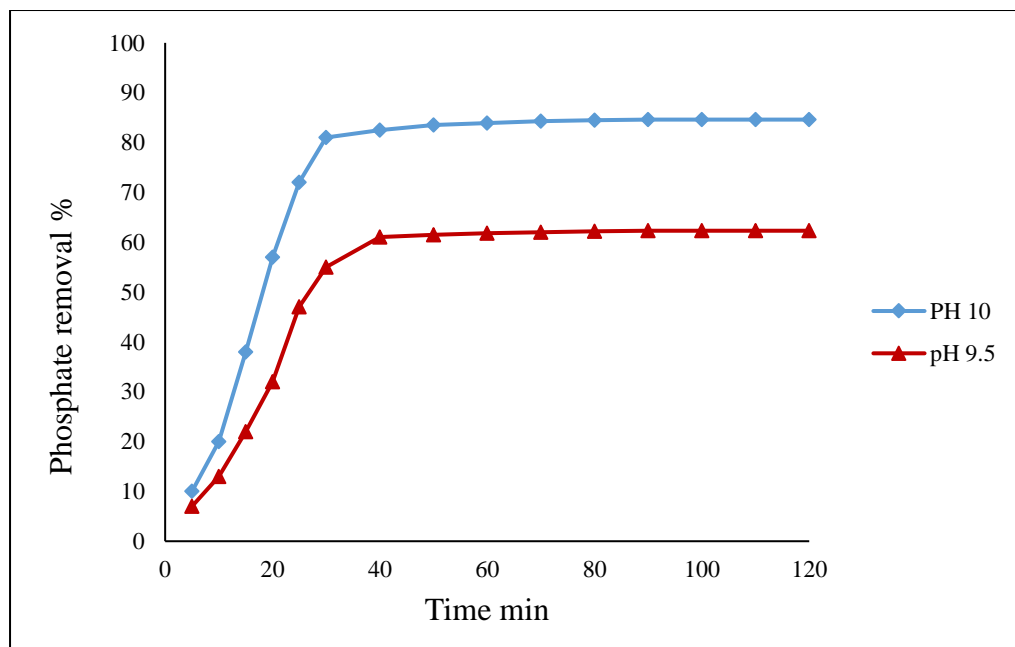


Figure 7.3. Phosphate removal efficiency via LFBA samples versus washing time

It is obvious the removal efficiency is increased with increasing contact time with both solutions. Specifically, the samples are regenerated in the first 30 and 40 min for washing solution pH 10 and 9.5, respectively. Then they are slowed down; for 90 and 80 min the removal efficiency only increased 3.6% and 2.3% for solution pH 10 and 9.5, respectively. Based on these results, washing LFBA for around 30 min has been adopted. Therefore, in the continuous washing method the washing solutions were pumped for 4 cycles at flow rate 1 l/min because each cycle requires 8 min for completion. While, in the intermittent method the washing solutions were pumped in 8 doses; each dose has a quantity of 1 L and submerges the LFBA for 4 min.

After washing the LFBA with solution at pH 9.5 and 10, influent at concentration 10 mg P/l was pumped for one cycle to detect if the LFBA is activated again to remove the phosphate effectively. Figure 7.4 and 7.5 illustrates the phosphate removal efficiency via LFBA after washing with solution at pH value 9.5 and 10, respectively.

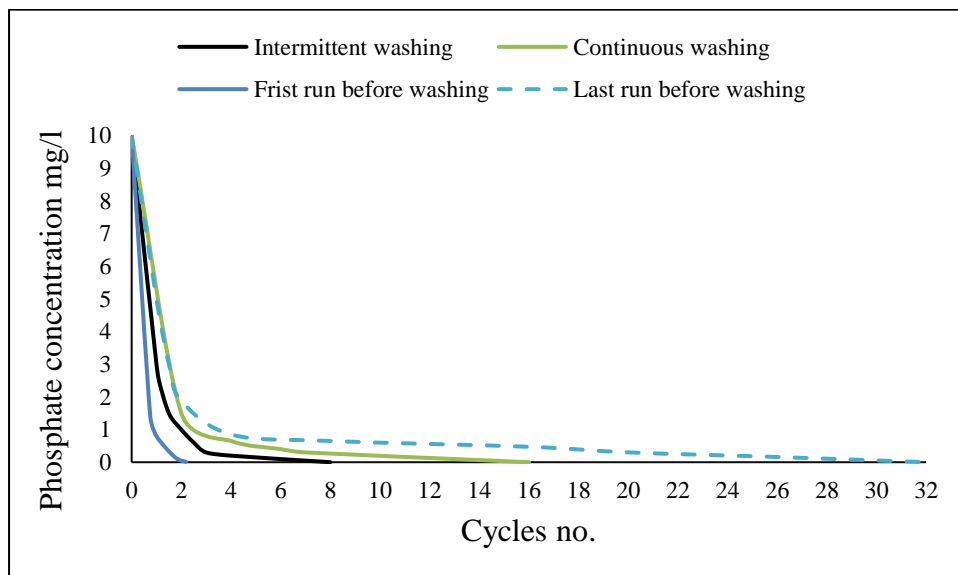


Figure 7.4. LFBA efficiency after washing with solution at pH 9.5

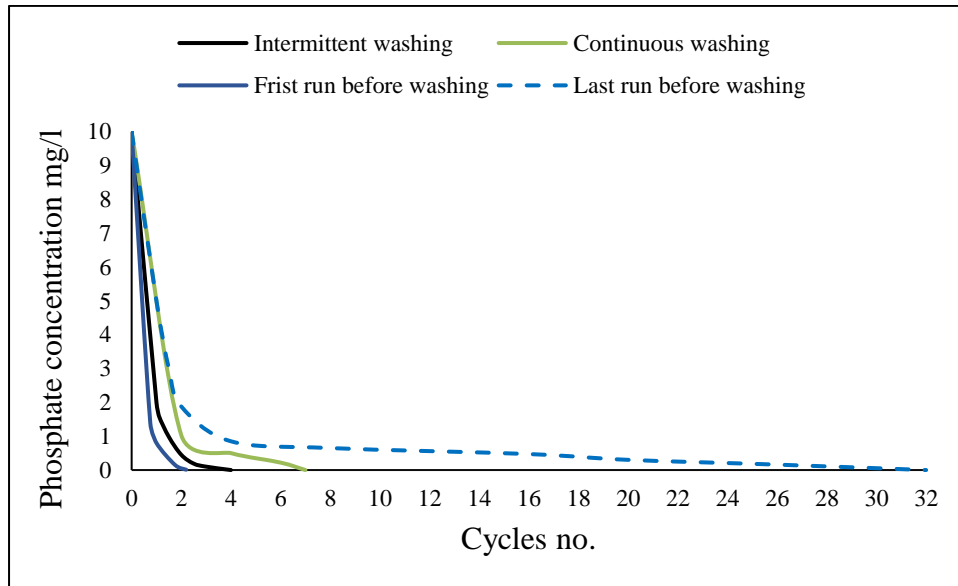


Figure 7.5. LFBA efficiency after washing with solution at pH 10

The results revealed that the LFBA showed better removal efficiency when it is activated via 10 pH solution in comparison with 9.5 pH washing solution. In addition, the intermittent method has presented better regeneration performance than the continuous method because the LFBA, which is activated by the intermittent method, introduced superior phosphate removal. The results have been compared with the LFBA removal efficiency for the first and last run before performing the washing process. The regeneration efficiency RE% was calculated by using following equation:

$$RE\% = \frac{C_o - C_{reg}}{C_o} \times 100 \quad \text{Equation 7.2}$$

Where C_o is initial phosphate concentration 10 mg P/l and C_{reg} phosphate concentration for regenerated LFBA at the time when complete removal occurred in first run before regeneration process. Table 7.1 shows the outcomes of the regeneration efficiency of LFBA in comparison to the efficiency of the first run before the regeneration process according to the pH values of solutions and the washing method.

Table 7.1. Regeneration efficiency of LFBA according to pH and method of washing

pH of washing solution	Washing method	RE%
	Intermittent	90
	Continuous	85
	Intermittent	95.5
	Continuous	89.7

Washing solution at pH 10 and intermittent washing method has achieved the highest LFBA regeneration efficiency. While, the lowest regeneration occurred at pH 9.5 and continuous washing method. It might be the LFBA has reached the highest regeneration efficiency at intermittent washing method because this method provides solution stagnation for a period, which allows better contact between solid and liquid phase.

7.4 Cost analysis of LFBA

The successful produced filter material should be characterized to fulfil any requirements besides the high treatment efficiency. Consequently, it is necessary to pay attention to analysis of other aspects that play a vital role in identifying the LFBA as an eligible filter material. The production cost of LFBA is one of the necessary aspects that is described in this section. Examination of the estimated or actual cost to determine the probable cost of the product is very important because the product cost may be significantly higher than the necessary level of wastewater treatment. The purpose is to get an idea on whether the suggested costs are in line with the required level of treatment. The production cost of LFBA was compared with the cost of

producing the Iron-oxide-coated sand IOCS filter media to illustrate the significance of LFBA in terms of cost. The main reason for comparing the cost of LFBA with the cost of IOCS production is that it is the most recently developed technique for coating metal oxides onto sand surface in order to avoid the problems of using metal oxides as a powder in wastewater treatment units. The method of metal-oxides-coated sand is widely tested for removal of several anions and cations such as phosphate, Arsenic, copper and lead (Thirunavukkarasu et al., 2003, Han et al., 2006, Jianbo et al., 2009).

7.4.1 Method of pricing

The creation process of the LFBA and IOCS includes consumption of materials and energy. Therefore, the cost of each filter material was calculated as the sum of the material cost and consumed energy. The cost of material can be simply calculated by taking the total material cost. The material prices have suggested depending on reliable vendors such as Sigma Aldrich and HachL; specifically, for chemicals. Some material pricing was adopted from commercial suppliers such as Wickes. On the other hand, the energy required in the production process of both filter materials was calculated according to the method of consuming this energy. A mixing process is required in the production of LFBA. Therefore, energy consumption occurs as a result of utilizing a mixer to achieve the mixing of the materials. The energy consumed by the mixer is calculated according to the mixer power that is provided by the vendor over the mixing time. While, the energy consumed in the method of creating the IOCS comes from material heating. The energy required to heat a material can be calculated from the equation below:

$$\text{Power} = \frac{M \times \text{Sp heat} \times T}{3600} \quad \text{Equation 7.3}$$

Where power is the required power to heat one kilogram of the material in kW, M is the mass of the heated material in kg, Sp heat is the specific heat of the heated material in kJ/kg K and T is the raised temperature in °C.

To evaluate the product profitability some external costs can be spread across the product to address the final cost of the product. For instance, the amount of labour cost should be estimated. The manufacturing process is associated with every step along the product routing. Commonly, each step requires labour time to carry out. Overhead cost is another type of external cost, and it includes many sorts of costs ranging from depreciation and taxes to various kinds of supplies. In this stage, the LFBA cost was calculated in the case of manufacturing without paying attention to the process of marketing, and the external costs are varied. Therefore, external cost has been peeled off from total cost to create a product cost, which can be used for decision-making.

7.4.2 Calculate the filter material cost

The listed materials in table 7.2 represent all the components, which contribute in making up the LFBA besides the mixing energy. Table 7.2 illustrates also the quantities, and the unit cost for each component. The summation of the material cost for each component gives the total material cost for the LFBA per kg. Energy consumption could take place as a result of material mixing. Therefore, the cost of consumed energy has been calculated to obtain a reliable estimated cost. Consequently, the required energy to produce 1kg of coated limestone is 0.025 kW as shown in table 7.2.

Table 7.2. Materials and energy costs for LFBA production

Item	Unit	Quantity	Unit cost	Extended cost
Limestone	g	1000	£0.19 per kg	£0.19
OPC	g	50	0.056 per kg	£ 2.8×10^{-3}
FBA	g	400	Free	Free
Water	ml	160	£1.705 per m ³	£ 0.27×10^{-3}
Energy	kW	0.025	£ 0.1147 per kW	£ 2.8×10^{-3}
Total LFBA cost per kg Limestone				£0.19587

The final cost of LFBA per 1 kg limestone is £0.19587. Based on these prices, 1 tonne of LFBA cost £195.86, and 1 tonne of limestone costs £190. Hence, the difference between these costs represents the cost of coating. In other words, only £5.86 is the cost of coating per 1 tonne of limestone.

As mentioned above the cost of IOCS has been estimated to evaluate the cost significance of LFBA. All components that form IOCS are listed in table 7.3, and the heating energy that is required in obtaining the coating over the sand. The same procedure of calculating the LFBA cost is utilized to estimate the cost of IOCS, and gather all listed components according to their quantities and costs.

Table 7.3. Materials and energy costs for IOCS production

Item	Unit	Quantity	Unit cost	Extended cost
sand	g	800	£0.279 per kg	£0.22
HCl	ml	----	£29.70 per 250 ml	----
FeCl ₃ ·6H ₂ O	ml	800	12.95 per 1000 ml	£10.36
NaOH	ml	2	£34.40 per 500 g	----
Energy	kW	3.792	£ 0.1147 per kW	£0.435
Total IOCS cost per 0.8 kg sand				£11.285

The heating energy could be estimated according to equation 7.2. The mass of heated material, temperature and time of heating are identified in the IOCS production method. The specific heat of sand is ranging from 0.669 to 0.753; the average value is adopted as a specific heat of sand. The results revealed the energy required to heat the sand according to the coating method IOCS is 3.792 kW. Extra energy has been consumed in this process, resulting from drying the material but the drying period is not given. In this case, this extra energy was not estimated. However, the final cost of 0.8 kg of IOCS is £11.285. If the cost of the sand is taken away from the total cost to obtain only the coating cost, 1 tonne of sand required £13,780 as a cost of coating.

Obviously, there is a huge difference between the coating cost of LFBA and IOCS. This indicates that the LFBA is able to be utilized in full-scale wastewater treatment plants depending on the economic considerations. While IOCS is only valid for research issues in terms of phosphate removal. LFBA is cost effective for different

reasons: it utilizes an easily available natural ingredient, the main material (FBA) is available free, the material which is paid for is very cheap such as limestone or consumed in small amounts like OPC and little energy is consumed in the preparation process. On the other hand, IOCS consumes high energy in the preparation process, and depends on expensive chemicals as coating material.

7.5 Phosphate removal from wastewater sample

Many filter materials have been examined for removal of various pollutants (Johansson Westholm, 2006a, Vohla et al., 2011) but it is still uncertain how most of them would work in real wastewater facilities. It would be beneficial to investigate the performance of suggested filter materials to remove the contaminants from real wastewater influent. The present study contributes to introducing a sound comparison by investigating the effect of influent source on the efficiency of phosphate removal. This study has been conducted by testing the removal capacity of LFBA for phosphate from real wastewater and comparing the results with the findings that were obtained previously for phosphate removal from synthetic phosphate solution. The real wastewater contains various types of contaminants that may have an influence on LFBA efficiency to remove the phosphate. While, during this research a synthetic phosphate solution has been used to test the efficiency of selected material as phosphate sorption material. Therefore, the final findings of this experiment will help to give an insight into the performance of LFBA about phosphate removal from wastewater.

The wastewater sample was collected from the secondary treatment of Liverpool wastewater treatment works LWTW, Sandon Docks, Liverpool, United Kingdom; the concentration of phosphate was 8 mg P/l. The concentration of synthetic phosphate

solution was altered to 8 mg P/l to resemble the wastewater concentration. Both solutions were pumped into the lab-scale upflow filter at the same conditions of the previous experiments. Figure 7.6 illustrates wastewater feeding into the lab-scale upflow filter.

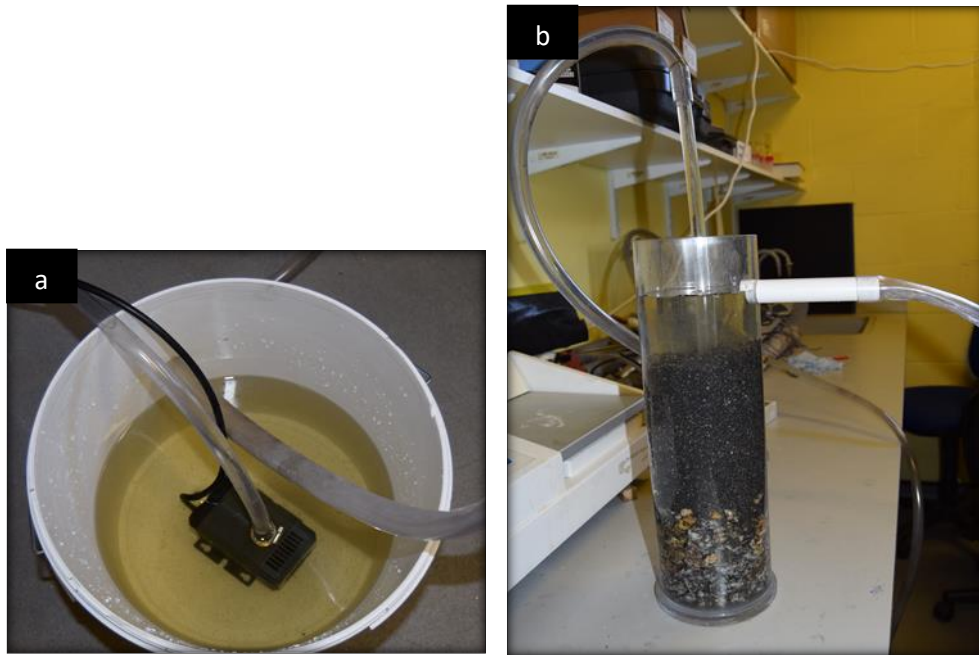


Figure 7.6. Treating wastewater influent via lab-scale upflow system (a) submersible pump (b) lab-scale upflow filter

The experimental results for both solutions was represented through plotting the adsorbed amount of phosphate, versus contact time as shown in figure 7.7.

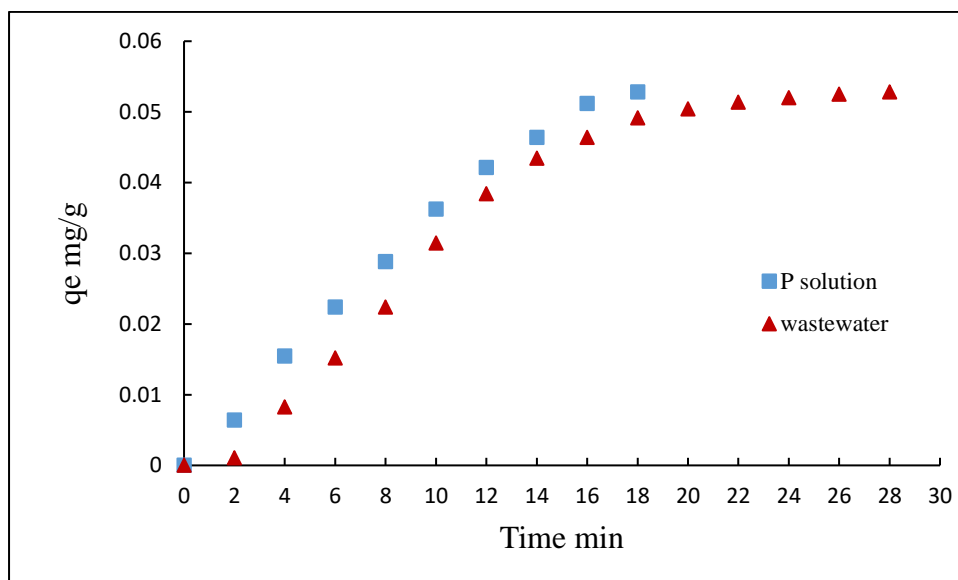


Figure 7.7. Adsorption of phosphate onto LFBA for wastewater and synthetic phosphate solutions (flow rate 1 L/min, temperature $(20 \pm 2 \text{ oC})$)

It is noticeable from figure 7.7, the LFBA removed the phosphate faster from the treated P solution in comparison with wastewater. The interference of pollutants with the removal mechanism might have an influence on the LFBA's efficiency in removing phosphate from wastewater. While LFBA has exhibited better phosphate removal from P solution because the solution is empty from ions except phosphate. However, there is no considerable difference between wastewater and P solution in terms of the time needed for phosphate to reach the required limit. The phosphate has reached the concentration of 0.1 mg P/l when the influent is wastewater after 24 min. While when the P solution is the influent the concentration became 0.1 mg P/l after 18 min. It is observed that the removal pattern for both solutions is the same, at the beginning a large amount of phosphate was removed then a decrease in influent concentration. This is might be due to that the concentration decrease with the passage of time reduces the chance of contact with captured ions onto the LFBA surface.

7.6 Effect of LFBA bed height

Several active materials have been applied as filter media in both small and large scales. According to Klimeski et al. (2012) the phosphate removal via PSM, which is packed in large scale is lower than applications in small scale. Increasing the scale leads to a reduction in the phosphate removal from the influent because of many obstacles (Lyngsie, 2013). The most significant obstacle that has an influence on phosphate removal is indicated by Lyngsie (2013) ‘ The incoming flow also tends to form preferential pathways in the material, resulting in a short retention time, limited contact between the phosphate and the material and consequently lower than expected removal efficiency of the filter system’.

In this part, the influence of filter media depth on the phosphate removal has been studied to obtain outcomes about the performance of LFBA during the change of the filter bed depth. In this stage, the parameters such as filter diameter and influent flow rate have been unchanged to focus on the influence of increasing the quantity of packed LFBA vertically.

As shown in figure 7.8 a new upflow filter was constructed to measure the phosphate removal at three different LFBA depths.

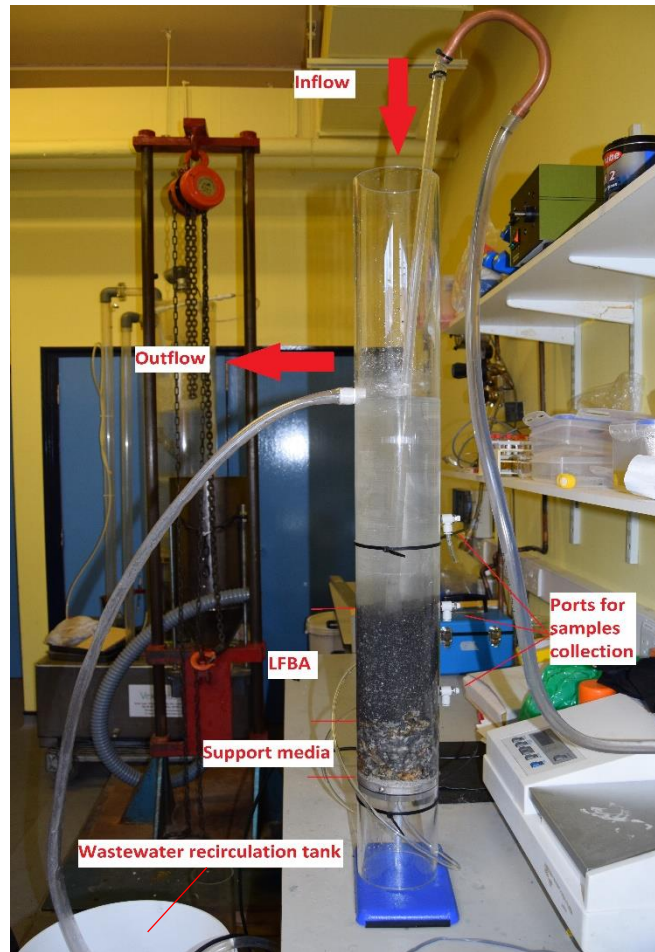


Figure 7.8. The second constructed lab-scale flow filter for measure phosphate removal at various LFBA depths

Table 7.4 illustrates the change in packed mass of LFBA according to depth change.

Wastewater was pumped as influent to obtain more findings that are realistic.

Table 7.4. Experimental conditions at each selected depth

Depth cm	Filter diameter cm	Filter volume m ³	LFBA packed mass kg	Flow rate L/min
13	10	0.001	1.5	1
24.5	10	0.002	2.88	1
37	10	0.0029	4.356	1
45.5	10	0.0035	5.357	1

The reaction of phosphate onto fresh LFBA material was determined at different filter media depths. As shown in figure 7.9 the higher phosphate uptake has occurred at the shallow zone. Specifically, at filter depth 24.5 cm.

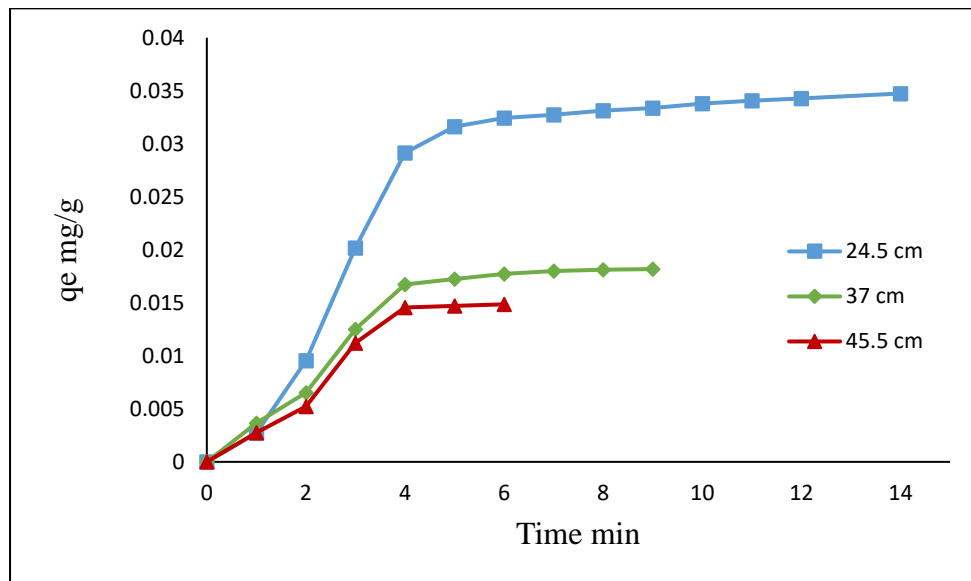


Figure 7.9. Phosphate adsorption at different depths, when LFBA fresh

It is could be observed from the maximum phosphate uptake at each depth; the final adsorbed phosphate were 0.0347, 0.0181 and 0.0148 mg/g for depths 24.5, 37 and 45.5 cm, respectively. This indicates that a significant phosphate uptake has taken place in

the lowest depth. Therefore, it is suggested that the LFBA depth 24.5 cm is sufficient to achieve the desirable phosphate removal when the LFBA is fresh.

According to figure 7.1, there is a dramatic shift in the LFBA saturation after 18 runs. Consequently, the previous experiment of investigating the LFBA performance at different depths has been repeated. However, this time the phosphate uptake was measured after 18 runs to examine the difference of phosphate removal at different depths between fresh and semi saturated LFBA.

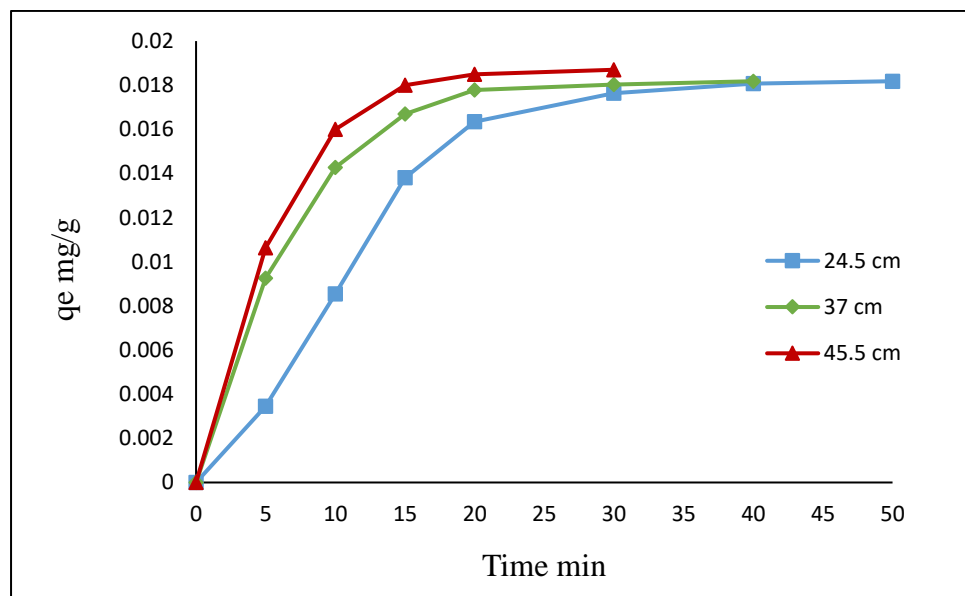


Figure 7.10. Phosphate adsorption at different depths, when LFBA semi saturated. As can be seen from the figure 7.10, phosphate uptake is faster at higher depth. It is true that there is not a big difference between the final phosphate uptakes at all depths but there is big difference in removal time. The phosphate removal time at depth, 45.5 cm is 30 min. While, phosphate removal time at depths 37 and 24.5 cm were 40 and 50 min, respectively.

Increasing the bed depth would provide a longer distance for the influent transfer to reach the outlet. Consequently, extending the contact time between the influent and

LFBA because it provides a large surface area. However, the lower depth has achieved better phosphate removal when the LFBA is fresh. It is first contact zone that captures the phosphate from influent better than the upper zones because at this point the phosphate concentration is the highest. In the case of measuring the phosphate uptake at semi saturated LFBA, the role of the higher part in the filter came into play. It might be the saturation of the lower zone which allows higher phosphate concentration to pass into upper zones, hence, increasing the phosphate removal at these zones. The experimental findings indicate that the increase of the depth of LFBA leads to a reduction in the phosphate removal time.

7.7 Comparison with related work

In this section, a discussion has been conducted about the related previous works of which we are aware, which have focused on the issue of phosphate removal via active materials. Also, the performance of LFBA was compared to these other works. This discussion has focused on the recent works to ensure comparison that is more reliable. Klimeski et al. (2012) were listed in many recent researches on phosphate removal via filter materials. Therefore, most researches that were utilized for comparison in this part have been obtained from this reference. However, it is difficult to obtain a comparison without drawbacks because some researchers used different parameters from our study. LFBA was tested according to column experiments, many researchers studied the phosphate removal via batch experiments. Researches based on batch experiments have been excluded from comparison. While the filter materials, which were tested via column experiments have been used instead as shown in table 7.5.

Table 7.5. LFBA and other filter materials used in flow column experiments

Material	Source	Test period days	P concentration mg l ⁻¹	Particle size mm	Loading rate l d ⁻¹ g ⁻¹	Volume of material cm ³	P retention mg g ⁻¹	Reference
LFBA	Warrington power station, North West England	0.127	10	0.9-2.3	0.96	1021	1.22	
Filtralite P	Saint-Gobain, Norway	229	4.9	0.5-4	0.00048	18800	0.473	(Ádám et al., 2007)
Shellsand	Natural material produced from shell, snail and alga, Norway	303	10	3-7	0.00027	18300	0.497	(Ádám et al., 2007)
Iron-coated sand	Someren, water treatment plant, Netherlands	238	3.95	< 2	0.0039	n.a	n.a	(Chardon et al., 2012)
Electric furnace slag	Steel mill Ft. smith, AR, USA	0.2	0.5-15	6.35-11	0.29-4.6	1.1	1.3	(Penn and McGrath, 2011)

The treatment method is not the only parameter that is considered to have a key impact on the phosphate retention capacity of filter materials. Many parameters have a significant influence on phosphate retention such as particle size of filter material, phosphate concentration in the influent and treatment time, which is related to flow rate of feed solution. High phosphate concentration may lead to a shortening of the required time to remove the phosphate. While, increasing the influent flow rate may decrease the phosphate uptake due to reducing the contact chance. On the other hand, small particle size of filter material offers a large surface area that increases the chance of contact between the feed solution and filter material. Based on these considerations, specific works have been selected to provide a more realistic insight into the efficiency of LFBA in comparison with related works. As listed in table 7.5, some filter material has been selected to compare their outcomes with LFBA where they have somewhat similar parameters.

It is observed that filter materials such as Filtralite P and Shellsand required test periods of 229 and 303 days at loading rate at 0.00048 and $0.00027 \text{ l d}^{-1} \text{ g}^{-1}$, respectively; to reach the saturation point. In contrast, the test period of LFBA is very short in comparison with Filtralite P and Shellsand; it was 0.127 days. While the loading rate is larger than their loading rates; it was $0.96 \text{ l d}^{-1} \text{ g}^{-1}$. As illustrated above the test period is related to the loading rate of feed solution, long contact time and low influent loading rate leads to higher phosphate retention. However, the LFBA retains phosphate much better than Filtralite P and Shellsand. Although the LFBA did not reach the saturation point at these parameters the phosphate retention was 1.22 mg g^{-1} . While, phosphate retention for Filtralite P and Shellsand was 0.473 and 0.497 mg g^{-1} , respectively.

Chardon et al. (2012) describe the phosphate removal via Iron-coated sand. It is a good opportunity to compare the phosphate uptake by LFBA with a coated filter material. The parameters of Iron-coated sand are somewhat similar to the parameters of Filtralite P and

Shellsand as shown in table 7.5. Chardon et al. (2012) did not mention the phosphate retention by Iron-coated sand; but he states that the final concentration of effluent is 90% less than the concentration of influent. Based on operating conditions and phosphate removal percentage of Iron-coated sand, the LFBA also showed better characteristics in terms of phosphate retention. Penn and McGrath (2011) estimate the phosphate retention capacity of electric furnace slag. The outcomes indicate an outstanding performance by electric furnace slag to remove the phosphate. Therefore, it looks a promising material to act as filter material for retaining the phosphate. Electric furnace slag achieved phosphate retention 1.3 mg g⁻¹ during the test period 0.2 days. However, Penn and McGrath (2011) indicate that electric furnace slag no longer retains phosphate after 0.2 days. Hence, electric furnace slag is saturated quickly, whereas LFBA is unsaturated at this point.

According to the findings of several researchers such as (Klimeski et al., 2012, Herrmann et al., 2013): phosphate removal varies depending on many parameters which have an influence on performance of filter material such as phosphate concentration, loading rate and quantity of packed material. However, these parameters do not have an influence on all materials performance in the same manner and same magnitude as illustrated above in comparison with LFBA with other materials in table 7.5. This leads the researcher to believe that chemical composition and physical characteristics play the key role in the process of phosphate removal via the PSMs. Specifically, LFBA results from the process of developing the physical and chemical characteristics that help to obtain an efficient material to act as phosphate sorption media in upflow system.

7.8 Chapter discussion

The long-term treatment is incompatible with economic considerations. Consequently, in terms of studying the LFBA longevity, the decision of stop pumping the phosphate solution into the lab-scale filter has been taken because the treatment time was increased.

The technique of measuring the point zero charge PZC is applied to determine the required pH value of the washing solution to regenerate the LFBA. Determination of the PZC for LFBA helps to avoid the random selection of the pH of the washing solution. The outcomes of PZC experiment indicates that the LFBA has an amphoteric behaviour, and ΔpH was zero when the initial pH was around 9 at all investigated temperatures.

The LFBA removed the phosphate faster when it was treating the P solution in comparison to wastewater. However, there is no considerable difference between wastewater and P solution in terms of the time needed for phosphate to reach the required limit. The performance of LFBA during the change of the filter bed depth has been studied. The experimental outcomes indicates that the increase of the depth of LFBA leads to a reduction in the phosphate removal time. According to comparison of the LFBA removal performance with other related works, the LFBA can be classified as a low cost and efficient filter material to pack in continuous upflow filters.

7.9 Chapter summary

LFBA longevity, adsorption regeneration, cost, utilizing real wastewater sample and influence of change of the filter scale are factors have been studied in this chapter.

Commonly, determining the saturation point for any filter material indicates to the lifetime of these materials. However, the longevity of LFBA was not determined by the saturation point. The decision to stop pumping the phosphate solution into the lab-scale filter was taken because the treatment time was increased. Long-term treatment is incompatible with economic considerations. The phosphate sorption rate is 0.053 mg P/g LFBA for each 8 L of phosphate solution which reached the required effluent limit of 0.1 mg P /l.

The process of regeneration of the LFBA was performed by washing it with an alkaline solution. The technique of measuring the point zero charge PZC is applied to determine the required pH value of the washing solution to regenerate the LFBA. Determination of the PZC for LFBA helps to avoid the random selection of the pH of the washing solution. The outcomes of PZC experiment indicates that the LFBA has an amphoteric behaviour, and ΔpH was zero when the initial pH was around 9 at all investigated temperatures. Continuous and intermittent washing are methods, which were adopted for washing the LFBA for the purpose of regenerating the LFBA efficiency. Washing solution at pH 10 and intermittent washing method has achieved the highest LFBA regeneration efficiency.

The cost of the coating process to produce LFBA is very low in comparison with other coated material.

The LFBA removed the phosphate faster when it was treating the P solution in comparison to wastewater. However, there is no considerable difference between wastewater and P solution in terms of the time needed for phosphate to reach the required limit.

The performance of LFBA during the change of the filter bed depth has been studied. The experimental outcomes indicate that the increase of the depth of LFBA leads to a reduction in the phosphate removal time.

According to comparison between the LFBA removal performance and other related works, the LFBA can be classified as a low cost and efficient filter material to pack in continuous upflow filters.

CHAPTER 8 CONCLUSION AND RECOMMENDATIONS

8.1 Chapter introduction

In this chapter, the key outcomes with regard to the research goals are summarised and major conclusions are described depending on the results of this study. Also the contribution of research findings in regards to utilizing the coated filter materials in removing the phosphate via upflow filters. Moreover, this chapter concludes with recommendations for further research in some aspects related to this research.

8.2 Thesis primary aim

In this present thesis, the primary aim was focused on determining a material capable of removing the phosphate from secondary treated wastewater with a fast retention time. Additionally, this material is suitable to pack in continuous upflow filters as filter media.

8.3 Major conclusions

- The literature review revealed that the effluent, which is released from WWTPs, is one of the main sources of phosphorus that leads to eutrophication of aquatic life. Recently, many researchers proposed that the phosphorus sorbing materials PSM are a sustainable method, which offer an attractive solution for treating municipal wastewater. The chemical composition of these PSMs is the key factor of phosphate removal; the mainly active PSMs that remove the phosphate contain metals such as Fe/Al and soluble Ca and Mg.
- The materials that are subjected to the examination of their capability for phosphate sorption are chosen according to several considerations. These considerations are based on the potential chemical composition, availability and cost.

- The batch experiments results revealed that the materials that consist of oxides of Al_2O_3 and Fe_2O_3 such as FBA and BBA have presented better performance than material consisting of oxides of CaO such as limestone and white dolomite.
- The decision to apply coating technology has been made due to the efficient phosphate removal by FBA and BBA, and the good physical characteristics of limestone, white dolomite and sand.
- The cost of the coating process to produce LFBA is very low in comparison with other coated material.
- According to comparison of the LFBA removal performance with other related works, the LFBA can be classified as a low cost and efficient filter material to pack in continuous upflow filters.

8.4 Thesis contribution to knowledge

The main aim of this study is to find a filter material suitable to pack in continuous upflow filters to remove the phosphate effectively from wastewater. However, the original contribution of this study is introduce a new approach regarding creating and developing the characteristics of the filter media which fit the economic and environmental requirements. The coating process was performed without needing a source of energy such as heat in order to set the coating material over the surface of supporting material. Instead, a small portion of cementitious material such as OPC was utilized as a binder for binding the mixture materials. The cementitious materials merely need water to activate them as a binder.

8.5 Minor contributions

- Adopting a method of image processing via MATLAB codes as an analysis tool to characterise the SEM images. In this present study, MATLAB codes are created to describe the surface morphology of the newly created materials after the coating

process. This method of image processing helps to provide a graphical and numerical finding, which can be adopted in validation of visual inspection of SEM images.

- The technique of measuring the point zero charge PZC was applied to determine the required pH value of the washing solution to regenerate the LFBA. In terms of studying the regeneration of materials, which contain Fe/Al oxides and saturated with phosphate ions, determining PZC for these materials is the key factor which helps to avoid the random selection of the pH of washing solutions, consequently, avoiding consuming any unnecessary time and materials.

8.6 Thesis recommendations

- Determining the effectiveness of various materials in filter systems such as continuous upflow filter leads to encouraging the research into the feasibility of utilizing different filter media in the future. Ashes have different physical and chemical characteristics based on several factors such as origin of the material and method of incineration. Consequently, their efficiency in contaminant removal is varying. Materials' validation as filter media can be achieved by following the same procedures as suggested in this study regarding identifying the physical and chemical characteristics of materials.
- A method developed for coating Limestone with FBA was chosen for this study. A small portion of OPC is added into the mixture to work as a binder, according to findings the OPC provided a durable coating that adsorbs phosphate effectively. The availability of high amounts of calcium and silicate in the composite of OPC leads to the production of the calcium-silicate hydrate (C-S-H) which acts as a binder. It is true that a small quantity of OPC was utilized in coating process, but it is considered a manufactured material. Therefore, it is recommended to search for by-product materials which may be available and contain of high amounts of calcium

and silicate to use as a binder instead of the OPC. This solution will help to enhance the approach of sustainability.

- In this study, the longevity of LFBA was not determined according to the saturation point because long-term treatment is incompatible with economic considerations. Additionally, the features of the LFBA regeneration process were not covered entirely: specifically, the optimal time of washing and hydraulic loading rate for the washing solution. These aspects are connected and both of them need further development. Especially, the performance of LFBA was examined for phosphate retention after one trial of regeneration. Increasing the trials of LFBA regeneration will help to identify the life span of utilizing the LFBA.

References

- Ádám, K.,Krogstad, T.,Vråle, L.,Søvik, A. K.and Jenssen, P. D. (2007) Phosphorus retention in the filter materials shellsand and Filtralite P®- Batch and column experiment with P solution and secondary wastewater. *Ecological Engineering*, 29, 200-208.
- Akhurst, D.,Jones, G.,Clark, M.and McConchie, D. (2006) Phosphate removal from aqueous solutions using neutralised bauxite refinery residues (Bauxsol™). *Environ Chem*, 3, 65–74.
- Anderson, M. A.,Rubin, A. J.and I., C. (1981) *Adsorption of inorganic at solid liquid interfaces*, MI, Ann Arbor Science Publishers.
- Barger, E. . (2013) *The 28-Day Myth* [Online]. Precast Magazines NPCA. Available: <http://precast.org/2013/10/28-day-myth/> [Accessed 11/07/2016 2016].
- Barnett, V.and Lewis, T. (1995) *Outliers in Statistical Data*, Chichester, John Wiley and Sons.
- Ben Aim, R.,Vigneswaran, S.,Prasanthi, H.and Jegatheesan, V. (1997) Influence of particle size and size distribution in granular bed filtration and dynamic microfiltration. *Water Science and Technology*, 36, 207-215.
- Benjamin, M.,Sletten, R.,Bailey, R.and Bennett, T. (1996) Sorption and filtration of metals using iron-oxide-coated sand. *Wat. Res.*, 30, 2609-262.
- Bennour, H. A. M. (2012) Influence of pH and Ionic Strength on the Adsorption of Copper and Zinc in Bentonite Clay. *Chemical Science Transactions*, 1, 371-381.
- Berryman, C. J. (2007) *Tracer tests for investigating flow and transport in the hyporheic zone*. UK: Environment Agency.
- Bourikas, K.,Kordulis, C.and Lycourghiotis, A. (2005) Differential potentiometric titration: development of a methodology for determining the point of zero charge of metal (hydr)oxides by one titration curve. *Environ. Sci. Technol.*, 39.
- Cardenas-Peña, A. M.,Ibanez, J. G.and Vasquez-Medrano, R. (2012) Determination of the point of zero charge for electrocoagulation precipitates from an iron anode. *Int. J. Electrochem. Sci.*, 7, 6142 - 6153.
- Cecil, D. L.and Green, J. R. (2000) *Radon-222. In: Environmental Tracers in Subsurface Hydrology*, Kluwer Academic Publishers.
- Chandler, A. J.,Eighmy, T. T.,Hjelmar, O.,Kosson, D. S.,Sawell, S. E.,Vehlow, J.,Sloot, H. A. v. d.and Hartlén, J. (1997) *Municipal Solid Waste Incinerator Residues*, Amsterdam, Netherland Elsevier.
- Chang, W.-S.,Tran, H.-T.,Park, D.-H.,Zhang, R.-H.and Ahn, D.-H. (2009) Ammonium nitrogen removal characteristics of zeolite media in a Biological Aerated Filter (BAF) for the treatment of textile wastewater. *Journal of Industrial and Engineering Chemistry*, 15, 524-528.

- Chardon, W. J., Groenenberg, J. E., Temminghoff, E. J. M. and Koopmans, G. F. (2012) Use of reactive materials to bind phosphorus. *Journal of Environmental Quality*, 41, 636-646.
- Chen, X. (2015) Modeling of Experimental Adsorption Isotherm Data. *Information*, 6, 14-22.
- Cheremisinoff, N. P. (2002) *Handbook of Water and Wastewater Treatment Technologies*, United States of America Butterworth-Heinemann.
- Cobos-Becerra, Y. L. and Gonzalez-Martinez, S. (2013) Influence of air flow rate and backwashing on the hydraulic behaviour of a submerged filter. *Water Sci Technol*, 68, 2000-6.
- Costa Reis, L. and Santa' Anna, G. (1985) 'Aerobic treatment of concentrated wastewater in a submerged bed reactor'. *Water Resources*, 19, 1341-1345.
- Crites, R. W. and Tchobanoglous, G. (1998) *Small and decentralized wastewater management systems*, WCB/McGraw-Hill.
- Cucarella, V. (2009) *Recycling filter substrates used for phosphorus removal from wastewater as soil amendments*. PhD, Royal Institute of Technology.
- Cucarella, V. and Renman, G. (2009) Phosphorus sorption capacity of filter materials used for on-site wastewater treatment determined in batch experiments – A Comparative Study. *Journal of Environmental Quality*, 38, 381-392.
- de-Bashan, L. E. and Bashan, Y. (2004) Recent advances in removing phosphorus from wastewater and its future use as fertilizer (1997-2003). *Water Res*, 38, 4222-46.
- De Souza Jr., L. R. and Lorenz, L. (2014) Residence Time Distribution for Tubular Reactors. *COMSOL Conference*. Curitiba.
- Defra (2014) Water Framework Directive implementation in England and Wales: new and updated standards to protect the water environment.
- Del Bubba, M., Arias, C. A. and Brix, H. (2003) Phosphorus adsorption maximum of sands for use as media in subsurface flow constructed reed beds as measured by the Langmuir isotherm. *Water Research*, 37, 3390-3400.
- Despland, L. M., Clark, M. W., Vancov, T. and Aragno, M. (2014) Nutrient removal and microbial communities' development in a young unplanted constructed wetland using Bauxsol pellets to treat wastewater. *Sci Total Environ*, 484, 167-75.
- Di Gianfilippo, M., Costa, G., Pantini, S., Allegrini, E., Lombardi, F. and Astrup, T. F. (2015) LCA of management strategies for RDF incineration and gasification bottom ash based on experimental leaching data. *Waste Manag.*
- Dils, R., Leaf, S., Robinson, R. and Sweet, N. (2001) Phosphorus in the environment – Why should recovery be a policy issue? . *2nd Int. Conf. on Recovery of Phosphates from Sewage and Animal Wastes*. Holland, NL.
- Donnert, D. and Salecker, M. (1999a) Elimination of phosphorus from municipal and industrial waste water. *Water Sci. Technol.*, 40, 195–202.

- Donnert, D. and Salecker, M. (1999b) Elimination of phosphorus from waste water by crystallization. *Environ. Technol.*, 20, 735–742.
- Dunstan Jr., P. E. (2011) How Does Pozzolanic Reaction Make Concrete “Green”? *2011 World of Coal Ash (WOCA) Conference*. Denver, CO, USA
- Ellins, K. K., Kincaid, T. R., Hisert, R. A., Johnson, N. A., Davison, C. A. and Wanninkhof, R. H. (1991) Using ^{222}Rn and SF_6 to determine groundwater gains and stream flow losses in the Santa Fe river: hydrogeology of the western Santa Fe river basin, Field Trip Guidebook No.32. Southeastern Geological Society.
- Ellins, K. K., Roman-Mas, A. and Lee, R. (1990) Using ^{222}Rn to examine groundwater/surface discharge interaction in the Rio Grande De Manati, Puerto Rico. *Journal of Hydrology*, 115, 319–341.
- Engelhardt, T. (2012) Granular media filtration for water treatment applications. Drinking Water Hach Company.
- EPA. (2016) *Table of Regulated Drinking Water Contaminants* [Online]. USA: EPA. Available: <https://www.epa.gov/ground-water-and-drinking-water/table-regulated-drinking-water-contaminants> [Accessed 25/06/2016 2016].
- Farmer, A. M. (2001) Reducing phosphate discharges: the role of the 1991 EC urban wastewater treatment directive. *Water Sci. Technol*, 44, 41-48.
- Fazolo, A., Pasotto, M. B., Foresti, E. and Zaiat, M. (2006) Kinetics, mass transfer and hydrodynamics in a packed bed aerobic reactor fed with anaerobically treated domestic sewage. *Environ Technol*, 27, 1125–1135.
- Field, A. (2008) Multiple regression using SPSS. *Research Methods in Psychology*, 1-11.
- Franklin, S., Thomas, S. and Brodeur, M. Robust multivariate outlier detection using mahalanobis’ distance and modified stahel-donoho estimators. Available: <https://ww2.amstat.org/meetings/ices/2000/proceedings/S33.pdf> [Accessed 06/01/2017].
- Galarneau, E. and Gehr, R. (1997) Phosphorus removal from wastewaters: experimental and theoretical support for alternative mechanisms. *Water Res.*, 31, 328–338.
- Grainger, S. and Blunt, J. (1998) *Engineering Coatings: Design and Application*, UK, Woodhead Publishing Ltd.
- Gray, E. (2012) *Laboratory Methods for the Advancement of Wastewater Treatment Modeling*. Master of Science, Wilfrid Laurier University.
- Gupta, G. and Torres, N. (1998) Use of fly ash in reducing toxicity of and heavy metals in wastewater effluent. *J. Hazard. Mater.*, 57, 243–248.
- Han, R., Zou, W. and Li, H. (2006) Copper(II) and lead(II) removal from aqueous solution in fixed-bed columns by manganese oxide coated zeolite. *Journal of Hazardous Materials*, 137, 934-942.

- Henry, J. G. and Heinke, G. W. (1989) *Environmental Science and Engineering*, Englewood Cliffs, NJ, Prentice-Hall.
- Herrmann, I., Jourak, A., Hedström, A., Lundström, S. and Viklander, M. (2013) The Effect of Hydraulic Loading Rate and Influent Source on the Binding Capacity of Phosphorus Filters. *PLoS ONE*, 8, 1-8.
- Hjelmar, O., Johnson, A. and Comans, R. (2010) Incineration: Solid Residues. In: Christensen, T. H. (ed.) *Solid Waste Technology and Management, Volume 1 and 2*. Chichester, UK: John Wiley & Sons, Ltd.
- Hydro. (2006) *Fiddler's Ferry Power Station* [Online]. Available: <http://web.archive.org/web/20060924222142/http://www.fhc.co.uk/powerprogramme/PDF/v4.pdf> [Accessed 22/03/2016].
- Ibanez, J. G., Hernandez-Esparza, M., Doria-Serrano, C., Fregoso-Infante, A. and Singh, M. M. (2007) *Environmental Chemistry: Fundamentals*, New York, Springer.
- Iida, Y. and Teranishi, A. (1984) 'Nitrogen removal from municipal wastewater by a single submerged filter'. *J. Water Pollut. Control Fed.*, 56, 251-258.
- Jenkins, D., Ferguson, J. and Menar, A. (1971) Chemical process for phosphate removal. *Water Research*, 5, 369-389.
- Jenkins, D. and Hermanowicz, S. W. E. n. e. (eds.) (1991) *Phosphorus and Nitrogen Removal from Municipal Wastewater: Principles and Practice*, Chelsea, MI: Lewis Publishers.
- Jianbo, L., Liping, S., Xinhua, Z., Bin, L., Yinlei, L. and Lei, Z. (2009) Removal of Phosphate from Aqueous Solution Using Iron-Oxide-Coated Sand Filter Media: Batch Studies. *International conference on environmental science and information application technology*. China.
- Johansson Westholm, L. (2006a) Substrates for phosphorus removal—Potential benefits for on-site wastewater treatment? *Water Research*, 40, 23–36.
- Johansson Westholm, L. (2006b) Substrates for phosphorus removal—Potential benefits for on-site wastewater treatment. *Water Research*, 40, 23-36.
- Kaasik, A., Vohla, C., Mötle, R., Mander, Ü. and Kirsimäe, K. (2008) Hydrated calcareous oil-shale ash as potential filter media for phosphorus removal in constructed wetlands. *Water Research*, 42, 1315-1323.
- Kadlec, R. and Wallace, S. (2009) *Treatment wetlands*, Boca Raton, FL, CRC Press.
- Kaminski, I., Vescan, N. and Adin, A. (1997) Particle size distribution and wastewater filter performance. *Water Science & Technology*, 36, 217- 224
- Kawamura, S. (2000) *Integrated Design of Water Treatment Facilities*, New Jersey, John Wiley & Sons.
- Kent, T., Fttzpatrick, C. and Williams, S. (1996) Testing of biological aerated filter (BAF) media. *Water Science Technology*, 34, 363-370.

- Kirk, D. W., Jia, C. Q., Yan, J. and Torrenueva, A. L. (2003) Wastewater remediation using coal ash. *Integrated Management of Hazardous Waste*, 5, 5-8.
- Klimeski, A., Wim, J. C., Turtola, E. and Uusitalo, R. (2012) Potential and limitations of phosphate retention media in water protection: A process-based review of laboratory and field-scale tests. *AGRICULTURAL AND FOOD SCIENCE*, 21, 206–223.
- Knofczynski, G. and Mundfrom, D. (2008) Sample sizes when using multiple linear regression for Prediction. *Educational and Psychological Measurement*, 68, 431-442.
- Kocamemi, B. (2014) Filtration. ENVE 301 Environmental Engineering Unit Operations.
- Kosmulski, M. (2006) pH-Dependent Surface Charging and Points of Zero Charge III. Update. *J. Colloid Interface Sci.*, 298, 730.
- Krishnaswamy, U., Muthuchamy, M. and Perumalsamy, L. (2011) Biological removal of phosphate from synthetic wastewater using bacterial consortium. *IRANIAN JOURNAL of BIOTECHNOLOGY*, 9, 37-49.
- Lau, P. S., Tam, N. F. Y. and Wong, Y. S. (1997) Wastewater Nutrients (N and P) Removal by Carrageenan and Alginate Immobilized *Chlorella Vulgaris*. *Environmental Technology*, 18, 945-951.
- Le Clorec, P. and Martin, G. (1984) 'The mean residential time application in an aerated immersed biological filter'. *Environment Technology Lett.*, 58, 275-282.
- Lenntech (2016) *Phosphorous removal from wastewater* [Online]. Available: <http://www.lenntech.com/phosphorous-removal.htm>.
- Levenspiel, O. (1999) *Chemical Reaction Engineering*, John Wiley & Sons.
- Levenspiel, O. (1972) *Chemical Reaction Engineering*, New York, Wiley.
- Li, S., Cui, J., Zhang, Q., Fu, J., Lian, J. and Li, C. (2010) Performance of blast furnace dust clay sodium silicate ceramic particles (BCSCP) for brewery wastewater treatment in a biological aerated filter. *Desalination*, 258, 12-18.
- Loffill, E. (2011) *The optimisation of nitrifying continuous up-flow filters for tertiary wastewater treatment*. PhD, Liverpool John Moores.
- Lyngsie, G. (2013) *Sorbents for phosphate removal from agricultural drainage water*. PhD, University of Copenhagen.
- Madigan, M., Martinko, J., Stahl, D. and Clark, D. (2012) *Brock biology of microorganisms*, Harlow, Pearson Education.
- Mahmood, T., Saddique, M. T., Naeem, A., Mustafa, S. and Dilara, B. (2011a) Cation Exchange Removal of Zn from Aqueous Solution by NiO. *J. Non Cryst. Solids*, 357, 1016.
- Mahmood, T., Saddique, M. T., Naeem, A., Westerhoff, P., Mustafa, S. and Alum, A. (2011b) Comparison of Different Methods for the Point of Zero Charge Determination of NiO. *Industrial & Engineering Chemistry Research*, 50, 10017-10023.

- Mangialardi, T., Piga, L., Schena, G. and Sirini, P. (1998) Characteristics of MSW incinerator ash for use in concrete, *Environ. Eng. Sci.*, 15, 291–297.
- Marais, G. (1983) Observation supporting phosphate removal by biological excess uptake - a review. *Water Sci. Tech.*, 15, 15-41.
- Maxwell, S. E. (2000) Sample size and multiple regression analysis. *Psychological Methods*, 5, 434-458.
- MECO. (2016). Available: <http://www.meco.com/product/food-and-beverages-ultrafiltration/> [Accessed 10th August 2016 2016].
- Mendoza, L. and Stephenson, T. (1999) A Review of Biological Aerated Filters (BAFs) of Wastewater Treatment *Environmental Engineering Science*, 16, 201-216.
- Mesquita, D. P., Amaral, A. L. and Ferreira, E. C. (2011) Identifying different types of bulking in an activated sludge system through quantitative image analysis. *Chemosphere*, 85, 643-52.
- Mesquita, D. P., Dias, O., Amaral, A. L. and Ferreira, E. C. (2010) A Comparison between bright field and phase-contrast image analysis techniques in activated sludge morphological characterization. *Microsc Microanal*, 16, 166-74.
- Montaigne, F. and Essick, P. (2002) Water Pressure. *Natl. Geog*, 202, 2–33.
- Morse, G., Lester, J. and Perry, R. (1993) *The economic and environmental impact of phosphorus removal from wastewater in the European Community*, London, Selpher Publications.
- Morse, G. K., Brett, S. W., Guy, J. A. and Lester, J. N. (1998) Review: Phosphorus removal and recovery technologies. *Sci. Total Environ.*, 212, 69–81.
- Naeem, A., Westerhoff, P. and Mustafa, S. (2007) Vanadium Removal by Metal (Hydr)Oxide Adsorbents. *Water Res.*, 41, 1596.
- Neethling, J. B., Bakke, B., Benisch, M., Gu, A., Stephens, A., Stensel, H. D. and Moore, R. (2005) Factors Influencing the Reliability of Enhanced Biological Phosphorus Removal. Alexandria, VA: Water Environment Research Foundation.
- NESC (2013) Phosphorus and Onsite Wastewater Systems. Virginia, USA: West Virginia University.
- Ntifo, S. (2004) *Water Framework Directive, Water UK Policy* [Online]. Available: <http://www.water.org.uk/>.
- Office of Geotechnical Engineering. (2008) *Design procedures for soil modification or stabilization*. Indianapolis, Indiana: Office of Geotechnical Engineering.
- Osorio, F. and Hontoria, E. (2002) Wastewater treatment with a double-layer submerged biological aerated filter, using waste materials as biofilm support. *J. Environ. Manag.*, 65, 79–84.

- P., C. J. and M., P. J. (1994) Biological aerated filters: assessment of the process based on 12 sewage treatment plants. *Water Science and Technology*, 29, 13–22.
- Pallant, J. (2005) *SPSS Survival Manual*, Australia, Allen & Unwin.
- Pant, H. J., Goswami, S., Samantray, J. S., Sharma, V. K. and Maheshwari, N. K. (2015) Residence time distribution measurements in a pilot-scale poison tank using radiotracer technique. *Appl Radiat Isot*, 103, 54-60.
- Penetra, R. G., Reali, M. A. P., Foresti, E. and Campos, J. R. (1999) Post-treatment of effluents from anaerobic reactor treating domestic sewage by dissolved-air flotation. *Water Sci. Technol.*, 40, 137–143.
- Penn, C. J. and McGrath, J. M. (2011) Predicting phosphorus sorption onto steel slag using a flow-through approach with application to a pilot scale system. *Journal of Water Resource and Protection*, 3, 235-244.
- Pradhan, S. and Raj Pokhrel, M. (2013) Spectrophotometric determination of phosphate in sugarcane juice, fertilizer, detergent and water samples by molybdenum blue method. *Scientific World*, 11.
- Pujol, R., Hamon, M., Kandel, X. and Lemmel, H. (1994) Biofilters: flexible, reliable biological reactors. *Water Science Technology*, 29, 33-38.
- Quickenden, J., Mittal, R. and Gros, H. (1992) Published. the European Conference on Nutrient Removal from Wastewater, 1992 Wakefield, UK.
- Reardon, R. (2006) Technical introduction of membrane separation processes for low TP limits. WERF.
- Rhue, R. and Harris, W. (eds.) (1999) *Phosphorus sorption desorption reactions in soils and sediments*, Florida: Lewis Publishers.
- Robinson, A., Brignal, W. and Smith, A. (1994) Construction and operation of a submerged aerated filter sewage treatment work. *J. IWEM*, 8, 215-227.
- Rogalla, F., Payraudeau, M., Bacquet, G., Bourbigot, M., Sibony, J. and Gilles, P. (1990) Nitrification and Phosphorus Precipitation with Biological Aerated Filters. *J. Water Pollut. Control Fed.*, 62, 169-176.
- Rolland, L., Molle, P., Liénard, A., Bouteldja, F. and Grasmick, A. (2009) Influence of the physical and mechanical characteristics of sands on the hydraulic and biological behaviors of sand filters. *Desalination*, 248, 998-1007.
- Rybicki, S. (1997) Phosphorus Removal from Wastewater: A Literature Review. In: Płaza, E., Levlin, E. and Hultman, B. (eds.). Royal Institute of Technology.
- Sagberg, P. and Berg, K. (1996) Published. Experiences with bio for reactors at Veas, Norway. the 2nd BAF Symposim, 1996 Cranfield, UK.
- Sakadevan, K. and Bavor, H. J. (1998) Phosphate adsorption characteristics of soils, slags and zeolite to be used as substrates in constructed wetland systems. *Water Res.*, 32, 393–399.

- Schauer, P., Rectanus, R., Debarbadillo, C., Barton, D., Gebbia, R., Boyd, B. and McGehee, M. (2006) Published. Pilot Testing of Upflow Continuous Backwash Filters for Tertiary Denitrification and Phosphorus Removal. WEFTEC, 2006. Water Environment Federation, 4751-4780.
- Sear, L. K. A. (2001) *The Properties and Use of Coal Fly Ash*, London, Thomas Telford.
- Seida, Y. and Nakano, Y. (2002) Removal of phosphate by layered double hydroxides containing iron. *Water Res.*, 36, 1306–1312.
- Shock, C. and Pratt, K. (2003) Phosphorus effects on surface water quality and phosphorus TMDL development. *Western Nutrient Management Conference*. Salt Lake City, UT.
- Shyla, B., Mahadevaiah and Nagendrappa, G. (2011) A simple spectrophotometric method for the determination of phosphate in soil, detergents, water, bone and food samples through the formation of phosphomolybdate complex followed by its reduction with thiourea. *Spectrochim Acta A Mol Biomol Spectrosc*, 78, 497-502.
- Smil, V. (2000) Phosphorus in the environment: natural flows and human interferences. *Annu. Rev. Energy Environ*, 25, 53–88.
- Smith, A. and Marsh, P. (1995) Enhanced wastewater treatment with lamella tube settlers, submerged aerated filters, and ultra-violet radiation. *the Water Environment Federation 68th Annual Conf.* Miami.
- Stensel, H., Reiber, S., Lee, K., Melcer, H. and Rakness, K. (1988) Biological aerated filter evaluation. *Environ. Prog.*, 114, 655-671.
- Strom, P. F. (2006) Introduction to phosphorus removal. Atlantic city, NJ: NJWEA.
- Szabo, A., Takas, I., Murthy, S., Daigger, G., Licsko, I. and Smith, S. (2008) Significance of Design and Operational Variables in Chemical Phosphorus Removal *Water Environment Research*, 80, 407-416.
- Tabachnick, B. G. and Fidell, L. S. (2001) *Using Multivariate Statistics*, Boston, Allyn and Bacon.
- Tarun, R. N., Shiw, S. S. and Amr, S. H. (1992) Effects of water to cementitious ratio on compressive strength of cement mortar containing fly ash. *Fourth international conference on fly ash, silica fume, slag and natural pozzolans in concrete*. Istanbul, Turkey.
- Tchobanoglous, G., Burton, F. L. and Stensel, H. D. (2003) *Wastewater Engineering: Treatment and Reuse*, New York, The McGraw-Hill Inc.
- Thirunavukkarasu, O. S., Viraraghavan, T. and Suvramanian, K. S. (2003) Arsenic removal from drinking water using iron oxide-coated sand. *Water, Air, and Soil Pollution*, 142, 95-111.
- Thomas, M. (2007) Optimizing the Use of Fly Ash in Concrete. United States: Portland Cement Association.

- UNEP (2004) Guidelines on sewage treatment and disposal for the Mediterranean region. Athens: United Nations Environment Programme.
- (2016) *Constructed wetlands* [Online]. Available: http://www.unep.or.jp/ietc/publications/freshwater/sb_summary/8.asp [Accessed 7th December 2016].
- Valentis, G. and Lesavre, J. (1989) waste-water treatment by attached-growth microorganisms on a geotextile support *Water Sci. Technol.*, 22, 43-51.
- vanLoon, G. W. and Duffy, S. J. (2000) *Environmental chemistry a global perspective*, New York, Oxford University Press.
- Vohla, C., Kořiv, M., Bavor, H. J., Chazarenc, F. and Mander, U. (2011) Filter materials for phosphorus removal from wastewater in treatment wetlands—A review. *Ecol. Eng.*, 37, 70–89.
- Wagener, C. (2000) *Evaluation of static low density media filters for use in domestic wastewater treatment*. MSc., Louisiana State University.
- Ward, R. S., Williams, A. T., Barker, J. A., Brewerton, L. J. and Gale, I. N. (1998) Groundwater Tracer Tests: a Review and Guidelines for Their Use in British Aquifers. Environment Agency R&D.
- Wen, Z., Zhang, Y. and Dai, C. (2014) Removal of phosphate from aqueous solution using nanoscale zerovalent iron (nZVI). *Colloids and Surfaces A: Physicochemical and Engineering Aspects*, 457, 433-440.
- Wilderer, P. A., Cunningham, A. and Schindler, U. (1995) Hydrodynamics and shear stress: report from the discussion session. *Water Science and Technology*, 32, 271-272.
- Wong, H. S. and Buenfeld, N. R. (2009) Determining the water-cement ratio, cement content, water content and degree of hydration of hardened cement paste: Method development and validation on 2 paste samples. *Cement & Concrete Research*, 39, 957-965.
- Water World. (2016) *Upflow Media Filtration Tackles Demanding Treatment Applications* [Online]. Water World. Available: <http://www.waterworld.com/articles/print/volume-23/issue-2/product-focus/upflow-media-filtration-tackles-demanding-treatment-applications.html> [Accessed 4th April 2016].
- Yi, W. G. and Lo, K. V. (2003) Phosphate recovery from greenhouse wastewater. *J. Environ. Sci. Heal.*, B 38, 501–509.
- Young, J. C., Baumann, E. R. and Wall, D. J. (1975) Packed-Bed Reactors for Secondary Effluent BOD and Ammonia Removal. *Water Pollution Control Federation*, 47, 46-56.
- Yousef, R. I., El-Eswed, B. and Al-Muhtaseb, A. a. H. (2011) Adsorption characteristics of natural zeolites as solid adsorbents for phenol removal from aqueous solutions: Kinetics, mechanism, and thermodynamics studies. *Chemical Engineering Journal*, 171, 1143-1149.
- Yu, Y., Feng, Y., Qiu, L., Han, W. and Guan, L. (2008) Effect of grain-slag media for the treatment of wastewater in a biological aerated filter. *Bioresour Technol*, 99, 4120-3.

- Zamani, A. and Maini, B. (2009) Flow of dispersed particles through porous media — Deep bed filtration. *Journal of Petroleum Science and Engineering*, 69, 71-88.
- Zbicinski, I., Stavenuiter, J., Kozłowska, B. and Van de Coevering, H. (2006) *Product Design and Life Cycle Assessment*, Sweden, The Baltic University.
- ZENG, H., FISHER, B. and GIAMMAR, D. (2008) Individual and Competitive Adsorption of Arsenate and Phosphate To a High-Surface-Area Iron Oxide-Based Sorbent. *Environ. Sci. Technol.*, 42, 147–152.

Appendices

Appendix A

Worksheets of the experiments

Specific gravity (Gas Jar Method)

Test Number	Measurements (g)
(M1) Mass of gas jar and plate	
(M2) Mass of gas jar, plate and dry material	
(M3) Mass of gas jar, plate, material and water	
(M3) Mass of gas jar and water	
Calculation of S.G $M2 - M1 / (M4 - M1) - (M3 - M2)$	
Specific Gravity (S.G)	

Coefficient of permeability K (Constant head permeameter method)

Sample diameter mm		74
Area of sample mm ²	A	4303
Distance between piezometer tapping's mm	I	100
Quantity of water collected ml		
Quantity of water collected mm ³	Q	

		Test 1	Test 2	Test 3	Test 4	Test 5
Manometer A						
Manometer B						
Head loss mm	h					
Time s	t					
Hydraulic gradient	$i = h / I$					

$q = Q / t$	mm/s					
-------------	------	--	--	--	--	--

Discharge velocity	$V = q / A$	mm/s				
--------------------	-------------	------	--	--	--	--

$K = QI / tAh$	mm/s					
----------------	------	--	--	--	--	--

Average	K	mm/s	
---------	---	------	--

Average	K	M/s × 10 ⁻ⁿ	
---------	---	------------------------	--

Porosity and bulk density

No.	Step	results
1	Weight of beaker	
2	Weight beaker & particles	
3	Weight of particles (2 -1)	
4	Bulk volume (particles + pore space)	
5	Initial volume of water in the 1000 graduated cylinder	
6	Final volume (level) of water in 1000 ml graduated cylinder after particles were added	
7	Volume of particles (6 – 5)	
8	Volume of pore space (4 -7)	
9	Percentage of Bulk volume (8/4) = porosity	
10	Bulk density (mass/Bulk volume) (3/4)	
11	Density of individual particles (mass/particle volume) (3/7)	

Appendix B

MATLAB codes for SEM image processing

LFBA and LBBA SEM image processing

```
>> %% Limestone SEM images processing
>> L1=imread('LFBA.jpg');
>> L2=imread('LBBA.jpg');
>> %% SEM images convert into grayscale
>> L1gray=rgb2gray(L1);
>> L2gray=rgb2gray(L2);
>> %% SEM images segmentation
>> L1thresh=im2bw(L1gray,0.3);
>> L2thresh=im2bw(L2gray,0.3);
>> %% Show images
>> subplot(2,2,1);
>> imshow(L1thresh);
>> title('LFBA');
>> subplot(2,2,2);
>> imshow(L2thresh);
>> title('LBBA');
>> %% Images Histogram
>> h1=imhist(L1gray);
>> subplot(2,2,3);
>> plot(h1);
>> xlabel('Intensity');
>> ylabel('Frequency');
>> h2=imhist(L2gray);
>> subplot(2,2,4);
>> plot(h2);
```

```

>> xlabel('Intensity');
>> ylabel('Frequency');
DFBA and DBBA SEM image processing

%% White dolomite SEM images processing
>> d1=imread('DFBA.jpg');
>> d2=imread('DBBA.jpg');
>> %% SEM images convert into grayscale
>> d1gray=rgb2gray(d1);
>> d2gray=rgb2gray(d2);
>> %% SEM images segmentation
>> d1thresh=im2bw(d1gray,0.3);
>> d2thresh=im2bw(d2gray,0.3);
>> %% show images
>> subplot(2,2,1);
>> imshow(d1thresh);
>> title('DFBA')
>> subplot(2,2,2);
>> imshow(d2thresh);
>> title('DBBA');
>> %% images Histogram
>> h1=imhist(d1gray);
>> subplot(2,2,3);
>> plot(h1);
>> xlabel('Intensity');
>> ylabel('Frequency');
>> h2=imhist(d2gray);
>> subplot(2,2,4);
>> plot(h2);
>> xlabel('Intensity');

```

```

>> ylabel('Frequency');
SFBA and SBBA SEM image processing

>> %% Sand SEM images processing
>> S1=imread('SFBA.jpg');
>> S2=imread('SBBA.jpg');
>> %% SEM images convert into grayscale
>> S1gray=rgb2gray(S1);
>> S2gray=rgb2gray(S2);
>> %% SEM images segmentation
>> S1thresh=im2bw(S1gray,0.3);
>> S2thresh=im2bw(S2gray,0.3);
>> %% Show images
>> subplot(2,2,1);
>> imshow(S1thresh);
>> title('SFBA');
>> subplot(2,2,2);
>> imshow(S2thresh);
>> title('SBBA');
>> %% Images Histogram
>> h1=imhist(S1gray);
>> subplot(2,2,3);
>> plot(h1);
>> xlabel('Intensity');
>> ylabel('Frequency');
>> h2=imhist(S2gray);
>> subplot(2,2,4);
>> plot(h2);
>> xlabel('Intensity');
>> ylabel('Frequency');

```